Université de Montréal

The viral diversity in the EPIC[4] cohort and the evolution of the size of the HIV-1 cellular reservoir in perinatally infected children and adolescents under cART

Par

Madeleine Aby Diallo

Département de microbiologie, infectiologie et immunologie

Faculté de Médecine

Mémoire présenté en vue de l'obtention du grade de M.Sc.

en Microbiologie et Immunologie

Décembre 2021

Université de Montréal

Département de microbiologie, infectiologie et immunologie

Faculté de Médecine

Ce mémoire intitulé

The viral diversity in the EPIC[4] cohort and the evolution of the size of the HIV-1 cellular reservoir in perinatally infected children and adolescents under cART

Présenté par

Madeleine Aby Diallo

A été évalué par un jury composé des personnes suivantes

Dr. Guy Lemay
Président-rapporteur

Dr. Hugo Soudeyns
Directeur de recherche

Dr. Daniel Kaufmann
Membre du jury

Résumé

Le VIH-1 reste incurable dû à sa diversité génétique et sa capacité à se cacher dans des réservoirs cellulaires. Certaines études ont révélé que le clade du VIH peut influencer l'issue de l'infection. D'autres études chez l'adulte et l'enfant ont montré que l'initiation précoce d'un traitement antirétroviral combiné (TARc) peut limiter la taille du réservoir et conduire à une suppression virale soutenue (SVS) après interruption du traitement.

Ici, nous allons génotyper le clade de 64 participants et allons examiner l'influence de l'âge, du maintien de la SVS et de l'initiation précoce du TARc sur la dynamique du réservoir chez 67 enfants et adolescents verticalement infectés (cohorte EPIC[4]).

Une analyse phylogénétique basée sur le gène *gag* du VIH-1 a démontré que la majorité était infectée par le clade C, puis A, B, CRF01_AE, CRF02_AG et G. La prévalence des sous-types non-B (77 %) est cohérente avec les tendances courantes et l'origine ethnique des participants.

L'ADN viral a été mesuré dans les cellules mononuclées du sang périphérique. L'ARN induit par un analogue de prostratin a été mesuré dans des cellules T CD4+. Nous avons démontré la corrélation positive entre les deux techniques. La taille du réservoir était similaire entre enfants et adolescents et est restée stable aux différents temps de mesures. Les participants avec SVS présentaient les niveaux médians d'ARN et d'ADN les plus bas. Une longue durée de la TARc et l'initiation précoce du traitement chez ceux qui ont maintenu une SVS étaient associées à un réservoir plus petit. La présence de « blips » a influencé la trajectoire et la taille du réservoir.

Mots-clés: VIH-1, enfants, TAR, suppression virale soutenue (SVS), réservoir du VIH, analyse phylogénétique, gène *gag*, ADN du VIH-1, prostratine, stimulation de lymphocytes T CD4+.

Abstract

HIV-1 infection remains incurable due to the genetic diversity of the virus and its ability to hide out of reach in cellular reservoirs. Some studies revealed that HIV clades may differently influence the outcome of HIV. Other studies in adults and children have shown that early initiation of combination antiretroviral therapy (cART) can limit the size of the reservoir and can lead to sustained viral suppression (SVS) after treatment interruption.

Here we genotyped the HIV-1 subtype in 64 participants and examined how the dynamics of the viral reservoir in 67 children and adolescents with vertically acquired HIV infection was influenced by age, maintenance of SVS, and early initiation of cART (EPIC[4] cohort).

Following a phylogenetic analysis based on HIV-1 *gag* gene, we discovered the majority were infected with clade C, then A, B, CRF01_AE, CRF02_AG and G. The high prevalence of non-B subtypes (77%) is consistent with current trends and the ethnic origin of study participants.

Viral DNA was measured in peripheral blood mononuclear cells, and RNA induced with an prostratin analog was measured in CD4+ T cells. We demonstrated the positive correlation between these two assays. The size of the reservoir was similar between children and adolescents and remained stable at different time-points. Participants with SVS presented the lowest median HIV-1 RNA and DNA levels. Longer duration of effective treatment and early initiation of treatment in participants who maintained SVS were associated with a smaller reservoir. The presence of « blips » influenced the trajectory of reservoir size over time.

Keywords: HIV-1, children, ART, sustained viral suppression (SVS), HIV reservoir, phylogenetic analysis, *gag* gene, HIV-1 DNA, prostratin, CD4 T cell stimulation.

Table des matières

Liste des tableaux

Liste des figures

Liste des sigles et abréviations

ADCC : antibody-dependent cellular cytotoxicity

AIDS: acquired immunodeficiency syndrome

ART : antiretroviral therapy

ARV : AIDS-associated retrovirus

AZT : azidothymidine

bNAb : broad spectrum neutralizing antibodies

cART : combined antiretroviral therapy

CD4+ or CD8+ T cells: CD4+ or CD8+ T lymphocytes

CHUL : Centre hospitalier de l'Université de Laval

cPLEC: cumulative proportion of life under effective treatment

cPLUS: cumulative proportion of life under sustained viral suppression

CRF : circular recombinant forms

DC : dendritic cells

ddPCR: digital droplet polymerase chain reaction

DNA : deoxyribonucleic acid

DRC : Democratic Republic of Congo

Env : envelope

EPIC[4]: Early Pediatric Initiation, Canada Child Cure Cohort Study

FBS : fetal bovine serum

FI : fusion inhibitors

Gag : group-specific antigen

HIV-1: human immunodeficiency virus type 1

HIV-2: human immunodeficiency virus type 2

HTLV-III : human T-lymphotropic virus type III

ICF: inducible cell-free

IFN-γ : interferon gamma

IgG : immunoglobulin G

IL-2: interleukin 2

INSTI : integrase strand transfer inhibitors

LANL : Los Alamos National Laboratory

LAV : lymphadenopathy-associated virus

LB medium : lysogeny broth medium

LPA : latency-promoting agents

LRA : latency reversing agents

LTR: long terminal repeat

mL: milliliter

mm : millimeter

N.A.: not available

NFAT : nuclear factor of activated T-cells

NF-kB: nuclear factor-kB

nm : nanometer

NNRTIs : non-nucleoside reverse transcriptase inhibitors

NRTIs : nucleoside reverse transcriptase inhibitors

ns: not significant

PBMC: peripheral blood mononuclear cell

PCR : polymerase chain reaction

PE : post-exposure

PEP : post-exposure prophylaxis

PI : protease inhibitors

PKC: protein kinase C

PLWH : people living with HIV

PMA : phorbol 12-myristate 13-acétate

POL: polymerase

PrEP : pre-exposure prophylaxis

QVOA : quantitative viral outgrowth assay

REV : regulator of expression of virion proteins

RNA : ribonucleic acid

RPMI : Roswell Park Memorial Institute

SIV: simian immunodeficiency virus

SIVcpz: simian immunodeficiency virus of chimpanzees

SIVgor: simian immunodeficiency virus of gorilla

SVS : sustained viral suppression

TAT : trans-activator of transcription

TCM : central memory CD4+ T cells

TEM : effector memory CD4+ T cells

TH: CD4+ T helper cells

Th2,17 : T helper 2, T helper 17 cells

Tregs : regulatory T cells

μg : micrograms

UNAIDS : United Nations Programme on HIV/AIDS

vif : viral infectivity factor

vpr : viral protein R

vpu : viral protein U

Remerciements

Je tiens avant tout à remercier le Dr Hugo Soudeyns pour m'avoir donné l'opportunité de réaliser ce fascinant projet dans son laboratoire. Je le remercie également pour sa gentillesse, son soutien, sa patiente et son encadrement.

Un gros merci à tous les membres du laboratoire pour leur aide, leur bonne humeur contagieuse et tous les moments de rires, d'échange et de réflexion qu'on a partagés: Hinatea Dieumegard, candidate au Ph.D.; Jade Canape, M.Sc.; Martine Caty, assistante de recherche; Ariane Larouche, Ph.D., associée de recherche et Doris Ransy, Ph.D., précédente associée de recherche.

Enfin, je tiens à remercier chaleureusement tous les participants de l'étude EPIC[4] ainsi que leurs familles sans qui le projet n'aurait pas eu lieu.

CHAPTER 1 – INTRODUCTION

Human immunodeficiency virus (HIV), which is the causative agent of AIDS, is a virus that has held the world in suspense since the end of the 20th century. However, the key to opening the door leading to a cure of HIV infection has eluded us to this day. The complexity and genetic diversity of this virus, as well as its ability to hide within its host in anatomical and cellular reservoirs beyond the reach of eradication treatments, are the fundamental reasons for this.

Here, we turn to basic biomolecular sciences in order to shed light on certain aspects of the course of HIV infection while paying particular attention to the perinatal transmission from infected mothers to their children. However, before we dive deeper into this matter, let us take a look back into the origins of the HIV pandemic.

1.1. HIV pandemic

1.1.1 Epidemiology

June 5, 2021, marked the 40th anniversary of the HIV Long-Term Survivors Awareness Day (HLTSAD), when is paid tribute to the millions of lives lost during this global pandemic and when countless heroes and survivors who paved the way for the progress we see today are celebrated. On this day, four decades ago, the United States Centers for Disease Control and Prevention reported the first five cases of rare *Pneumocystis carinii* pneumonia (PCP) in young gay men in Los Angeles [1, 2]. In 1982, this condition was termed as Acquired Immune Deficiency Syndrome (AIDS), as more young people continued to die due to opportunistic infections their immune systems should have been able to fend off [3]. Following that, the situation only got worse and by the end of 1985, almost every region of the world had reported at least one case of AIDS.

Since then, the HIV/AIDS pandemic has dominated the world. In 2020, The United Nations Programme on HIV/AIDS (UNAIDS) estimated that 37.7 million people were living with HIV and amidst them were 1.7 million children aged 0 to 14 [4]. Today, the vast majority of people living with HIV (PLWH) are located in East and Southern Africa, and other low- and middle- income

regions [4]. In Canada, 2,242 new HIV infections were reported in 2018, amounting to 62,050 PLWH in total [5].

As treatment continued to improve and different preventive measures were implemented, such as daily-oral pre-exposure prophylaxis (PrEP) for the HIV-negative, a steady decrease in the incidence of new infections worldwide was observed, with a 52% reduction since the peak in 1997 [4]. Another key strategy in driving down the incidence of new HIV infections was the 90-90-90 treatment targets for 2020 [6]. These were presented in December 2013 by UNAIDS and aimed to ensure that 90% of all PLWH knew their status, 90% of all diagnosed PLWH were receiving sustainable antiretroviral therapy (ART) and 90% of all PLWH receiving ART maintained an undetectable viral load. Fourteen countries have achieved the targets [7]. Although Canada did not reach this goal (2018 Results: 87%, 85%, 94%), significant improvements were still observed as they were in other parts of the world [5].

The goal of ending the HIV/AIDS pandemic requires universal access to all HIV services for each and every infected person. This can only be achieved through global solidarity and partnership. However, stigma, discrimination and inequalities remain pervasive in the HIV pandemic. It wasn't until 2010 that US President Obama lifted the travel ban on visitors with HIV, which had been put in place in 1987 [8]. Around that period, some schools wouldn't even allow the attendance of HIV-infected children [8]. This stigma born from the lack of awareness and misinformation still persists to this day and causes the marginalization and criminalization of the HIV-positive population. This, alongside a multitude of social, environmental, economic and legal factors unfavourably impact the HIV cascade of care, making it so that in 2020, 10 million PLWH were still not accessing treatment, the great majority of them originating from low/middle income countries [4].

Furthermore, as the current COVID-19 pandemic continues to spread out, HIV is also dropping down the priority list of health issues. The restrictions born from COVID-19 pandemic have limited provision of HIV services while studies show that PLWH are more likely to suffer severe outcomes from the COVID-19 infection [9, 10]. This dangerous combination threatens the welfare of an already vulnerable population.

As the number of PLWH continues to increase due to ongoing transmission and increased longevity amongst those infected, it is essential to identify and tear down the barriers that limit the access and utilization of HIV testing and treatment services [11]. This will be pursued in the updated 95-95-95 targets of UNAIDS as the world learns to narrow these inequality gaps by removing the societal and legal impediments to the delivery of HIV service [12].

1.1.2. Origin and viral diversity.

Over the period of 1983 to 1984, the team of Françoise Barré-Sinoussi and Luc Montagnier from the Pasteur Institute in France, Robert Gallo's group at the US National Cancer Institute and Jay Levy's team at the University of California all isolated the same retrovirus they would respectively name lymphadenopathy-associated virus (LAV), human T-lymphotropic virus type III (HTLV-III) and AIDS-associated Retrovirus (ARV) [13-15]. In 1986, a consensus was reached within the scientific community to call the new retrovirus HIV [16].

HIV is an example of cross-species, or 'zoonotic', viral transmission. Indeed, it is of simian descent [17]. The "spillover" was estimated to have occurred at the beginning of the 20th century in the Democratic Republic of Congo (DRC) [17]. The oldest HIV sequence was recovered in a 1959 plasma sample from a Congolese male [18]. The most common origin theory proposes that transmission occurred from a simian immunodeficiency virus (SIV)-carrying primate to a Congolese hunter during the killing rituals of the animal or from a bite. This virus can also cause the equivalent of AIDS in non-human primates [17].

There are two types of HIV currently circulating: HIV-1 and HIV-2; they originated from SIV strains found in chimpanzees and sooty mangabeys, respectively [19]. They exhibit differences in the organization of their genome, their pathogenesis and their epidemiology [20]. For example, HIV-1 is more virulent and reaches higher viral loads than HIV-2, which is therefore less infectious [20]. This reduced pathogenicity of HIV-2 is mainly associated with its expression of the accessory protein Vpx instead of HIV-1's Vpu [20, 21].

While HIV-2 is endemic in West Africa, it is rarely found elsewhere [20]. HIV-1, on the other hand, dominates the pandemic. It displays extensive genetic heterogeneity, as the various groups that compose this type are the result of different zoonotic transfers between non-human primates and humans [22]. These transfers gave birth to the 4 branches of HIV-1: M (Major), O (Outlier), N (Non O—Non M) and P [17, 23]. The four groups have different geographic distributions but produce relatively similar clinical symptoms [24]. Group M is the result of a single transmission event involving SIV-infecting chimpanzees from Cameroon and is the most widespread, mainly due to the fact that it was the most disseminated group at the beginning of the pandemic [17]. Group M separates into different clades/subtypes that were characterized and classified by phylogenetic analysis: A (A1, A2, A3, A4 and A6), B, C, D, F (F1 and F2), G, H, J, K and L [25, 26]. Current HIV nomenclature guidelines indicate that, in order to classify a new subtype, at least three full-length sequences must be identified from nonlinked transmission events, with no evidence of recombination. For HIV-1L, all three samples were recovered in DRC in 1983, 1990 and 2001 [26, 27]. However, it was only in 2019 that technology advanced enough to allow the sequencing of the most recent sample, where the virus was in low quantity.

The development of phylodynamic methods have greatly improved epidemiological reconstruction and prediction, making it easier and more accurate. This allows us to map the evolution of HIV-1 all around the world, as we observe the ever-changing subtype distribution patterns caused by population migration (Figure 1) [28]. 46.6% of global HIV infections are caused by clade C [29]. This clade is predominant in regions such as South and East Africa and India [29, 30]. In developed countries located in America, Western Europe, North Africa and Oceania, it is clade B, which represents 12% of all HIV infections, that is predominant [29, 30].
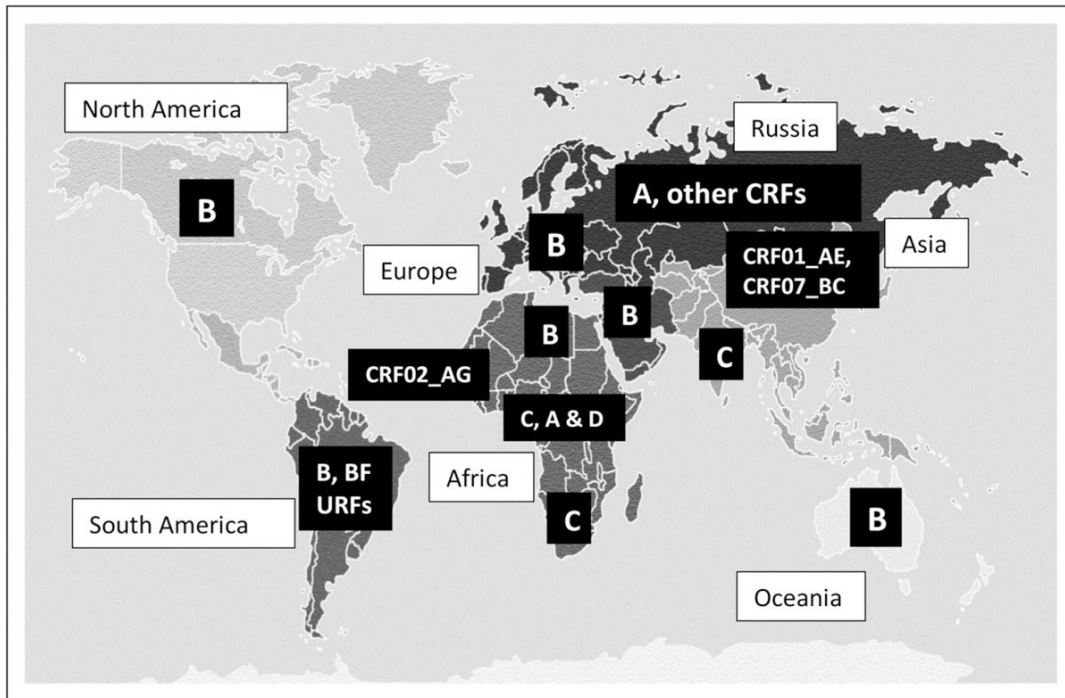
Figure 1. Global distribution of the major HIV-1 subtypes and recombinant forms [30].

This important biological property of HIV-1 allows the virus to evade the immune response and antiretroviral treatments [31]. Genetic variation can be anywhere from 15 to 20% within one subtype and 25 to 35% between subtypes [22]. Recombination between different subtypes of group M can also occur, resulting in circulating recombinant forms (CRF) and unique recombinant forms (URF). CRFs are recombinant forms spreading within a population, whereas URFs are often unique to a given individual [22]. Currently, there are 118 registered CRF in the Los Alamos National Laboratory (LANL) HIV sequence database and recombinants now predominate in regions such as West Africa and Asia [30, 32].

1.1.3. Structure and genomic organization of HIV-1

HIV-1 is a retrovirus of the lentivirus subfamily [33]. The spherical and enveloped virion has a diameter of approximately 100 nm [34]. Its lipid membrane results from the budding step of the HIV life cycle. Therefore, it is possible to find a few cell surface proteins on the viral envelope.

Envelope (Env) trimers are composed of three gp120 units each of which is non-covalently anchored to a gp41 transmembrane protein [34]. Env represents a major obstacle to the development of vaccines [35]. Not only does its coding sequences undergo rapid variation, but its glycosylation also acts as a shield against immune recognition [35, 36]. To add to this, the Env trimer can adopt different conformational structures in order to limit recognition by the immune system with immune cells [35, 36].

Right underneath the envelope is the matrix, which consists of thousands of copies of the p17 protein [37]. Surrounded by the matrix is the capsid. It is composed of the p24 protein and it encloses two positive-sense single-stranded RNA genomes bound to the p7 nucleocapsid protein, and other viral enzymes such as reverse transcriptase, integrase and proteases (Figure 2) [37].
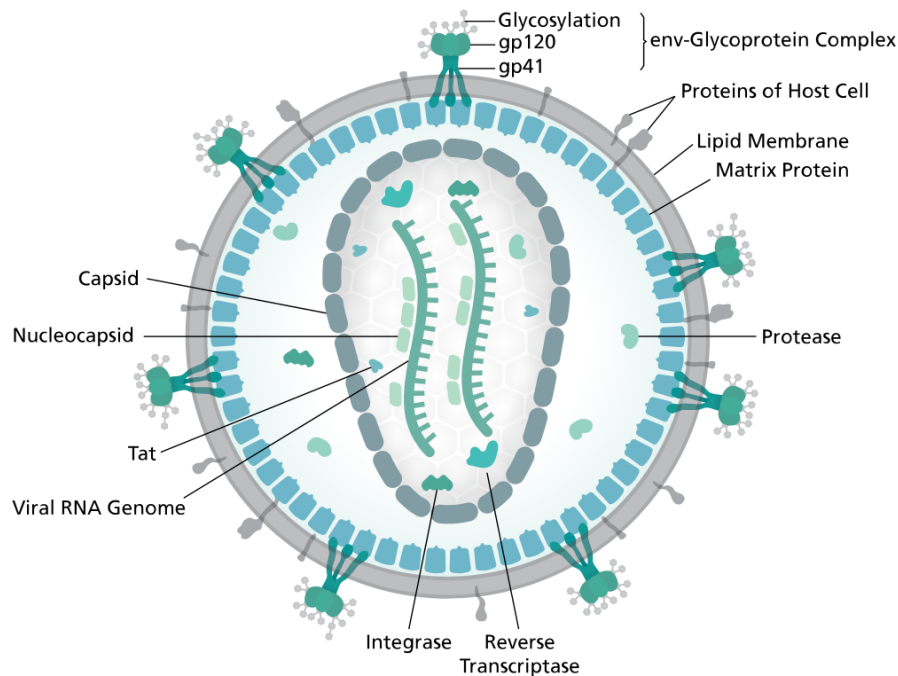
Figure 2. Structure of HIV. Adapted from Diagram of the HIV virion, 2014 by Thomas Splettstoesser (www.scistyle.com) [38].

The purpose of RNA dimerization has not been confirmed [39]. However, different hypotheses have been proposed. For example, this mechanism could allow the viral retrotranscriptase to switch RNA templates in order to rescue the genetic information following an encounter with a

damaged site [39]. It has also been proposed that this ability to switch could allow a higher frequency of recombination and thus an increase in genetic diversity [39].

The HIV genome of 9 kb includes 9 open reading frames (15 proteins) and long terminal repeats (LTR) at its ends, which contain important regulatory regions (Figure 3) [33]. The *gag*, *pol* and *env* genes encode for polyproteins: Gag produces the structural proteins (matrix/p17, capsid/p24, nucleocapsid/p7 and p6); Pol produces the enzymes (reverse transcriptase/p51, integrase/p32, RNase H/p15/p66, and protease/p10) and Env produces the glycoproteins which form the envelope (gp120 and gp41) [33]. The reverse transcriptase, which copies the single-stranded viral RNA into a double-stranded DNA, has an important role in immune evasion [40]. Reverse transcriptase does not have a corrective function and thus introduces a high level of mutations in the viral genome [40]. This, coupled with high-rate recombination between strains of HIV, generates more than 10 trillion different virions per day within a single host [41].
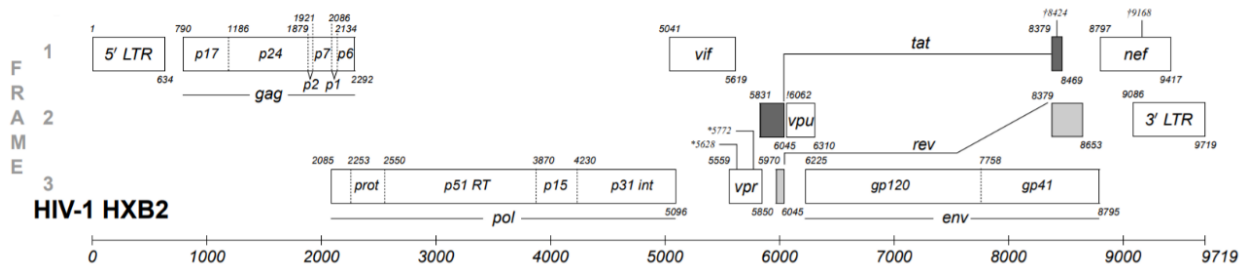
Figure 3. Mosaic structure of the HIV-1 genome (HXB2 Strain). Open reading frames are shown as rectangles [33].

The viral genome also codes for the regulatory proteins Tat (transcriptional transactivator) and Rev (regulator of expression of viral genes) and the accessory proteins Vif (viral infectivity factor), Vpr (viral protein R), Vpu (viral protein U) and Nef (negative regulatory factor) that play important roles in viral replication, viral dissemination and immune evasion [42].

1.1.4. Life cycle of HIV-1

The HIV-1 life cycle can be divided in two phases: early and late (Figure 4).

8
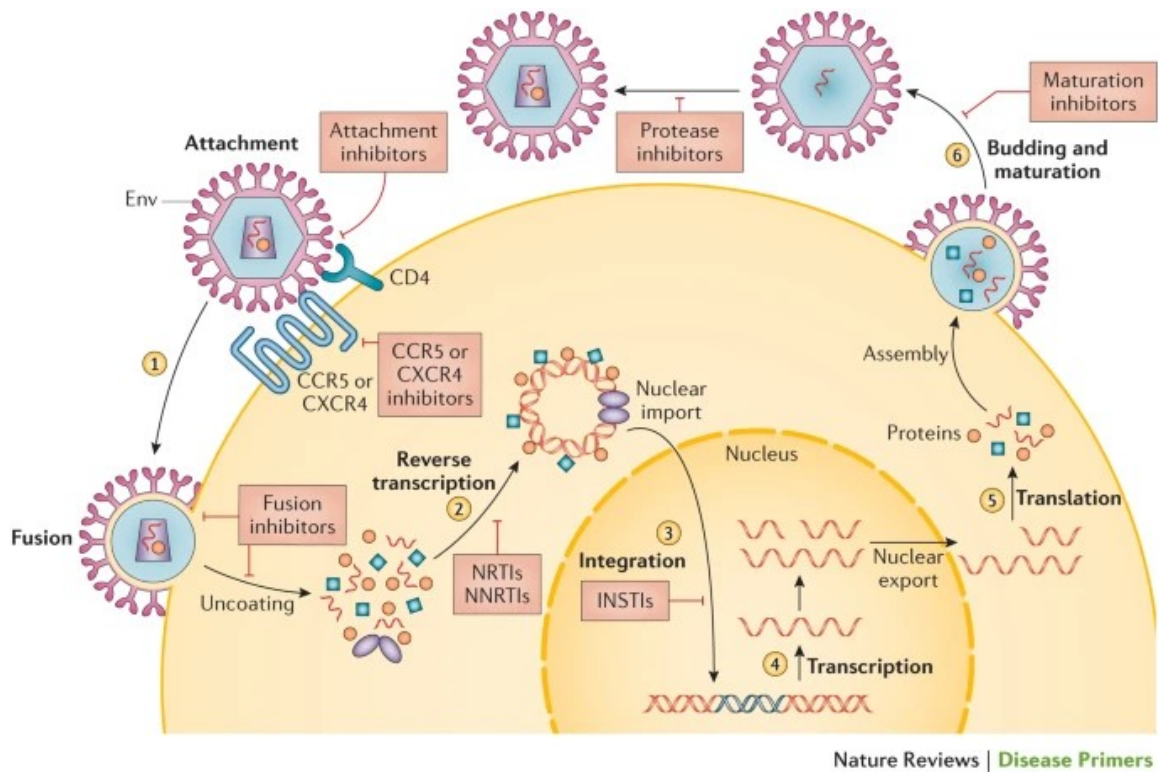
Figure 4. The HIV-1 life cycle. From Deeks, S. G., Overbaugh, J., Phillips, A. & Buchbinder, S. HIV infection [43].

In the early phase, the virus binds to the surface of the target cell via attachment of the viral gp120/gp41 glycoprotein complex to the primary cell receptor CD4 [44]. This is followed by an interaction between gp120 and the chemokine coreceptors CXCR4 or CCR5, which allows the fusion of the viral and cellular lipid membranes, and the entry of the nucleocapsid into the cytoplasm. Once inside the cell, the virus loses the capsid which results in the release of viral proteins and RNA into the cytoplasm. Reverse transcriptase can then transcribe the viral genome into a complementary double-stranded DNA which will be transported into the nucleus and incorporated into the cellular genome by viral integrase [44]. Notably, the integration sites can sometimes include genes associated with cellular proliferation or cancer which may contribute to the persistence of the viral reservoir [45].

The late phase includes the expression of the integrated proviral DNA, also called the provirus, and the assembly and release of new virions. This phase is regulated by both cellular and viral proteins [44]. As the virus mainly targets immune cells, a stimulus such as an infection will usually activate the host cell machinery and simultaneously allow the production of viral

proteins [44]. The initial activation of the provirus is mainly accomplished by NF-κB, a transcription factor which migrates to the nucleus following antigen recognition and binds to different promoters including HIV LTRs; this allows the production of primarily short transcripts [46, 47]. High level expression of full-length viral RNA is, however, induced by Tat [46, 47]. Rev will then promote the export of incompletely spliced viral RNAs into the cytoplasm where they can be translated [48]. The translated viral proteins will then assemble with full-length viral RNAs to form new virions that will bud off the surface of the cell, simultaneously acquiring a lipidic envelope containing both viral glycoproteins and a few cellular surface proteins [44]. The life cycle of HIV is completed when the viral protease cleaves the polyproteins and assures the maturation of virions into infectious particles.

1.1.5. Pathogenesis of HIV infection

1.1.5.1. How is HIV-1 transmitted?
A single HIV-1 virion is enough to establish infection [49]. The virus is transmitted primarily via sexual intercourse. Some transmission events have resulted from contaminated blood (transfusion or contaminated syringes) [49].

When it comes to children from 0 - 14, the great majority of HIV infections will occur via vertical transmission, meaning during gestation, childbirth or while breastfeeding. 15 to 45% of HIV-positive women will transmit the virus to their child during pregnancy [50]. However, this event becomes rare, below 1%, when mothers are treated with ART during and after pregnancy [50]. In 2020, 150,000 new infections among children were reported by UNAIDS [4]. A great improvement in comparison to the estimated 500,000 new cases back in 2001 and the 370,000 cases in 2009 [51].

1.1.5.2. After exposure: Viral tropism

HIV-1 mainly targets the cells of the immune system. Upon entry in the body of its host, HIV-1 will usually first encounter dendritic cells (DC) [52]. Infected DCs will then migrate to lymph nodes, thus transmitting the virus via cell-to-cell contact to naïve CD4+ T cells [52].

The chemokine receptors present on the surface of HIV-1 target cells determine viral tropism. R5 HIV-1 strains, present in the early stages of infection, will preferentially bind to CCR5 coreceptors found on macrophages, DC and effector memory CD4+ T cells [52-54]. As disease progresses, there may be a switch towards X4 strains or dual-tropic infection [54]. X4 variants are linked to a rapid progression to AIDS and are able to bind to CXCR4 expressed on naive CD4+ T cells and central memory T cells [54, 55].

1.1.5.3 Clinical phases of HIV-1 infection

Three clinical phases are observed. During the acute phase, which mainly involves R5 viral strains, a large number of virions are produced, causing a rapid decline in the number of CD4+ T cells, both at the mucosal and systemic levels [55, 56]. Following this decline, the immune system attacks and attempts to control viral replication, allowing levels of CD4+ T cells to recover [55]. The viral load will also drop and settle in what is called a viral setpoint, where viral replication is maintained at a relatively stable rate. With adults, this phase takes place 2 to 6 weeks post-exposure (PE) and patients may experience cold-like symptoms [55]. The chronic phase is long and largely asymptomatic [55]. Viral replication persists at low levels, whereas the number of CD4+ T cells gradually decreases to <500 T cells/mm^3 due to viral cytopathogenicity and as a resulting consequence of the effect of persistent immune activation on cellular proliferation and survival [57]. In this phase, uptake in X4 strains which migrate to the lymphoid tissues and infect T cells is observed [55, 56]. Treated patients can survive this chronic phase for several decades, depending on many individual factors such as age and effectiveness of treatment [55]. Untreated patients, however, will eventually progress to the last phase, 5 to 10 years post-exposure [58]. AIDS occurs when the immune system of the infected individual are defeated by the virus and degenerate to the point where the host becomes vulnerable to

opportunistic diseases, almost invariably leading to death in absence of treatment [55]. When the frequency of CD4+ T cells falls <200 cells/mm^3, viral replication is no longer controlled [55]. At this point, PLWH will survive for <3 years if anti-HIV treatment is not administered. [55].

The course of HIV-1 infection is different in vertically infected children. Indeed, in the absence of treatment, a faster and more intense progression of the disease is observed [58]. For the pediatric population, the median time to AIDS stage is 1 year PE and, in many cases, infected children die before the age of 2, before the viral setpoint is reached (Figure 5) [58]. Furthermore, studies on the effect of in-utero exposure to HIV-1 and treatment show that both HIV-1-exposed uninfected and infected children present higher morbidity and mortality rate compared to uninfected children [59]. They also present a higher risk of premature birth, impaired growth and poorer neurodevelopmental outcomes/cognitive abilities [59, 60]. As for the effect of treatment on children, studies show mixed results. Due to the challenges in finding treatment-naive HIV-1 infected children, it is hard to differentiate the effect of HIV-1 exposure from exposure to ART [60].
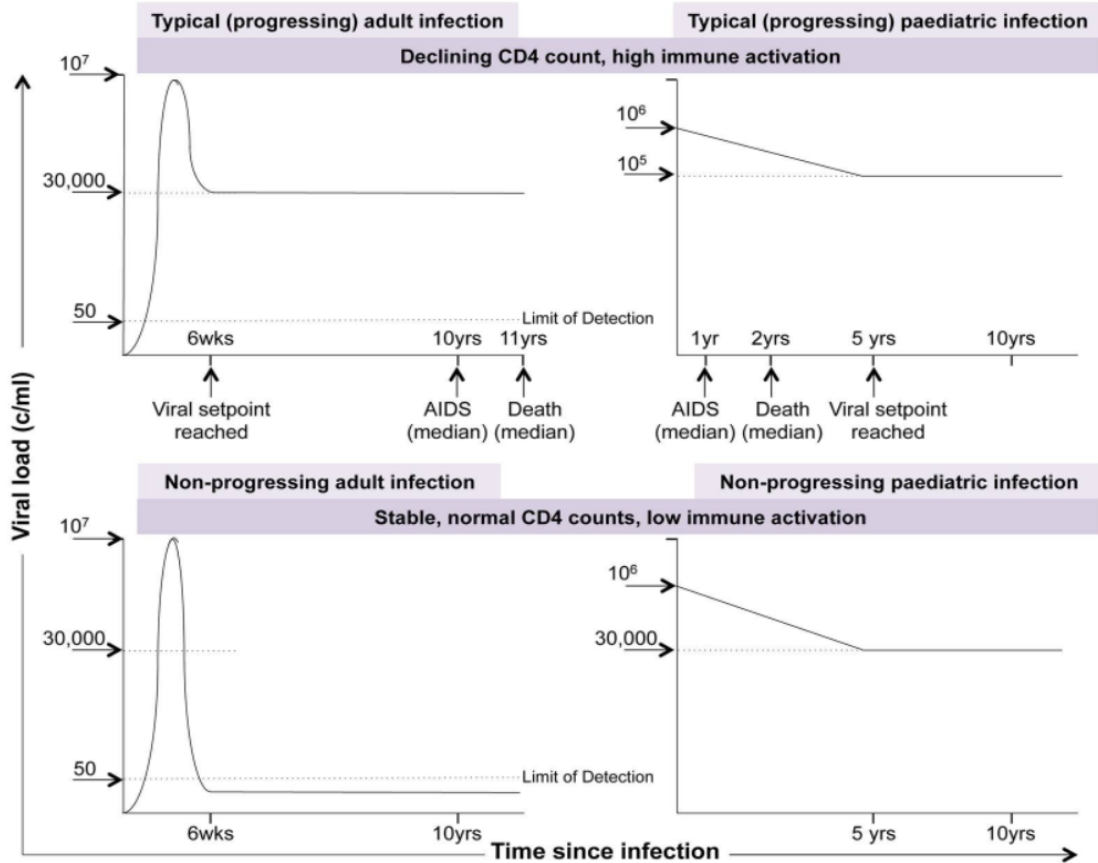
Figure 5. Evolution of viremia in pediatric cases compared to adult cases. Adults present a lower viral setpoint (30,000 copies/mL) that they reach in 6 weeks while children take longer (5 years) to stabilize viral load to a setpoint of 100,000 copies/mL [58].

1.1.5.4. How do we explain the differences observed between adults and children during the progression of HIV-1 infection?

Vertical transmission is relatively inefficient.

13 to 42% of HIV-infected mothers who do not receive ART will transmit the virus [61] with transplacental HIV transmission, which is associated with elevated inflammatory cytokines and chemokines in the placenta, being the least efficient [62, 63]. Most transmissions occur in the last weeks of pregnancy and the mechanism by which this transpires is poorly understood [64]. However, transplacental microtransfusions of maternal lymphocytes is one of the hypotheses [65, 66].

The low transmission rate in comparison to other transmission routes is most probably a combination of different factors. First, most fetal cells are quiescent whereas HIV prefers activated cells [64]. Additionally, the crossing of maternal cells over the placenta induces the development of fetal CD4+CD25highFoxP3+ regulatory T cells (Tregs) that suppress antimaternal immune response [67, 68]. Finally, maternal immunoglobulin G (IgG) anti-HIV antibodies are transferred in the 3rd trimester [69, 70] and can assist in viral control and as well as enhance B cell responses, as shown in infant macaques, by accelerating the development of neutralizing antibodies [71].

Transmission of a "Veteran-Type" pre-adapted virus.

In some cases, the developing immune system of infected children is exposed to a "veteran" ART-hardened virus with ample experience in overcoming their mother's immune system and pre-adapted to T-cell responses [58] The obligate presence of shared HLA alleles between mom and baby may also fortify this effect [72, 73]

The developing immune system.

The immune system of children generates a response that is qualitatively and quantitatively different from adults and continues its development until adolescence [64]. The function and number of innate immunity cells are moderate at the beginning of life compared to later in life. A sacrifice that enables the fetus to tolerate his mother's antigens [74].

The thymus, which plays a vital role in the training and development of T cells, is largest in the first years of life [74]. This is coupled with a lager frequency of CD4+ T cells that decreases with age [64]. Seeing that these cells are the preferred targets of HIV, it is important to understand their development when studying HIV infection in children. The frequency of CD4+ T cells subsets changes with age and differs from person to person. For example, naïve cells represent 86% of the CD4+ T cell pool in infants and merely 46% in adults. For central memory (TCM) and effector memory (TEM) T cells, the opposite correlation is observed, with TCM representing 13% in infants vs 42% in adults and TEM constituting 0.052% vs 5% [75]. In utero, the fetal immune system must be tolerant to the mother. Thus, naïve CD4+ T cells preferably adopt a Treg fate in response to maternal alloantigens [74]. These cells persist after birth, making early-life adaptive

immunity tolerogeneic and poorly responsive to foreign antigen. Babies also present a higher population of unconventional γδ T cells which can produce significant amounts of IFN-γ and act against infectious agents [76].

Abnormalities in the immune system of infected children.

The main abnormalities are as follows: decreased T-cell function and restricted development of immune cells, increased differentiation of Treg and Th2 cells, decreased cytokine production, decreased natural killer cell antibody-dependent cellular cytotoxicity [77] and poor stimulation of B cells [64]. Soon after birth, it is possible to notice increased immune activation which correlates with increased viral replication [64]. This is followed by CD4+ T cell depletion caused by the cytopathic effect of the virus and the host immune response that targets HIV-infected cells [75]. Moreover, a massive depletion of Th17 cells can be seen in the intestinal mucosa, causing an altered integrity of the epithelium which leads to microbial translocation [78-80]. This depletion of cells in the gastrointestinal tract is a critical early event in HIV-1 pathogenesis in adults, hinting at the importance of the gut as an important site of viral replication in infants as well [64].

1.2. Antiretroviral therapy

The first antiretroviral inhibitor zidovudine or azidothymidine (AZT) was introduced as a treatment in 1987 [81]. The drug was initially used in cancer treatment but was later found to be somewhat effective in inhibiting HIV replication [81]. However, this drug, along with the others used individually around that time, was ineffective in the long-term, triggered sometimes severe side-effects and most patients didn't survive very long [81]. Since then, much was accomplished in treatment development. Nowadays, ART has turned the infection into a chronic, manageable disease and significantly lengthened the life expectancy of those infected [82].

1.2.1. Antiretroviral inhibitors

Antiretroviral agents suppress HIV-1 replication by targeting different key elements of the HIV life cycle [82]. They are separated into different classes depending on their mechanism of action: CCR5 antagonists bind to CCR5 and prevent viral entry into target cells; fusion inhibitors (FI) block the fusion of viral and cellular membranes; nucleoside reverse transcriptase inhibitors (NRTIs) and non-nucleoside reverse transcriptase inhibitors (NNRTIs) target the viral reverse transcriptase; integrase strand transfer inhibitors (INSTI) block the integration of HIV in the cellular genome; and finally, protease inhibitors (PI) targets the viral protease, thus preventing virion maturation (Table 1) [82].

Table 1. Classification of antiretroviral drugs [82]

Mechanism of action	Commonly used drugs
Fusion inhibitor (FI)	Enfuvirtide
Nucleoside reverse transcriptase inhibitors (NRTI)	Lamivudine, Tenofovir, Abacavir, Didanosine, Zidovudine, Emtricitabine
Non-nucleoside reverse transcriptase inhibitor (NNRTI)	Efavirenz, Nevirapine, Rilpivirine, Delavirdine
Integrase strand transfer inhibitor (INSTI)	Dolutegravir, Raltegravir, Elvitegravir
Protease inhibitor (PI)	Darunavir, Atazanavir, Indinavir
Chemokine receptor antagonist (CCR5 antagonist)	Maraviroc

* Adapted from Deeks, S. G., Overbaugh, J., Phillips, A. & Buchbinder, S. HIV infection. Nat Rev Dis Primers 1, 15,035 (2015). https://doi.org/10.1038/nrdp.2015.35

In 1995, with the introduction of the first PI, combination ART (cART) was born in which two or more antiretroviral drugs are prescribed [83]. This provides a powerful attack against HIV and prevents new cells from being infected, allowing PLWH to live longer and healthier lives. It also reduces the incidence of viral transmissions by maintaining viremia to undetectable levels [84, 85]. Furthermore, cART provides the advantage of lowering the emergence of drug resistance [82]. It also played a major role in HIV prevention, with the development of PrEP, which combines two HIV inhibitors in a single once-daily pill, and post-exposure prophylaxis (PEP), a

combination of three inhibitors taken within 72 hours post HIV-exposure and daily for the following 28 days [86].

The choice and dosage of cART varies from patient to patient, as it can be influenced by multiple factors such as age, weight, disease progression (CD4+ T cell counts and viral load), side effects, acquired drug resistance or the presence of other diseases or conditions. Most treatments will combine two NRTIs and a third inhibitor with a different mechanism of action, such as an INSTI, an NNRTI, or a boosted PI [87]. NRTIs were the first class of inhibitors to be approved for treatment. They are effective, less expensive and are shown to be safe for both adults and children [88].

For adults, including pregnant women, and adolescents ≥12 years old, the most common combination include Abacavir/Lamivudine (ABC/3TC) combined with the widely used Dolutegravir (DTG) [87, 89, 90]. For children aged ≥4 weeks and <12 years old, the preferred NRTI combinations are Emtricitabine (FTC) and Tenofovir (TAF) combined with DTG [91]. Newborns, on the other hand, are either given infant PEP, Zidovudine (ZDV), for 4 weeks after birth, when there is a low risk of perinatal acquisition of HIV or administered a presumptive HIV therapy including ZDV/3TC and Nevirapine (NVP) in higher risk settings [91].

Taking daily medication for a long period of time can sometimes prove to be a challenge for PLWH. In recent years, multiple studies on long-acting treatments have been initiated in order to develop a more practical yet effective solution for medication intake. Candidates for these regimens include, for example, Lenacapavir (GS-6207), a capsid inhibitor which can be taken once every six months and Ibalizumab, an antibody used in cases of multi-resistance, which can be administered through intravenous infusion on a weekly basis [92, 93]. For the first time in 2021, we saw the approval of a long-acting regimen, called Cabenuva, in Europe, the United Kingdom, the United States, Canada, and Australia. This injectable medication combines Cabotegravir (an INSTI) and Rilpivirine (an NNRTI) and can be administered once a month or every two months [94]. These alternative treatments could greatly help PLWH to improve their adherence to treatment and thus offer them a better control of the infection.

1.2.2. HIV treatments are not a cure.

cART cannot eliminate HIV and interruption of therapy will usually cause viremia to rebound [95]. Persistence of the virus in cellular and anatomical reservoirs and its ability to escape the immune system are the main reasons [96]. Indeed, HIV is able to integrate in the cellular genome and maintain itself in a state of dormance until reactivation of the infected cell [55]. The virus also tends to hide in immunological sanctuaries that are beyond the reach of HIV inhibitors, such as the central nervous system [55].

To date, only two people are known to have been cured of HIV: the Berlin patient and the London patient [97-99]. Both patients had a form of blood cancer and required a bone marrow transplant. But rather than choosing any donor, they received stem cells transplanted from donors presenting a homozygous CCR5Δ32 mutation. After a few months, T cells circulating in those patients no longer expressed CCR5 at the cell surface and *in vitro* HIV infection of those cells could not be accomplished. The transplant essentially provided them with a new and resistant immune system against HIV infection [100-102]. However, a bone marrow transplant is an arduous and perilous procedure that demands life-long follow-up, and thus, it is not a practical strategy for HIV cure.

Many strategies are currently being developed with the goal of eradicating the virus from its infected host. First, the "shock and kill" strategy is based on the reactivation of infected cells using latency reversing agents (LRA), such as NF-κB or protein kinase C (PKC) agonists. This is followed by the destruction of the infected host cells by viral cytopathic effects or the antiviral immune response [40]. Another strategy is the "block and lock", which aims to firmly block the reactivation and replication of HIV using latency-promoting agents (LPA) such as inhibitors of NF-κB or NFAT [103].

1.3. Reservoir

1.3.1. Where is the viral reservoir?

In adults not treated with ART, the reservoir consists mainly of short-lived activated CD4+ T cells with a half-life around 0.7 days [104]. Under ART, the long-lived memory CD4+ T cells (T stem cell memory (TSCM), TCM, T transitional memory (TTM) and TEM) are the main targets of HIV-1, with each subset contributing differentially to the reservoir pool and presenting varying levels of HIV activity and proportion of inducible proviruses [105]. CD4+ TCM are the long-lasting and low-proliferative contributors to the reservoir under effective ART. They contain the highest levels of integrated HIV DNA and the higher proportion of replication-competent proviruses amongst the different subsets [105]. CD4+ TTM, characterized by persistent immune activation, are the main reservoir in individuals with low CD4+ counts [105]. The composition of the reservoir can also vary depending on treatment initiation. If treatment is initiated well into the chronic phase, the cell reservoir is mainly made up of TCM and TSCM CD4+ T cells [105, 106]. In an early treatment initiation setting, TTM CD4+ cells predominate [105, 106].

The HIV reservoir in children is not well characterized. Since their proportions of CD4+ T cell subsets is different compared to adults, it is fair to think that the reservoir could be found in different compartments [58]. A study by Mavigner et al. where they measured virus persistence in blood and tissues after 6 to 9 months under ART in antiretroviral therapy-suppressed infant rhesus macaques showed a high contribution of naïve CD4+ T cells to the viral reservoir compared to what is observed in adult macaques [107].

HIV is also capable of persisting in multiple anatomical reservoirs spread throughout the body. The virus resides mostly in lymphoid tissues (lymph nodes and spleen) and the gastrointestinal tract but can also be detected in the liver, bone marrow, nervous system, lungs, kidneys, male and female reproductive tract, placenta, skin and adipose tissues [108]. Theses different sites vary in terms of the distribution of infectable cells types and thus contribute to the complexity of the viral reservoir [108].

1.3.2. How does the cellular reservoir persist in infected patients?

HIV uses a variety of mechanisms in order to persist in its host [104]. The major mechanism is through IL-7 mediated homeostatic proliferation of infected memory CD4+ T cells as a response to CD4+ T cell depletion [105, 109]. In addition to this, the long-lasting characteristics of these cells indirectly provide stability to the viral reservoir. Another mechanism is antigen driven proliferation, which can occur when there is reactivation of the infected immune cell, for example following an opportunistic infection [104]. There is also the openly debated mechanism of persistent viral replication. This is based of the fact that many patients will show transient episodes of detectable viremia under effective and suppressive ART. Some studies argue that this illustrates the phenomenon of low-level residual viral replication, which allows the virus to replenish the reservoir [110]. These findings remain controversial, as many studies were not able to find evidence of this mechanism [111].

1.3.3. Evolution of the HIV reservoir

In adults, the HIV reservoir is established very early in the acute phase of the infection. A study by Whitney et al. on adult rhesus monkeys showed a rapid seeding of the reservoir that occurred as early as 3 days post infection [112]. There is a rapid decay of HIV-1 DNA in the blood during the first 4 years following the initiation of treatment [113]. After that period, the slope plateaus, regardless of determinants such as regimens, immune activation, and age. Different factors such as the nadir CD4+ T cell count [114] and the initial HIV DNA level [113] are predictors of the evolution of reservoir size: A high CD4 nadir and low HIV DNA level at baseline usually reflect a low reservoir establishment. The initial HIV-1 DNA decay is faster in children. This is shown in the study of Veldsman et al., who also demonstrated by quantifying total cellular HIV-1 DNA and RNA in infants where early ART initiation occurred that 27% (3/11) of these children became undetectable after 6 days to 4 months on treatment [115]. Of the remaining 8 children, 7 of them presented fewer than 10 copies/million PBMCs within 13 months after birth [115].

1.3.4. Measurement of the viral reservoir

The HIV reservoir is complex to say the least. It is widely spread-out in different organs of the host, as HIV can integrate its genome in various cells types [116]. Accurate characterization of the HIV reservoir is necessary to assess and demonstrate the efficacy of treatment regimens, eradication strategies or a potential cure [116]. Many techniques were developed over the years to measure the viral reservoir, each targeting different aspects of the viral reservoir (Figure 6)
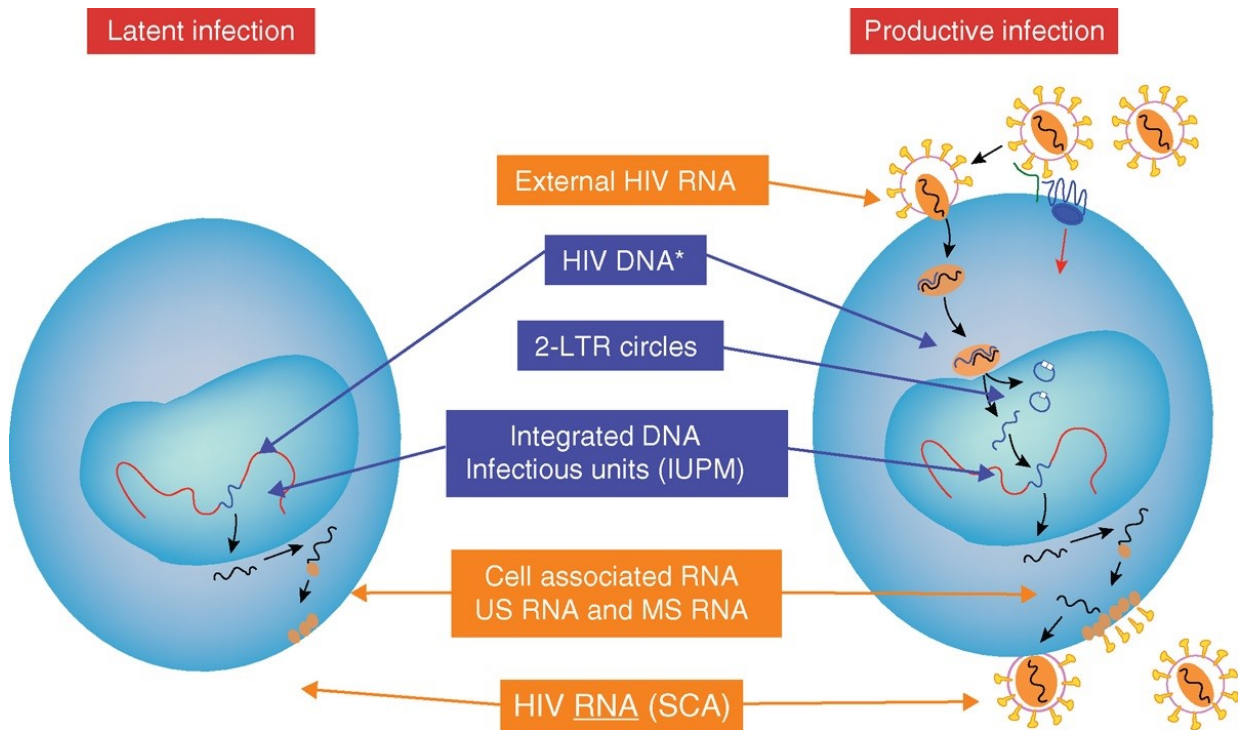
Figure 6. Quantification tests to measure the HIV-1 reservoir. Latently infected cell (left) and productively infected cell (right). HIV RNA (orange boxes and arrows) and HIV DNA (blue boxes and arrows). From Lewin and Rouzioux, 2011 [117].

The quantitative viral outgrowth assay (QVOA) is considered as a "gold-standard assay" for quantifying the HIV-1 reservoir. It is a co-culturing method used to stimulate viral replication in infected CD4+ T cells and to measure replication competent virus [96]. This technique is, however, difficult, long, expensive, requires large amounts of blood and can be imprecise [117].

Total HIV-1 DNA is a widely used marker for its clinical implications as it has a highly predictive value for disease progression [118]. The total HIV-1 DNA assay is a quick and easy technique that measures different forms of HIV-1 DNA in infected cells that can produce competent or defective virus [96, 119]. The reverse transcription of the viral RNA generates linear double-stranded cDNA, which is processed in an appropriate form which can be integrated into the cellular genome. This pathway generates multiple forms of DNA be they integrated, such as the proviral DNA, or unintegrated, such as the linear cDNA and the two forms of LTR circular viral DNA that results from its processing [120].

The total DNA assay overestimates the replication-competent reservoir which is, on the other hand, underestimated by the QVOA assay [120, 121]. To develop and accurately evaluate eradication strategies, it is important to be able to quantify the pool of cells harbouring replication-competent proviruses. Other potential candidates are viral induction assays for their capacity to measure the inducible reservoir [122]. They consist of stimulating infected cells, more commonly CD4+ T cells, which leads to viral RNA production that can be measured in cellular extracts or culture supernatants [122]. The different inducing agents include anti-CD3/CD28 antibodies, phorbol 12-myristate 13-acetate (PMA) and ionomycin, or LRA such as prostratin [122, 123]. This technique is, however, not without its limitations. Like the QVOA, it may underestimate the level of inducible viral genome, as only one round of stimulation is executed. Also, the primers used in quantitative PCR may not recognize all subtypes of HIV-1. In any case, the method is more sensitive, less costly, faster and provides an increased dynamic range over QVOA assays [124].

None of the known measurement techniques is considered the "best". To draw an accurate picture of the viral reservoir in an infected patient, it is critical to use multiple methods simultaneously.

1.4. RATIONALE, HYPOTHESES AND OBJECTIVES

The Early Pediatric Initiation: Canada Child Cure Cohort (EPIC[4]) regroups 228 children vertically infected by HIV-1 and under antiretroviral therapy and is the largest pediatric HIV cohort in Canada. The main objectives of the multicentric project, which ran from to 2015 to 2019, were to study the size of the viral reservoir at different time points and in different cell subsets and determine the presence and level of markers of immune activation, tissue inflammation, microbial translocation, and endothelial dysfunction. The research in this master's project falls within the EPIC[4] study and is divided into two distinctive parts. In the first part, we studied the HIV-1 clade of the remaining 64 participants of the cohort whose HIV-1 clade previously remained unknown, either due to an absence of prior genotyping and/or SVS. In the second part, we investigated the size of the viral reservoir in a different selection of 67 participants.

FIRST STUDY: Phylogenetic study of HIV-1 isolates.

The ever-expanding diversification of HIV is the result of an extremely high mutation rate of $(4.1 \pm 1.7) \times 10\text{-}3$ per base per cell and the selective pressure exerted by the immune system [22, 125]. This genetic diversity has been suggested to have impacts on the transmission rate, HIV disease progression, response to therapy and drug resistance [28, 126]. For example, some groups have reported that infections by subtypes C and D progressed more rapidly and aggressively, and that some non-B subtypes seemed to develop drug resistance easier [24].

The genetic complexity of the pandemic continues to increase as time moves on. The increase of non-B infections in previously B-predominant regions, the rising number of CRFs and the new HIV-1L all link to an increase in coinfections and superinfections [30]. This could easily become an issue as the majority of treatment and vaccine studies and advancement have been catered to subtype B, as this subtype is predominant in developed and wealthier countries [22]. Thus, considering the far-reaching impacts this has on phylogenetic reconstructions, on ensuring that treatments and diagnostic testing remain effective and up-to-date, and most importantly on

vaccine development, it is clear that epidemiologic surveillance and the study of dynamic changes in HIV-1 subtypes are of high importance [30, 126, 127].

HYPOTHESIS 1. HIV-1 can be isolated and genotyped from young and vertically infected patients even after long-term SVS and cART.

OBJECTIVE 1. Amplify the HIV-1 *gag* gene from PBMC samples using a nested PCR and sequence isolated clones. By analysing the phylogenetic relationship between the recovered sequences and references of HIV-1 subtypes, we will determine the viral subtypes that are infecting our study participants.

SECOND STUDY: HIV-1 reservoir study.

Many cases of long-term remission were observed in children [128-137]. The most mediatized case is the Mississippi Baby back in 2013 [133, 134]. The little girl received cART 30 hours after birth and her treatment was maintained for 18 months [133]. Then, she stopped receiving treatment and yet was able to remain HIV-undetectable for 27 months before the virus resurfaced [133]. Other examples include the French Teenager and the South African Child, who controlled viral replication without drugs for more than 8 years [130, 137].

Although these cases illustrate the challenges of eradicating HIV, they reinvigorated the efforts to find a functional cure that would allow patients to bypass lifelong ART and the potential immunological consequences entailed by long-term HIV-infection. They have also taught us important lessons. First, it seems that the faster a patient reaches virological control, the lower is the size of their viral reservoir [138]. Also, the earlier the treatment is initiated, the better [128]. Some studies on long-term suppressed prenatally infected children show that early treatment initiation results in reduced morbidity and mortality, in low levels of replication-competent provirus, an absence of HIV-specific immunity, a significantly reduced reservoir and the capacity to generate immune responses to immunotherapeutic interventions [139].

The HIV-1 reservoirs in children, however, still remains poorly characterized in terms of their composition and their dynamics.

HYPOTHESIS 2. The size and evolution of the HIV-1 reservoir in children and adolescents is influenced by age, maintenance of SVS, and early initiation of cART.

OBJECTIVE 2.A. Measure the size of the viral reservoir in a group of children and adolescents infected with HIV-1 who have been treated with cART and in whom SVS has been fully or less fully achieved.

OBJECTIVE 2.B Analyze the evolution of the reservoir between infancy, childhood and adolescence.

CHAPTER 2 – MATERIAL AND METHODS

2.1. Phylogenetic study of HIV-1 isolates

2.1.1. Study subjects

We obtained blood samples from 67 participants of the Early Pediatric Initiation, Canada Child Cure Cohort Study (EPIC[4]), whose HIV-1 subtype remained unknown due to low levels of the virus in the samples. EPIC[4] study was conducted from 2015 to 2019 and regrouped 228 vertically HIV-infected children and adolescents recruited across 9 pediatric clinical centers all over Canada [CHU Sainte-Justine (Montreal); Montreal Children's Hospital (Montreal); Hospital for Sick Children (Toronto); Children's Hospital of Eastern Ontario (Ottawa); Stollery Children's Hospital (Edmonton); BC Women's Hospital and Health Center of British Columbia (Vancouver); McMaster Children's Hospital (Hamilton); Royal University Hospital (Saskatoon)]. Written informed consent was obtained from the parents or legal guardians of all participants. The study protocol was approved by institutional review boards for ethics at each of the participating institutions.

2.1.2. Sample preparation

PBMC were separated from whole blood by density centrifugation using Leucosep tubes (Greiner Bio-One, Germany) and then cryopreserved in liquid nitrogen until use. Frozen PBMC were thawed in a 37 °C water bath and emptied in a tube containing warm fetal bovine serum (FBS) (Wisent BioProducts, Canada). RPMI medium (Wisent BioProducts, Canada) was then slowly added to the suspension. After centrifugation [1'500 RPM, 15 min], the pellets were resuspended in supplemented RPMI (RPMI + 10% FBS + 1% Gentamicin) and cell count was determined by Trypan Blue staining. Cell suspensions were subsequently split into aliquots of 1×10^6 cells and, after centrifugation [12'000 RPM, 5 min], the supernatant was discarded and the final pellet was resuspended in a lysis buffer containing 10 mg proteinase K per mL (Thermo Fisher Scientific, USA), Tris HCl [0.1 M, pH 8] and KCl [0.5 M]. An appropriate volume of lysis buffer was added to have a maximum of 5'333 cells/µL. Cells were then incubated overnight at 55 °C, after which proteinase K was inactivated at 95 °C for 10 minutes.

2.1.3. Amplification of the HIV-1 *gag* gene by nested PCR

Amplification reactions were performed with 15 μL of sample lysate in a 50 μL reaction volume using the *Taq* PCR Master Mix kit (QIAGEN, Netherlands) which includes 2.5 units of *Taq* DNA Polymerase, 1X PCR Buffer, 1.5 mM $MgCl_2$ and each dNTP at 200 μM. Primers pairs at 0.6 μM were added to the mixture. Both primers pairs were designed to match the DNA sequence at either end of the *gag* gene. For the first round PCR, the primers we used were P17-out1 (5'-TCT CTC GAC GCA GGA CTC GGC TTG CTG-3', sense, nucleotide position on HIV-1 HXB2 682 → 708) and P17-out2 (5'-TAA CAT TTG CAT GGC TGC TTG ATG TCC-3', antisense, 1392 → 1366). Amplification conditions consisted of 30 cycles of 94 ℃ for 30s, 60 ℃ for 45s and 72 ℃ for 1 min; followed by a final cycle of 72 °C for 10 min. PCR reactions were run on a Biometra PCR T Gradient thermocycler (MBI, Canada). The first-round PCR product was diluted 1:10 and 15 μL of the dilution was used for the second amplification. The primers used in second-round PCR were P17-in1 (5'-CTA GAA GGA GAG AGA GAT GGG TGC GAG-3', sense, 776 → 800) and P17-in2 (5'-CTT GTG GGG TGG CTC CTT CTG ATA ATG-3', antisense, 1336 → 1310). Amplification cycles were identical to first-round PCR. A participant whose HIV-1 subtype was known was used as a positive control (participant 01-005-DQS) and negative controls (water instead of template) were added at every PCR to very absence of contamination.

2.1.4. Purification of PCR products

20 μL of the final products of both rounds of PCR were separated by electrophoresis in a 1% agarose gel (1X TAE, 135 V, 80 min) supplemented with GelRED (Biotium, USA) at 0.1 μL per mL. The amplified 711bp and 561bp fragments of respectively the first and second round of PCR were then cut from the gel under UV light and purified through a silica membrane using GE Healthcare illustra™ GFX™ PCR DNA and Gel Band Purification Kit (Thermo Fisher Scientific, USA). Each fragment was cut from the gel using a different razor so to avoid cross contamination during extraction.

2.1.5. Cloning, transformation and plasmid extraction

Molecular cloning was used to separate the multiple *gag* gene variants present within each participant. Cloning was executed using the TOPO® TA Cloning® Kit for Sequencing. First,

purified *gag* amplicons were subcloned into the pCR™ 4-TOPO® vector (Thermo Fisher Scientific, USA) and then used to transform One Shot™ TOP10 Chemically Competent *E. coli* (Thermo Fisher Scientific, USA). All bacterial cultures were grown overnight on LB plates containing ampicillin at 100 µg/mL and X-GAL (Wisent BioProducts, Canada) at 100 µg/mL. The vector contains an ampicillin resistance gene and *lacZα-ccdB* gene fusion which allows selection of recombinant. The product of the *ccdb* gene kills bacteria by interfering with genome replication [140]. Successful ligation disrupts the expression of the *lacZα-ccdB* gene fusion, permitting the growth of positive recombinants [140]. The pUC19 plasmid included in the kit was used as a positive control for transformation.

For each participant, 3 recombinant colonies were selected and cultured overnight in 3 mL of LB supplemented with ampicillin (100 µg/mL). Cloning vectors were extracted from transformed *E. coli* clones using QIAprep membranes in the QIAprep Spin Miniprep Kit (QIAGEN, Netherlands) according to the manufacturer's instructions.

2.1.6. Restriction analysis

The presence of correctly sized inserts in recombinant plasmids were verified by enzymatic digestion using FastDigest EcoRI (Thermo Fisher Scientific, USA), which recognizes two sites on either side of the insertion site on the pCR4-TOPO vector. Following digestion, we obtained two DNA fragments by electrophoresis (1% agarose gel): the 560 bp *gag* fragment and the linearized vector at 3.9 kb.

2.1.7. Sequencing of HIV-1 *gag* gene fragments

The purified, plasmid recombinant vectors were sent to the Plateforme de séquençage et de génotypage du CHUL (Quebec, Canada) for sequencing, which was performed using the Sanger technique on an ABI 3730xl DNA Analyzer (Thermo Fisher Scientific, USA).

2.1.8. Phylogenetic analysis and HIV-1 genotyping

The Sequence Locator web tool (Los Alamos National Laboratory, USA) was used to locate the *gag* gene sequences on the genome of the HIV-1 reference strain, HXB2 (Subtype B, France,

1983) [141]. Sequences fragments were edited, assembled and aligned using MEGA 11 [142]. Reference *gag* sequences for all HIV-1 subtypes were downloaded from the LANL database. Sequences included group M, N, O and P and 118 CRFs. Reference sequences were aligned with our *gag* gene sequences using the Clustal W tool embedded in MEGA 11 and manually adjusted [143]. Phylogenetic trees were built with using the Neighbour-Joining method with bootstrap analysis (1 000 replicates) and rooted on a SIVcpz reference sequence [141, 144, 145]. Subtyping was based on reliable groupings with reference sequences (bootstrap value >70%).

2.2. HIV-1 reservoir study

2.2.1. Study subjects

PBMCs were obtained from 67 participants of the EPIC[4] study. Blood samples along with clinical and laboratory data (e.g., country of origin, HIV-1 subtypes, viremia, age at initiation of first ART, time under effective treatment, absolute and relative CD4+ and CD8+ T cell counts, etc.) were collected every 3 months. Study participants were stratified in 9 groups according to their age (<6, 6–10, and >10 years of age) and their control of viral replication (sustained viral suppression, [SVS]; "blips" in viremia, [BLIPS], and without SVS, [No SVS]).

2.2.2. Sample preparation

Whole venous blood from participants was separated by density gradient centrifugation using Leucosep tubes (Greiner Bio-One, Germany) into plasma, serum and PBMC, which were cryopreserved in liquid nitrogen until use. Frozen PBMC were thawed in a 37 °C water bath and transferred into a tube containing warm FBS (Wisent BioProducts, Canada). RPMI medium (Wisent BioProducts, Canada) was then slowly added to the suspension. After a centrifugation cycle (1'500 RPM, 15 min), pellets were resuspended in 15 mL of supplemented RPMI (RPMI + 10% FBS + 1% Gentamicin) and cell count was determined by Trypan Blue staining. The cell suspension was subsequently split into one aliquot of 0.5 x 10^6 cells for HIV-1 DNA quantification and one aliquot containing the remaining cells to be used in the prostratin stimulation assay (see below).

2.2.3. DNA extraction and quantification of total HIV-1 DNA

After centrifugation (12'000 RPM, 5 min), the supernatant was discarded and the cell pellet was resuspended in a lysis buffer containing 10 mg proteinase K per mL (Thermo Fisher Scientific, USA), 0.1 M Tris HCl pH 8 and 0.5 M KCl. The appropriate volume of lysis buffer was added to obtain a maximum of 5'333 cells/µL. The cells were then incubated overnight at 55 °C, after which proteinase K was inactivated at 95 °C for 10 minutes.

The PCR protocol used was developed by Vandergeeten et. al and adapted to run on a LightCycler® 96 (Roche, Basel, Switzerland) [146]. In each assay, two pairs of primers allow the simultaneous amplification of HIV-1 DNA (1 copy per cell) and CD3 epsilon gene (2 copies per cell). This procedure was optimized to allow the precise quantification of levels of total HIV-1 DNA from subtypes A, B, C, D and CRF01_AE.

First-round PCR (pre-amplification) was performed with 15 µL of sample lysate in a 50 µL reaction volume containing 2.5 U Taq DNA polymerase, 1X PCR Buffer and 1.5 mM $MgCl_2$ using the Taq DNA Polymerase kit (Thermo Fisher Scientific, USA). To this mixture was added each dNTP at 300 µM and primers at 300 nM. The CD3 primers were HCD3out5' (5'-ACT GAC ATG GAA CAG GGG AAG-3') and HCD3out3' (5'-CCA GCT CTG AAG TAG GGA ACA TAT-3'), and the HIV primers were ULF1 (5'- ATG CCA CGT AAG CGA AAC TCT GGG TCT CTC TDG TTA GAC -3', nucleotide position on HIV-1 HXB2 452 → 471) and UR1 (5'-CCA TCT CTC TCC TTC TAG C-3', 793 → 775). Amplification conditions consisted of a denaturation cycle of 95°C for 10 min, followed by 12 cycles of 95°C for 60s, 55°C for 40s and 72°C for 60s, and a final elongation cycle of 72°C for 15 min. The first-round PCR product (360 bp for HIV) was diluted 1:10 and 6.4 µL of the dilution was used in the second round of amplification for a total reaction volume of 20 µL.

For the second-round PCR (Real-time PCR), we used the PerfeCta qPCR ToughMix Low ROX 1X (QuantaBio, Beverly, Massachusetts, USA), primers at 1 250 nM and a probe at 100 nM. For the CD3 gene reaction mixture, internal region primers were HCD3in5' (5'-GGC TAT CAT TCT TCT TCA AGG T-3') and HCD3in3' (5'-CCT CTC TTC AGC CAT TTA AGT A-3'), and the CD3 FamZen

probe was 5'-/56-FAM/AG CAG AGA A/ZEN/C AGT TAA GAG CCT CCA T/3IABkFQ/-3'. For HIV, the primers were LambdaT (5'-ATG CCA CGT AAG CGA AAC T-3', [phage-specific heel sequence]) and UR2 (5'-CTG AGG GAT CTC TAG TTA CC-3', 583 → 602), and the UHIV FamZen probe was (5'-/56-FAM/CA CTC AAG G/ZEN/C AAG CTT TAT TGA GGC /3IABkFQ/-3'). The reaction conditions were: one denaturation cycle of 95℃ for 4 min and 40 cycles of 95℃ for 10s and 60℃ for 20s. The size of the resulting HIV fragment is 169 bp.

A standard curve based on extracts from ACH-2 cells was prepared for each reaction and allowed the determination of the number of HIV-1 copies [147]. ACH-2 cells derive from a human T cell line of lymphoblastic leukemia and harbour 1 copy of integrated HIV proviral DNA (LAV strain/HIV-1 Bru) per cell [147]. Negative controls (water instead of DNA template) were added in every experiment to monitor potential contamination.

2.2.4. CD4+ T cell isolation

CD4+ T cells were isolated from PBMC using immunomagnetic negative selection with the EasySep™ Human CD4+ T Cell Isolation Kit (STEMCELL Technologies, Vancouver, Canada) according to the manufacturer's instructions. The purity of enriched CD4+ T cells was >93%, as assessed by flow cytometry.

2.2.5. Prostratin stimulation assay

Purified CD4+ T cells were counted using Trypan Blue staining and resuspended at 1×10^7 cells/mL in RPMI supplemented with 10% FBS, 1'000 IU/mL interleukin-2 (IL-2), and 50 nM prostratin analogue SUW013 ([Stanford University Wender lab compound 013] or compound "11c") at 37 ℃ for 48 hours. SUW013 is a synthetic analogue which exhibits a higher affinity to PKC and a superior potency (100-fold) at inducing the expression of dormant HIV compared to the plant-derived prostratin [123]. SUW013 was provided by Dr. Paul A. Wender (Department of Chemistry, Stanford University, Stanford, California).

Cells were resuspended 24 hours post-stimulation. At the end of the incubation period, samples were centrifuged (2'000 RPM for 5 min) and supernatants were filtered through the 0.65 μm

pore membrane of an Ultrafree-MC Centrifugal Filter device (MilliporeSigma, Burlington, Massachusetts) by centrifugation at 2'000 RPM for 5 min. The filtrate was collected in a microtube and the volume was completed to 1 mL with RPMI.

Quantification of inducible cell-free HIV-1 RNA was performed by our collaborator Dr. John Kim at the National Laboratory for HIV Reference Services (JC Wilt Infectious Diseases Research Centre, Winnipeg, Canada) using two-step RT-qPCR. First-strand cDNA was synthesized using SuperScript™ VILO™ Master Mix (Thermo Fisher Scientific, USA). Quantification was then made using a QX200 Droplet Digital PCR device (Bio-Rad Laboratories, California, USA). This allowed absolute quantification of target DNA in the entire 1 mL sample. Results were then expressed as the number of HIV-1 RNA copies produced by 1×10^6 CD4+ T cells.

2.3 Statistical analysis

Statistical analysis was performed using GraphPad Prism 9 (GraphPad Software, La Jolla, CA) and correlations were considered statistically significant when $p < 0.05$.

- correlations were assessed using Spearman's non-parametric correlation test;
- comparison between groups was accomplished using the Kruskal-Wallis test and Dunn's multiple comparisons test; and,
- slopes were calculated using a linear regression model.

The mean accompanied with the standard deviation illustrated the range of measured HIV-1 RNA and DNA as this value is used in the corresponding statistical tests.

CHAPTER 3 – RESULTS

3.1. Phylogenetic study of HIV-1 isolates

3.1.1. Clinical characteristics of HIV-1 phylogenetic study participants

The clinical characteristics of the vertically infected participants are shown in Table 2. 56.3% (36/64) of them were female. Most participants (44/64, 68.8%) were immigrants with the four most frequent countries of origin being Vietnam (10.9%), Ethiopia (7.8%), Lesotho (6.3%) and Burundi (4.7%). Participants with mothers of Black ethnicity were a majority (54.7%), followed by Asian (14.1%), Aboriginal (6.3%) and Latino (4.7%) mothers. For the 64 participants, the median viral load was 0 copies/mL, as it ranged from undetectable for 56 participants (87.5%) to 8'280 copies/mL. Median T cell counts and percentages were respectively 757 cells/mm^3 (range: 119 to 2'250) and 37.5% (range: 7 to 49) for CD4$^+$ cells and 755 cells/mm^3 (range: 264 to 2'320) and 32.5% (range: 21 to 60) for CD8$^+$ cells. Median age at ART initiation was 1.7 years (range: 0 to 14.74) with the majority of participants (54.7%) starting ART within the first two years of life. All but two participants were receiving cART regimens at the time of sample collection, one was under AZT only and the other was treatment naïve. SVS was achieved in 87.5% of participants. The rest either presented measured blips of viremia overtime (9.4%) or were unsuccessful in controlling viral replication (3.1%). We calculated respective median values of 52.5% (range: 0 to 98) and 85% (range: 4 to 100) for the cumulative proportion of life during which patients were under effective ART (cPLEC) or sustained viral suppression (cPLUS). Participants' ages ranged from 2.19 to 25.81 years, with a median of 12.93 years.

Table 2. Clinical characteristics of the 64 participants in the HIV-1 phylogenetic study.

Patient ID	Gender	Age at Baseline (years)	Ethnicity of mother	Birth country of mother	Age at ART initiation (years)	Current ART Regimen	Median CD4+ T cell count (cells/mm3)	Median proportion of CD4+ T cells (%)	Median CD8+ T cell count (cells/mm3)	Median proportion of CD8+ T cells (%)	Median viral load (copies per ml of plasma)*	Control of viral replication (SVS, NoSVS, Blips)	cPLEC	CPLUS
01-002-BLY	F	8.45	Black	Ghana	0.00	3TC/AZT/NVP	1134	40	920	33	<40	SVS	0.97	1.00
01-003-FUO	M	4.52	Black	Ethiopia	1.12	3TC/AZT/NVP	817	31	918	33	<40	SVS	0.58	0.58
01-009-EKR	F	18.92	Black	Burundi	1.14	3TC/ABC/NFV	727	46	588	36	<40	SVS	0.78	0.91
01-011-TAG	F	18.93	Black	Botswana	6.05	EFV/FTC/TDF	718	30	695	31	<40	SVS	0.16	0.68
01-013-HWE	F	17.24	Asian	Laos	3.71	EFV/FTC/TDF	723	41	500	27	<40	SVS	0.73	0.78
01-014-IPC	M	13.68	Asian	Vietnam	4.88	3TC/AZT/NVP	711	30	737	32	<40	SVS	0.43	0.62
01-026-ZIY	M	13.82	Asian	Guyana	1.23	3TC/ABC/LPV/RTVb	699	34	792	39	3.6	Blips	0.79	0.89
01-038-CJC	F	15.50	Arab	Sri Lanka	0.88	EFV/FTC/TDF	994	42	696	30	<40	SVS	0.86	0.87
01-042-PAH	M	10.75	Asian	Vietnam	1.72	ABC/LPV/RTVb/ddl	877	31	982	35	<40	SVS	0.35	0.84
01-045-ASZ	M	16.24	Black	Burundi	4.17	3TC/ABC/NVP	509	49	264	25	<40	SVS	0.53	0.74
01-049-GBW	F	17.20	White	Canada	0.00	3TC/AZT/NFV	533	41	478	36	<40	SVS	0.94	0.95
01-054-RXI	M	10.28	Black	Ghana	1.49	3TC/AZT/NVP	1075	38	870	31	<40	SVS	0.37	0.85
01-057-UBN	F	14.37	Latino	El Salvador	0.47	3TC/AZT/NFV	1071	37	1233	42	<40	SVS	0.93	0.95
01-059-DVH	F	25.81	Black	Guyana	3.38	No ARV	119	7	931	56	151.0	noSVS	0.23	0.25
01-063-AIO	F	22.13	Black	Canada	1.61	DRV/DTG/MVC/RTVb	554	27	773	36	<40	SVS	0.52	0.67
01-071-HSZ	F	24.05	Latino	Nicaragua	1.16	FTC/RAL/TDF	689	27	1375	53	<40	SVS	0.37	0.57
01-072-XIZ	F	12.70	Black	Nigeria	2.86	3TC/ABC/LPV/RTVb	507	26	476	25	<40	SVS	0.12	0.54
01-074-ZIK	M	23.74	Black	Ethiopia	2.31	RV/DTG/FTC/RTVb/TD	389	26	784	52	<40	SVS	0.16	0.16
01-076-EOY	F	13.74	Black	Botswana	1.94	3TC/ABC/DTG	679	44	377	26	<40	SVS	0.55	0.86
02-015-DED	M	17.99	Black	Haiti	2.61	EFV/FTC/TDF	672	44	375	26	<40	SVS	0.79	0.85
02-039-YTH	F	15.67	Black	Burundi	4.45	3TC/AZT/EFV	1015	39	792	31	<40	SVS	0.01	0.36
02-040-LVQ	F	12.60	Black	Ivory Coast	0.22	3TC/ABC/RAL	1120	40	567	21	<40	SVS	0.05	0.34
02-042-UWP	F	16.76	Black	Congo	7.56	COBI/EVG/FTC/TDF	796	22	1964	51	8279.5	Blips	0.16	0.17
03-006-JJW	M	10.69	Black	Nigeria	0.01	ABC/AZT/SQV/RTV	756	41	685	35	<40	SVS	0.97	0.99
03-007-DGV	M	17.50	Black	Uganda	2.24	EFV/FTC/TDF	490	36	550	38	<40	SVS	0.83	0.87
03-008-QKI	M	16.92	Black	Chad	N.A.	N.A.	595	45	504	36	20.6	Blips	0.78	N.A.
03-012-CZZ	F	10.73	White	Canada	0.00	3TC/AZT/LPV/RTVb	758	32	745	31	<40	SVS	0.91	0.97
03-016-AIA	F	22.57	Black	Gabon	3.43	COBI/EVG/FTC/TDF	592	40	418	29	<40	SVS	0.75	0.82
03-018-NMU	F	20.73	White	Canada	4.17	3TC/ABC/ATV/RTV	790	39	896	43	<40	SVS	0.65	0.67
03-019-YTD	M	20.97	Black	Chad	N.A.	N.A.	917	36	862	33	<40	SVS	0.74	N.A.
03-023-UDJ	F	5.34	Asian	Vietnam	2.88	3TC/AZT/NVP	2250	46	1236	27	<40	SVS	0.07	0.46
03-027-EJC	F	13.21	Black	Congo	0.15	3TC/ABC/DTG	561	44	418	30	<40	SVS	0.98	0.99
04-003-OEZ	F	9.53	Aboriginal	Canada	0.20	3TC/AZT/LPV/RTVb	270	18	880	60	5106.1	noSVS	0.64	0.83
04-004-WWY	M	8.16	Black	Lesotho	4.70	3TC/ABC/EFV	730	35	580	27	<40	SVS	0.03	0.41
04-007-LPR	F	6.12	N.A.	N.A.	0.39	3TC/AZT/LPV/RTVb	1200	42	800	29	<40	SVS	0.74	0.94
04-008-XIH	F	11.61	Black	Lesotho	1.93	3TC/AZT/NVP	690	34	830	40	<40	SVS	0.16	0.83
04-009-RDQ	M	4.14	Black	Lesotho	0.04	3TC/ABC/LPV/RTVb	1020	34	830	28	<40	SVS	0.74	0.93
04-014-OEX	F	15.66	Latino	Bolivia	7.03	3TC/AZT/EFV	370	23	860	53	3836.2	Blips	0.43	0.47
04-015-ZTQ	M	5.92	Asian	Vietnam	0.08	3TC/AZT/LPV/RTVb	1060	38	760	27	<40	SVS	0.61	0.86
04-021-XBD	M	11.31	Aboriginal	Canada	0.02	3TC/ABC/ATV/RTV	760	47	500	32	<40	SVS	0.89	0.99
04-023-ZSY	M	15.51	Black	Ethiopia	1.00	DTG/FTC/TAF	550	30	890	49	<40	SVS	0.03	0.64
04-025-HMY	F	16.82	Black	Ethiopia	14.74	3TC/ABC/DTG	340	32	545	51	<40	SVS	0.02	0.04
05-001-DFD	F	15.30	White	Canada	4.22	3TC/ABC/NVP	720	46	585	35	4444.0	Blips	0.71	0.72
05-009-WJR	F	5.93	Asian	Vietnam	0.37	3TC/AZT/NVP	1130	40	610	22	<40	SVS	0.51	0.94
05-017-LMZ	F	7.11	Black	Lesotho	0.84	3TC/AZT/NVP	1170	40	1040	32	<40	SVS	0.62	0.88
05-018-BLD	F	16.45	Black	N.A.	7.79	COBI/EVG/FTC/TDF	690	39	580	35	<40	SVS	0.09	0.53
05-019-JDQ	F	2.19	Asian	Vietnam	0.08	3TC/AZT/LPV/RTVb	2060	29	2320	37	<40	SVS	0.38	0.91
05-020-BEQ	F	7.59	Black	Kenya	1.13	3TC/AZT/NVP	1255	49	1005	35	<40	SVS	0.71	0.80
05-024-TCK	M	6.75	Black	N.A.	0.23	3TC/ABC/EFV	1300	42	860	30	<40	SVS	0.23	0.55
05-025-UHW	F	9.20	Black	N.A.	0.50	3TC/ABC/EFV	1160	42	820	30	<40	SVS	0.17	0.52
05-026-HVX	F	10.09	Black	N.A.	1.81	3TC/ABC/EFV	1200	45	570	23	<40	SVS	0.16	0.47
05-027-KYN	M	13.16	Black	Ethiopia	3.66	3TC/ABC/RAL	720	35	940	45	<40	SVS	0.70	0.72
05-028-IGT	F	4.84	Black	N.A.	0.29	3TC/AZT/LPV/RTVb	1320	38	865	27	<40	SVS	0.72	0.94
07-001-ZTJ	M	4.89	N.A.	N.A.	N.A.	N.A.	830	37	620	28	<40	SVS	0.41	N.A.
07-005-ZJV	M	21.21	N.A.	N.A.	12.93	3TC/ABC/DTG	635	33	750	38	<40	SVS	0.38	0.39
08-001-DDN	F	9.70	Asian	Vietnam	1.70	3TC/ABC/LPV/RTV	847	42	576	25	<40	SVS	0.08	0.37
08-009-SKP	M	13.57	Black	Congo	11.81	3TC/EFV/TDF	640	34	625	34	<40	SVS	0.00	0.12
09-002-HSQ	M	8.17	N.A.	Canada	0.00	3TC/AZT/NVP	903	38	672	29	<40	SVS	0.79	0.95
09-003-TPH	F	7.46	N.A.	N.A.	6.19	3TC/AZT/ATV/RTV	1199	30	1445	36	16.0	Blips	0.09	0.17
09-004-UKN	M	5.50	N.A.	N.A.	2.85	3TC/AZT/ATV/RTV	1115	36	1157	37	<40	SVS	0.25	0.48
09-005-BMR	M	16.12	N.A.	N.A.	3.69	DRV/FTC/TDF/RTV	409	26	407	29	<40	SVS	0.41	0.50
09-006-VYY	M	6.06	N.A.	N.A.	3.35	AZT	1087	34	857	26	<40	SVS	0.40	0.45
09-009-SOF	F	11.05	Aboriginal	Canada	1.25	3TC/ABC/ATV/RTV	1082	40	639	27	<40	SVS	0.84	0.89

Legend: F, female; M, male; N.A., Not available; cPLEC, cumulative proportion of life under effective antiretroviral therapy; cPLUS, cumulative proportion of life under sustained viral suppression; *Measured viral load during the EPIC[4] study; <40: viral load measurement under the lower limit of detection

3.1.2. *gag* gene amplification and isolation

With the great majority of our participants having successfully suppressed viral replication during the course of our study, we attempted to amplify the HIV-1 *gag* gene by performing nested PCR on samples of PBMC lysates. Amplification was successful in 61 of the 64 participants. No band was detected in the well of negative controls and all positive controls generated the expected amplicons (data not shown). The amplified bands were visualized on 1% agarose gels (Figure 7A). The first-round of PCR resulted in most cases in smeared PCR products on the gels, instead of the expected 711 bp. This was most likely due to a high concentration of DNA template or non-specific annealing of primers. To bypass this limitation, the second-round PCR was performed on diluted PCR products. This generated the expected 561 bp fragment (Figure 7B).

All three participants for whom amplification failed (01-002-BLY, 05-028-IGT and 09-09-SOF) were young girls who initiated ART at birth or before the end of their second year of life, who achieved SVS and who presented a cPLUS value >89%. However, while this could explain the difficulty in isolating HIV-1 in these participants, these clinical characteristics were shared with others for whom amplification was a success.
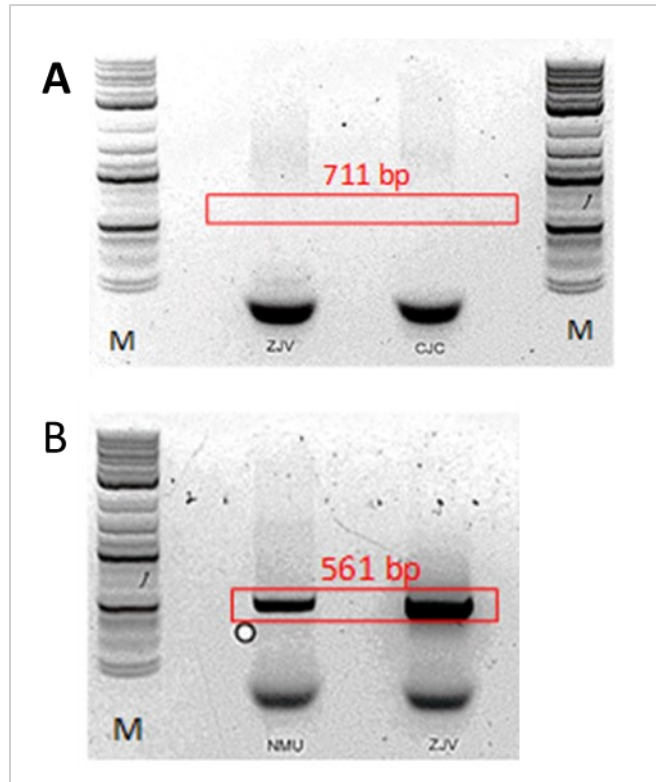
Figure 7. Agarose gel electrophoresis of *gag* fragments generated by first-round (A) and second-round PCR (B). The fragments are respectively positioned at approximately 711 bp and 561 bp. The gels were migrated for 80 minutes at 135 V and 400 mA. Red frames indicate the position of the fragments; Well M shows the molecular size marker; ZJV, CJC and NMU are examples of participants' results.

The 561 bp bands were then excised from the gel and purified using a PCR-DNA extraction and purification kit. We used molecular cloning to examine variations of the *gag* gene in each participant sample by subcloning the purified *gag* amplicons into pCR 4-TOPO vectors and transforming chemically induced competent *E. coli* with the recombinant vectors. Selective genes on the plasmids allowed us to differentiate positive recombinant colonies each carrying a variant of the HIV-1 *gag* gene. Two to five variants were selected for each participant and the positive recombinant vectors were extracted from the colonies using a Miniprep Kit. The presence of the fragment of interest was verified by performing a restriction analysis using the EcoRI and visualizing the resulting fragments in 1% agarose gels (Figure 8). The band at 3.9 kb represented the linearized vector and the second band at 560 bp, the *gag* fragment insert.

Purified recombinant plasmids were sent to the *Plateforme de séquençage et de génotypage du CHUL,* where they were sequenced by the Sanger method.
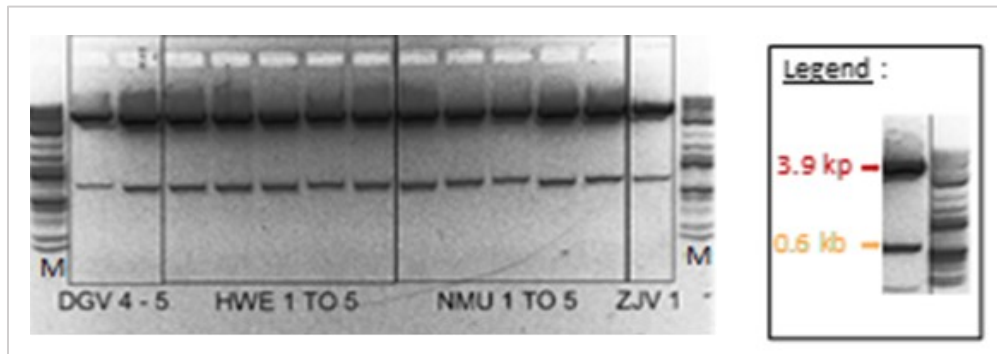
Figure 8. Restriction analysis of cloning vectors with EcoRI. 1% agarose gels were migrated for 80 minutes at 135 V and 400 mA. Fragments at 560 bp are the insert and fragments at 3.9 kb are linear vectors. M, molecular size marker; Wells DGV, HWE, NMU and ZJV are examples of participants results.

3.1.3. Phylogenetic analysis

Using the Sequence Locator feature of the online LANL HIV Sequence Database, we confirmed the location of all sequences on the genome of HIV-1 reference strain, HXB2. Then, using the Clustal W frame within the MEGA 11 software, we aligned participants and HIV-1 representative sequences. Those that were visibly too divergent from their clones or contained too many deletions were discarded. Two phylogenetic trees were constructed with different combinations of reference sequences. In the first tree, along with all recovered *gag* clones from each participant, we included two to four reference sequences for each subtype of group M (A1, A2, A3, A4, A6, B, C, D, F1, F2, G, H, J, K & L), for common CRFs (01_AE, 02_AG, 03_AB, 04_AGHKU, 05_DF, 06cpx 07_BC, 08_BC, 09_cpx, 10_CD, 11 cpx12_BF, 13cpx,14_BG 15_01B, 16_A2D) and finally for groups N, O and P. The tree was rooted on a representative SIVcpz sequence to better understand the evolutionary relationships between groups and clades. In Figure 9, we omitted CRFs and groups where no clustering was observed with participants' *gag* genes. We also discarded all but one representative *gag* clone for each participant to simplify visualization of the clusters (Figure 9).
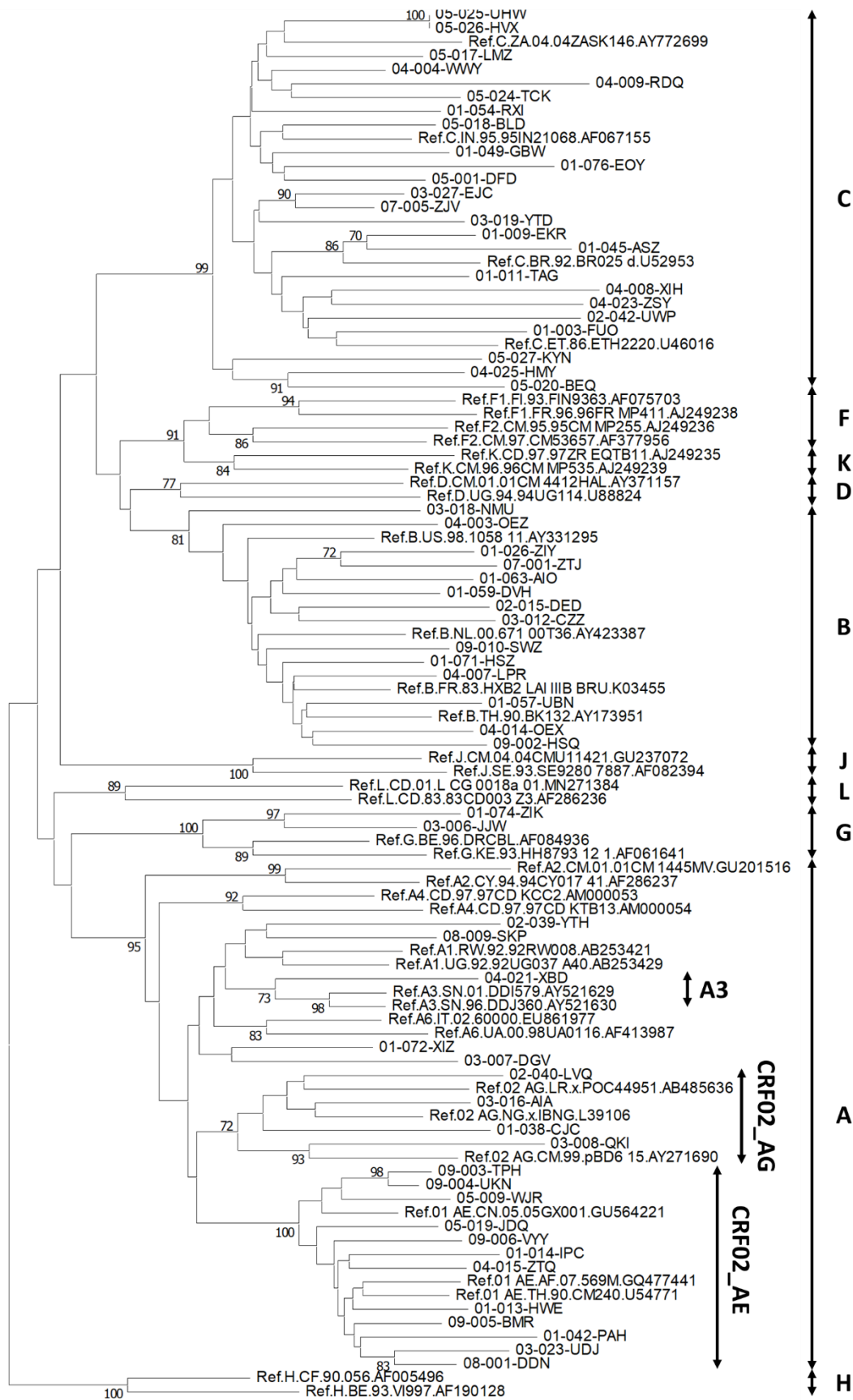
Figure 9. Phylogenetic analysis of HIV-1 *gag* gene isolated from vertically infected children and adolescents of the EPIC[4] cohort. Sequence relatedness was inferred using the Neighbor-Joining method. The optimal tree is shown. The percentage of replicate trees in which the associated taxa clustered together in the bootstrap test (1'000 replicates) are shown next to the branches. The tree is drawn to scale, with branch lengths in the same units as those of the evolutionary distances used to infer the phylogenetic tree. Evolutionary distances were computed using the Maximum Composite Likelihood method and are in the units of the number of base substitutions per site. Evolutionary analyses were conducted using MEGA 11.

Sequences from 61 participants clustered within group M. Clade assessment was based on reliable groupings with reference sequences supported by >70% bootstrap. First, we found that the *gag* sequences of 24 participants (39.3%) grouped with subtype C (99% bootstrap). Next, 21 participants (34.4%) clustered within subtype A (95% bootstrap). Amongst them: one was further classified as subtype A3 (73% bootstrap), twelve clustered alongside CRF01_AE references (100% bootstrap), four with CRF_02AG (72% bootstrap), while the last four did not reliably group within any A sub-subtype. Finally, sequences from 14 participants (22.9%) grouped with clade B (81% bootstrap) and the last two sequences (3.2%) grouped with clade G (100% bootstrap).

We turned to the clinical history of our participants to study the impact of the viral subtypes. However, we did not observe any significant correlations between the subtypes of HIV-1 isolates and the median viral load during EPIC[4], the median $CD4^+$ and $CD8^+$ T cell counts and frequencies and the cPLUS (Table 3). Intraclade and interclade variability were calculated in MEGA 11 by evaluating the nucleotide sequence variation of the *gag* gene fragments (802-1327bp). The average genetic variability between all participant sequences was 0.18 base substitutions per site. The mean variability within a clade varied between 0.07 base substitutions per site for clade A (including A3), 0.10 for clade B, 0.12 for clade C, 0.06 for clade G, 0.06 for CRF01_AE and 0.02 for CRF02_AG (Table 3).

Table 3. Clinical factors and sequence variability vs HIV-1 subtypes.

|	Subtype A (N = 4)	Subtype A3 (N = 1)	Subtype B (N = 14)	Subtype C (N = 24)	Subtype G (N = 2)	CRF01_AE (N = 12)	CRF02_AG (N = 4)
Gender, n (%)							
Female	1 (25)		9 (64)	14 (58)		6 (50)	3 (75)
Male	3 (75)	1 (100)	5 (36)	10 (42)	2 (100)	6 (50)	1 (25)
Ethnicity of mother, n (%)							
Black	4 (100)		3 (21.4)	21 (87.5)	2 (100)	8 (67)	3 (75)
Asian			1 (7.1)				
White			2 (14.3)	2 (8.3)			
Aboriginal		1 (100)	2 (14.3)				
Latino			3 (21.4)				
Arab							1 (25)
Not available			3 (21.4)	1 (4.2)		4 (33)	
Median age at ART initiation (years) (Range)	3.65 (2.240-11.81)	0.02	1.16 (0.00-7.030)	1.81 (0.00-14.74)	1.16 (0.01-2.31)	2.87 (0.08-6.20)	0.88 (0.22-3.43)
Median CD4$^+$ T cell count (Range)							
Frequency (cells/ mm3)	573.5 (490.0-1015.0)	760	694.0 (119.0-1200.0)	723.5 (340.0-1300.0)	572.5 (389.0-756.0)	1074.0 (409.0-2250.0)	794.5 (592.0-1120.0)
Proportion (%)	35.0 (26.0-39.0)	46.5	33.0 (7.0-44.0)	38.5 (22.0-49.0)	33.5 (26.00-41.00)	35.0 (26.0-46.0)	41.0 (40.0-45.0)
Median CD8$^+$ T cell count (Range)							
Frequency (cells/ mm3)	587.5 (476.0-792.0)	500	796.0 (362.0-1375)	785.0 (264.0-1964.0)	734.5 (685.0-784.0)	808.5 (407.0-2320.0)	535.5 (418.0-696.0)
Proportion (%)	32.5(25.0-38.0)	31.5	38.5 (26.0-60.0)	33.0 (23.0-51.0)	43.5(35.00-52.00)	28.0 (22.0-37.0)	29.5 21.0-36.0
Median viral load during EPIC^4 study (copies per ml of plasma)* (Range)	0.00 (0.00-0.00)	0.00	0 (0-5106)	0.00 (0.00-8280)	0.00 (0.00-0.00)	0.00 (0.00-16)	0.00 (0.00-21)
Median cPLEC, % (Range)	65.0 (0.0-83.0)	89.5	69.5 (23.0 - 93.0)	45.5 (2.0-98.0)	56.5 (16.0-97.0)	39.0 (7.0-73.0)	76.5 (5.0-86.0)
Median cPLUS, % (Range)	45.0 (12.0-87.0)	99	85.0 (25.0-98.0)	72.0 (4.0-99.0)	57.5 (16.0-99.0)	56.0 (17.0-94.0)	82.0 (34.0-87.0)
Mean intra-clade variability (base substitutions per site ± standard error)	0.07 ± 0.02		0.10 ± 0.02	0.12 ± 0.01	0.06 ± 0.01	0.06 ± 0.01	0.02 ± 0.03

Legend: cPLEC, cumulative proportion of life under effective antiretroviral therapy; cPLUS, cumulative proportion of life under sustained viral. *A value 0 means that viral load was undetectable.

3.2. HIV-1 reservoir study

3.2.1. Clinical characteristics of HIV-1 reservoir study participants

The clinical characteristics of the vertically infected participants from the EPIC[4] study are shown in Table 1. 67 children and adolescents under cART were selected and stratified in three groups according to their control of viral replication, with 29 presenting SVS at all time-points (**SVS** group); 27 with occasionally detectable "blips" in viremia (**BLIP** group), and finally, 11 lacking SVS (**No SVS** group). In Figure 10, we show an example of each profile of viral control. The participants were further stratified in three age subgroups (<6, 6 to 10 and >10 years old) so as to better examine the impact of age on reservoir size.
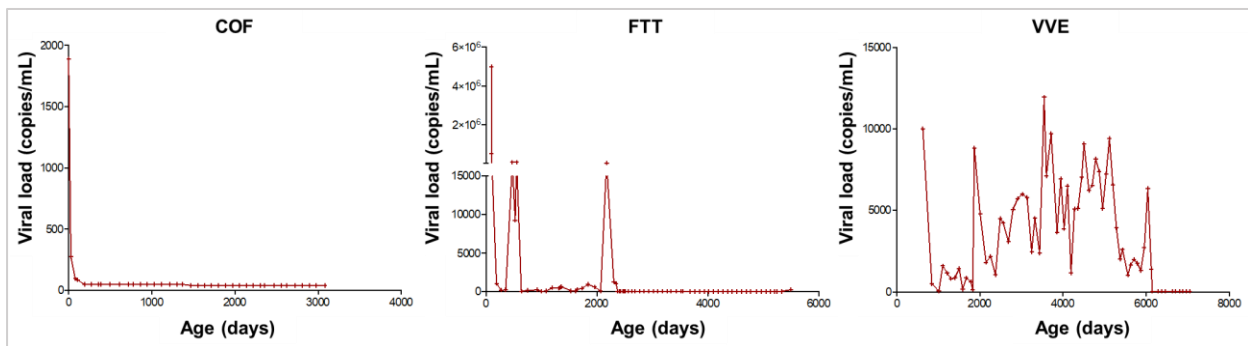
Figure 10. Examples for each profile of viral replication control. The three graphs show the measured viremia (HIV-1 RNA per mL of plasma) over time. (Left) Participant COF with sustained suppression of viral replication. (Middle) Participant FTT with occasional viremic "blips". (Right) Participant VVE without control over viral replication. The figure was provided by Hinatea Dieumegard, Ph.D. candidate.

The three groups exhibited similar clinical and sociodemographic characteristics at baseline. In fact, in each group, most of the participants were of Black ethnicity, originated from outside of Canada and had mothers who were diagnosed after their pregnancy and thus did not receive antepartum ART. Additionally, we observed similar levels of nadir CD4+ T cell counts and frequencies. There were, however, differences in terms of cPLEC and cPLUS, as the proportions were significantly higher amongst the children in the **SVS** group (cPLUS: 59.1 [Range: 3.1 - 97.1]; cPLEC: 76.8 % [Range: 76.8 - 100]) compared to the **No SVS** group (cPLUS: p=0.0169; cPLEC: p=

0.0072) and the **BLIP** group (cPLUS: p=ns ; cPLEC: p=0.0031). Notably, we also observed in the **No SVS** group lower counts (496.0 cells/mm^3 [Range: 150.0 - 1197]; p_{vsSVS}=0.0454; p_{vsBLIP}=0.0236) and frequencies (25.0% [Range: 14.0 - 39.0] ; p_{vsSVS}=0.0126 ; p_{vsBLIP}=0.0294) of CD4+ T cells along with higher frequencies of CD8+ T cells (45.0% [Range: 22.0 - 67.0]; p_{vsSVS}= 0.0008 ; p_{vsBLIP}= 0.0481). This analysis was accomplished using the Kruskal-Wallis test and Dunn's multiple comparisons test.

Table 4. Clinical characteristics of the 67 participants in the HIV-1 reservoir study.

Caracterisitics	Children with sutained viral suppression during study; <SVS> (n=29)	Children presenting occasional viremic blips; <BLIPS> (n=27)	Children without sutained viral suppression; <No SVS> (n=11)
Age group (n)			
<6 years	9	6	3
6 to 10 years	10	6	2
≥ 10 years	10	15	6
Sex (%)			
Female	14	15	7
Male	15	12	4
Mother's ethnic group (%)			
Black	58,6	74,1	72,7
White	10,3	3,7	0,0
Asian or Arab	13,7	11,1	18,2
Native american	6,9	3,7	9,1
Other	10,3	7,4	0,0
Birth country (%)			
Canada	52,7	37,0	81,8
Other	48,3	63,0	18,2
Timing of mother's diagnosis relative to pregnancy (%)			
Before	17,2	14,8	18,2
During	3,4	7,4	9,1
After	41,3	51,9	54,5
Unknown	37,9	25,9	18,2
ART administred during pregnancy (%)			
Yes	13,7	7,4	18,2
No	62,1	74,1	72,7
Unknown	24,1	18,5	9,1
Mother achived SVS during pregnancy (%)			
Yes	0,0	0,0	9,1
No	44,8	29,6	36,4
Unknown	55,2	70,4	54,5
Congenital infection during pregnancy (%)	20,7	3,0	27,3
Premature birth (%)	10,0	7,4	0,0
Median Viremia at diagnosis (range) (copies/mL)	61451 (0,0 - 2880000)	111445 (1066 - 1636046)	32968 (108,0 - 10916500)
Age at diagnostic (range) (years)	0,8 (0,0 - 9,6)	2,1 (0,0 - 13,1)	0,4 (0 - 4,3)
Median Age at ART initiation (range) (years)	1,1 (0,0 - 11,0)	4,0 (0,0 - 13,2)	0,4 (0 - 13,9)
Median Cumulative proportion of life under SVS at baseline (range) (%)	59,1 (3,1 - 97,1)	24,7 (0,0 - 95,5)	20,9 (0 - 76,7)
Median Cumulative proportion of life under effective ART at baseline (range) (%)	76,8 (5,8 - 100)	30,0 (0,0 - 96,7)	27,0 (0 - 96,7)
Median CD4 nadir at baseline (range) (cells/mm3)	494,0 (5,0 - 1250)	426,0 (20,0 - 1628)	288,0 (54,0 - 702,0)
Median CD4 % nadir at baseline (range)	23,0 (0,0 - 47,0)	20,0 (2,0 - 40,0)	17,0 (6,0 -24,0)
Median CD4 at baseline (range) (cells/mm3)	872,0 (38,0 - 2269)	883,0 (437,0 - 2940)	496,0 (150,0 - 1197)
Median CD4 % at baseline (range)	39,0 (7,1 - 52,0)	36,0 (23,0 - 50,0)	25,0 (14,0 - 39,0)
Median CD8 at baseline (range) (cells/mm3)	740,0 (156,0 - 1724)	788,0 (357,0 - 1848)	1069 (323,0 - 2428)
Median CD8 % at baseline (range)	30,0 (19,0 - 56,0)	35,0 (17,0 - 46,0)	45,0 (22,0 -67,0)

3.2.2. Measurement of HIV-1 reservoirs

Study participants were followed every 3 months for an average of 2.63 years (range: 0.94 – 3.53). Using PBMC samples collected at different time-points, HIV-1 reservoir size was quantified using two methods. The first method, measuring inducible cell-free (ICF) HIV-1 RNA, consisted of performing digital droplet PCR on the supernatant of isolated CD4+ T cells following a 48h stimulation using the SUW013 analogue of prostratin and IL-2. The second method, the HIV-1 DNA assay, allowed the quantification of total viral DNA present in PBMC lysates using real time quantitative PCR. This allowed us to portray the evolution of the HIV-1 reservoirs in our study group (Figures 11 and 12).
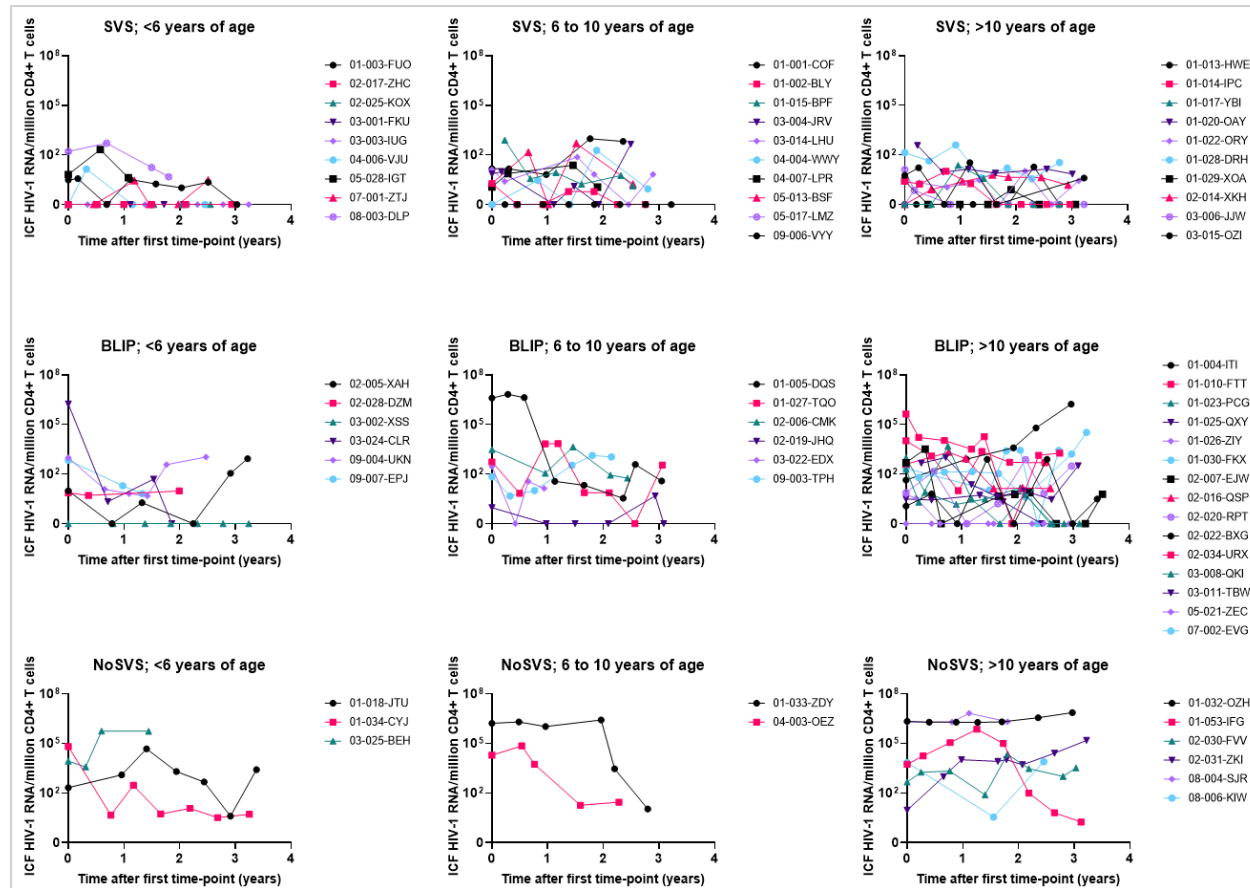
Figure 11. Dynamics of the inducible HIV-1 peripheral reservoir measured using the SUW013-stimulation assay in 67 children and adolescents over up to 3.53 years. Digital droplet PCR (ddPCR) was conducted in the supernatant of SUW013-stimulated CD4+ T cells isolated from PBMC samples collected every 3 months on average. Participants were stratified based on their control of viral replication (SVS, BLIP, No SVS) and their age (<6, 6–10, >10 years). Each dot represents a separate reservoir measurement. During experimentation, 8 participants from the BLIP and No SVS groups (03-024-CLR, 01-005-DQS, 01-010-FTT, 02-022-BXG, 03-025-BEH, 01-033-ZDY, 01-032-OZH and 08-004-SJR) presented some measures above the upper limit of detection in ddPCR. Due to low numbers of remaining samples, the experiments were not repeated. Instead, a calculation was made to estimate the reservoir (see Table 5 in annex). ICF = Inducible cell-free.
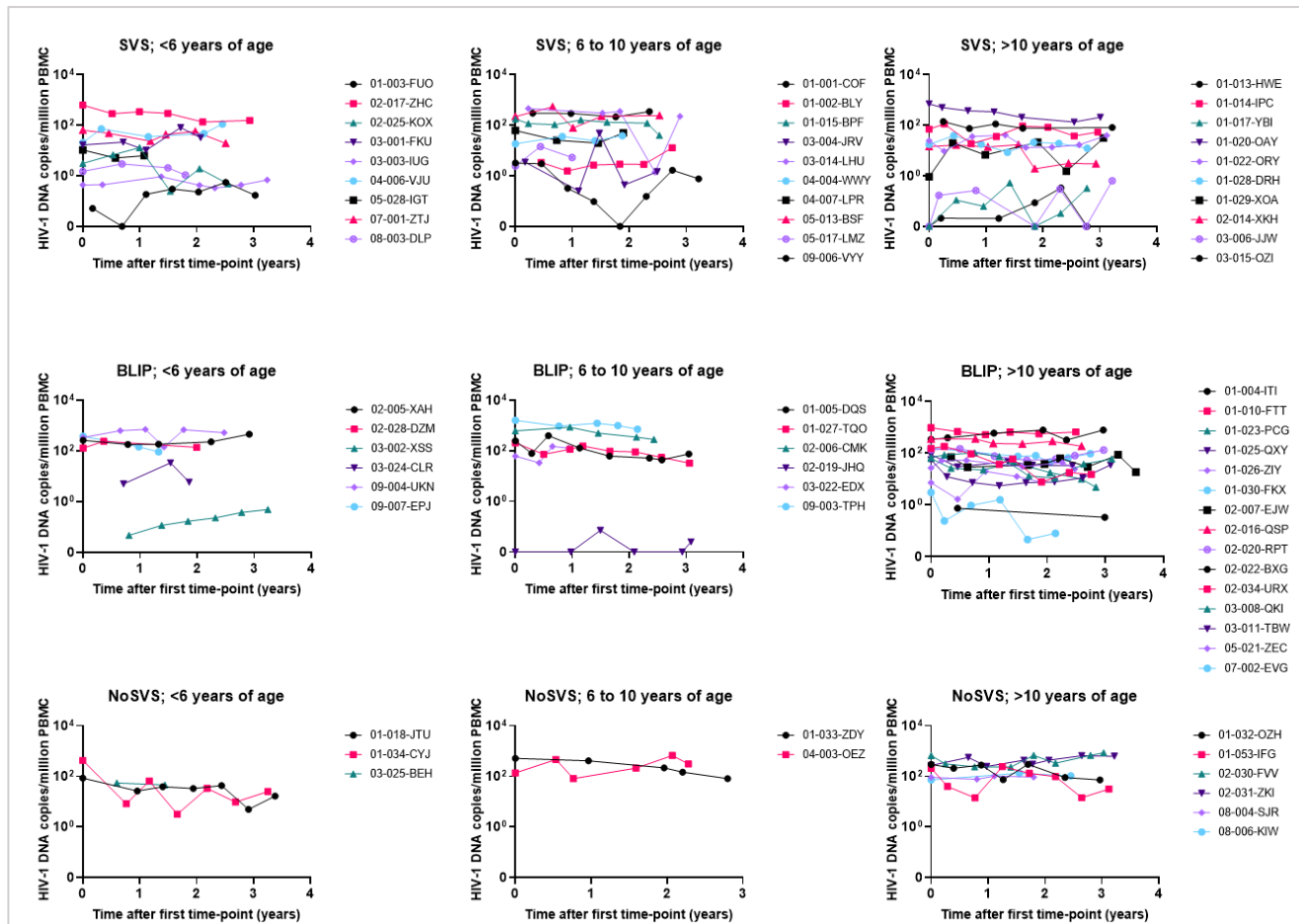
Figure 12. Dynamics of the HIV-1 peripheral reservoir measured using the total viral DNA quantification assay in 67 children and adolescents over up to 3.53 years. Quantitative PCR was conducted in PBMC lysates from samples collected every 3 months on average. Participants were stratified based on their control of viral replication (SVS, BLIP, No SVS) and their age (<6, 6–10, >10 years). Each dot represents a separate reservoir measurement.

Within the **SVS**, **BLIP** and **No SVS** groups, we observed no statistically significant differences between age-subgroups in the size of the viral reservoir, regardless of the quantification method used (Figure 13A and 13B). ICF HIV-1 RNA levels were highest amongst participants without SVS with a median of 6'953 copies/10^6 CD4+ T cells and ranging from 1.769 to 7'326'000, when compared to "blippers" (median = 9.884; range = 0.000 – 6'711'409; p<0.0001) and participants with SVS (median = 0.6174; range = 0.000 - 971.5; p<0.0001) whose levels where the lowest (Figure 13C). Total HIV-1 DNA followed a similar trend, with the **SVS** group presenting the lowest levels (median = 16.64 copies/10^6 PBMC; range = 0.00 - 705.0) compared to **BLIP** group (Median = 63.99; Range = 0.00 – 1'622; p=0.0001) and the **No SVS** group (median = 132.0; range = 3.167 – 838.2; p<0.0001) (Figure 13C). However, it was noted in this last case that the difference between the later groups was not statistically significant (p=0.2784).
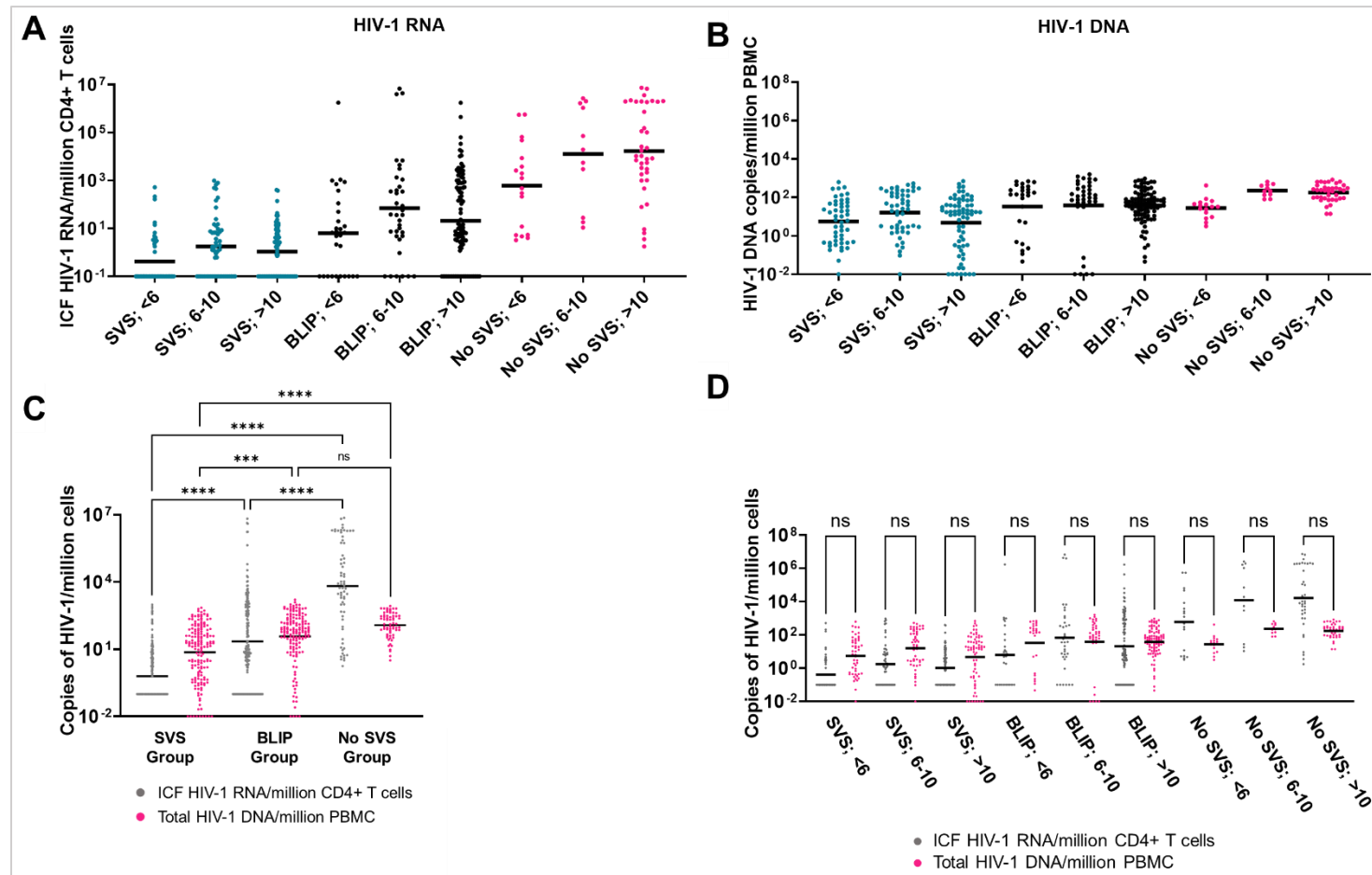
Figure 13. Size of the HIV-1 reservoir in samples of PBMC and SUW013-stimulated CD4+ T cells from 67 vertically infected children and adolescents. Participants were stratified according to their control of viral replication (SVS, BLIP, No SVS) and age (<6, 6–10, >10 years). Reservoir measurement was performed at different time points for up to 3.53 years. (A) Representation of ICF RNA levels measured in each subgroup. (B) Representation of Total DNA levels measured in each study subgroup. (C) Difference in viral RNA and DNA levels between viral control groups. (D) Comparison between viral RNA and DNA levels within each subgroup. Horizontal Lines indicate median values. Comparison between groups was done using the Kruskal-Wallis test and Dunn's multiple comparisons test. *** = p=0.001; **** = p<0.0001; ns = not significant; ICF = Inducible cell-free.

Despite the lack of a significant difference between the total measured levels of HIV-1 DNA in PBMC and ICF HIV-1 RNA in CD4+ T cells, we noticed that in the **SVS** group, RNA levels give the impression of being lower than DNA levels, whereas the **No SVS** group displays an opposite trend (Figure 13C and 13D). Nonetheless, as demonstrated in our previous article [148], correlation was observed between Total HIV-1 DNA and induced cell-free RNA (p<000.1; r=0.56) in our study group (Figure 14). Despite a high number of undetectable measures of ICF RNA, we still observed a significant correlation when these measures, in addition to undetectable DNA measures, where excluded from the analysis (p<0.0001; r=0.4409).
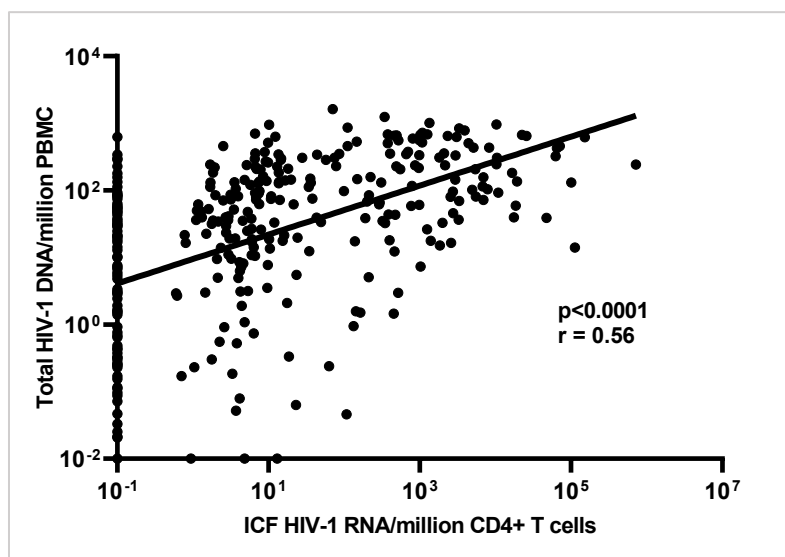
Figure 14. Correlation between HIV-1 peripheral reservoirs measured using the total HIV-1 DNA assay in PBMCs and the SUW013-stimulation assay in CD4+ T cells. The correlation was assessed using Spearman's non-parametric correlation test. ICF = inducible cell-free.

To describe the trajectory of the HIV-1 reservoir throughout childhood and adolescence, we realized a linear regression analysis in each of the previously mentioned subgroups (Figures 15 and 16). Overall, the median slope for inducible HIV-1 RNA was -0.12 $\log_{10}$ ICF HIV-1 RNA/10^6 CD4+ T cells (Range: -3.08 to 1.47) and was twice higher compared to the median of total HIV-1 DNA slopes which was calculated at -0.056 $\log_{10}$ HIV-1 DNA/10^6 PBMC (Range: -0.62 to 0.46). The lower range observed with the second quantification method (4.25 times lower) indicates a higher stability over time in terms of total HIV DNA compared to inducible cell-free RNA.

Generally, the linear relationship between time and the size of the reservoir was similar between participants within the same subgroup. For the SUW013-stimulation assay, differences were only supported statistically in the three *BLIP* age-subgroups (*BLIP <6 years of age* [p=0.0235], *BLIP 6-10 years of age* [p=0.0280] and *BLIP >10 years of age* [p=0.0253]) (Figure 15). For the total HIV-1 DNA assay, however, we noted statistically significant variations within the *SVS <6 years of age* subgroup (p=0.0282), and the *BLIP 6–10 years of age* subgroup (p=0.0143) (Figure 16).
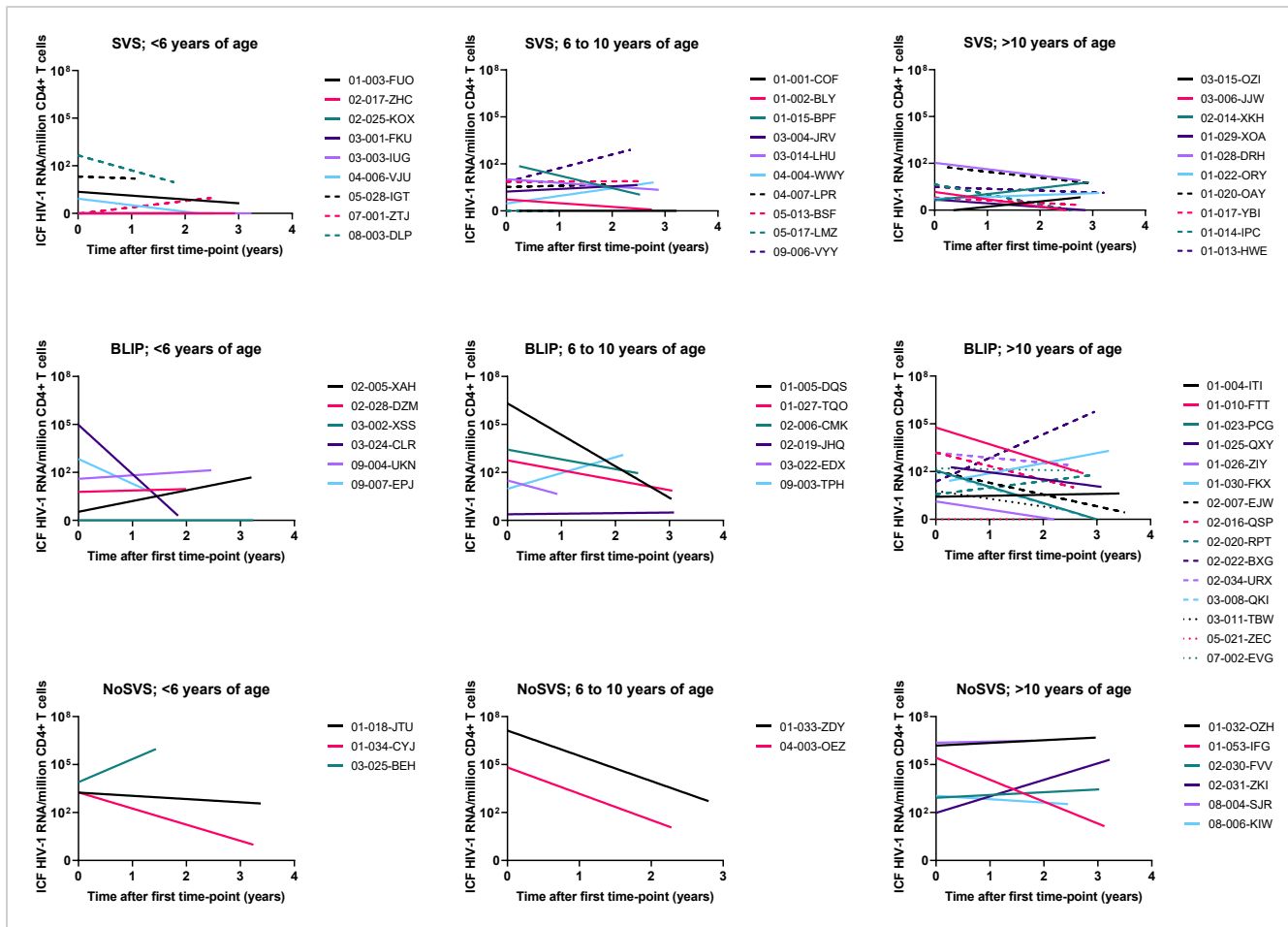
Figure 15. Trajectory of the inducible HIV-1 peripheral reservoir measured using the SUW013-stimulation assay in 67 children and adolescents over up to 3.53 years. Participants were stratified according to their control of viral replication (SVS, BLIP, No SVS) and age (<6, 6–10, >10 years). Digital droplet PCR (ddPCR) was conducted in the supernatant of SUW013-stimulated CD4+ T cells isolated from PBMC samples collected every 3 months on average. 8 participants from the BLIP and No SVS groups (03-024-CLR, 01-005-DQS, 01-010-FTT, 02-022-BXG, 03-025-BEH, 01-033-ZDY, 01-032-OZH and 08-004-SJR) presented measures above the upper limit of detection in ddPCR; a calculation was made to estimate the reservoir (see Table 5 in annex). ICF = Inducible cell-free.

52
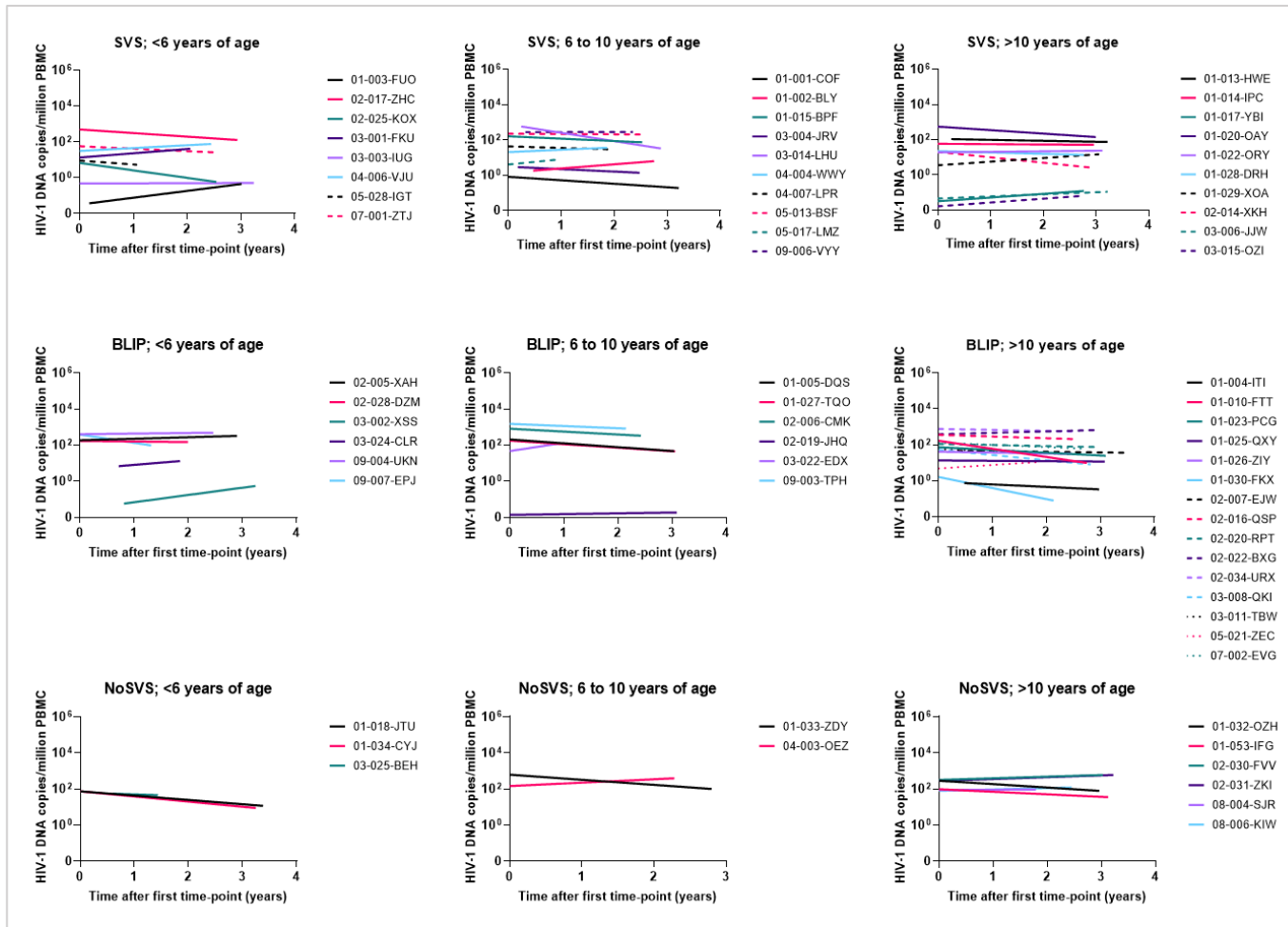
Figure 16. Trajectory of the HIV-1 peripheral reservoir measured using the total viral DNA quantification assay in 67 children and adolescents over up to 3.53 years. Participants were stratified based on their control of viral replication (SVS, BLIP, No SVS) and age (<6, 6–10, >10 years). Quantitative PCR was conducted in PBMC lysates from samples collected every 3 months on average. Slopes were calculated using a linear regression model.

Regardless of the quantification method used, the calculated slopes did not differ between subgroups (Figure 17), and seldom were those which significantly deviated from zero. For the SUW013-stimulation assay, this represents 11 out of 67 participants (16.4%) with a median slope of -0.64 $\log_{10}$ ICF HIV-1 RNA/10^6 CD4+ T cells and ranging from -1.97 to 1.49. Out of those eleven, the majority (63.6%) showed a negative slope. Comparably, the total HIV-1 DNA assay yielded only 10 participants (14.9%) who had regression lines deviating significantly from zero, with 9 out of 10 (90%) presenting a negative slope. In this instance, the median slope was -0.25 $\log_{10}$ HIV-1 DNA/10^6 PBMC and ranged from -0.47 to 0.40. Interestingly, we noted that 50% (12/21) of all these slopes originated from participants with viremic "blips". The variability of their reservoirs is thus consistent with the irregularity of their measured viremia as time goes by.
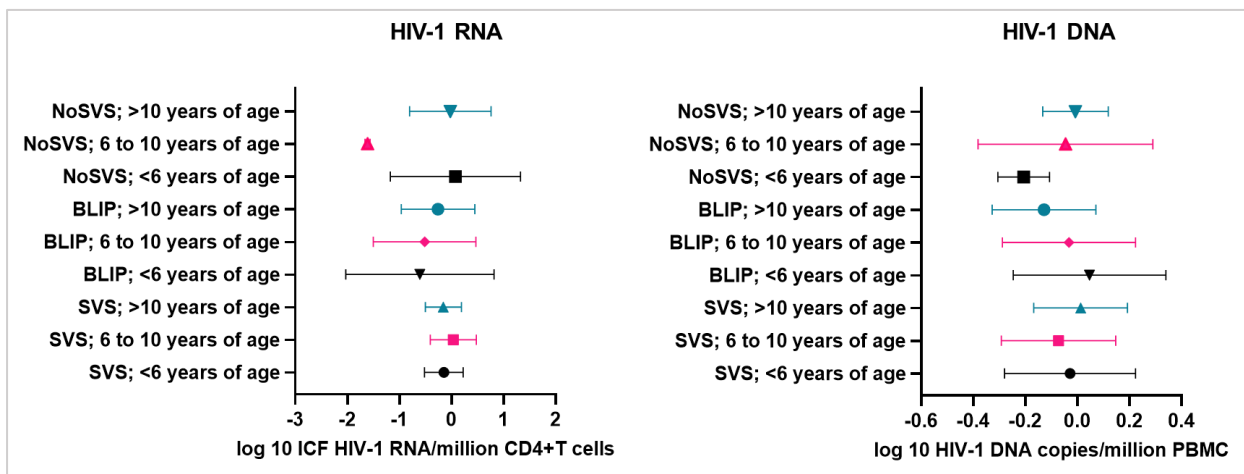
Figure 17. Regression analysis of the evolution the size of the HIV-1 reservoir over up to 3.53 years. The graphs were drawn using reservoir measures from the SUW013-stimulation assay (left) and the total HIV-1 DNA assay (right). Participants were stratified based on control of viral replication (SVS, BLIP, No SVS) and age (<6, 6–10, >10 years). Graphs represent mean with error bars showing the standard deviation. Comparison between groups was done using the Kruskal-Wallis test and Dunn's multiple comparisons test. ICF = Inducible cell-free.

54

All these results suggest a general stability in the measured viral reservoirs. This is further demonstrated by the lack of significant differences between the first and last measures of the reservoir, which is observed in all but one subgroup, ***BLIP>10 years of age*** (median difference =-20.68 HIV-1 DNA/10^6 PBMC; p= 0.0103), and only with the HIV-1 DNA assay.

3.2.3. Impacts of different clinical and viral factors on the size and evolution of the HIV-1 reservoir.

Next, we sought to determine the impact of different clinical and viral factors on the size and evolution of the HIV-1 reservoir in vertically infected children and adolescents. Having used two quantification methods, which target inducible HIV-1 RNA or total HIV-1 DNA, the correlations were studied separately, to allow a broader perspective.

Reservoir size estimated using the two methods negatively correlated with cPLUS (RNA: p<0.0001, r=- 0.3673 and DNA: p<0.0001, r=-0.3787) and cPLEC (p<0.0001 r=-0.3314, p<0.0001, r=-0.3459) (Figure 18A and 18B). Inversely, viremia was correlated positively with reservoir size (p<0.0001, r=0.4438, p<0.0001, r=0.3315) (Figure 18C).

ICF HIV-1 RNA levels correlated negatively with clinical parameters such as CD4+ T cell counts (p=0.003, r=-0.1524) and frequencies (p<0.0001, r=-0.229) (Figure 18D and 18E), and positively with CD8+ T cell counts (p=0.0184, r=0.1215) and frequencies (p=0.0001, r=0.1979) (Figure 18F and 18G) and the age of participants at the time of sample collection (p=0.0138, r=0.1251) (Figure 18H). The viral DNA reservoir had no significant relationship with these last factors except the count of CD4+ T cells, with which it correlated negatively (p=0.0045, r=0.1456).

Notably, the correlation coefficients were rather small, ranging from 0.1215 to 0.4438 for statistically significant linear relationships, indicating a generally weak association between the studied factors and reservoir size. Considering this and the high number of undetectable measures regrouped in our data, the analysis was repeated, and this time, we omitted these values to study their influence on our conclusions and correlation coefficients (Figure S1 in annex). We mostly observed similar associations in this analysis. On one hand, P values were

lower in 62.5% of the lines. On the other, absolute r values were increased in 62.5% of the lines and ranged generally from 0.1596 to 0.3855, with a unique outlier calculated at 0.6372. This value represented the strongest correlation observed, which linked viremia and ICF HIV-1 RNA. It should be noted that, in this analysis, three associations became nonsignificant: HIV-1 RNA vs CD8+ T cell counts (p=0.1268, r=0.09682), HIV-1 RNA vs age at visit (p=0.1120, r=0.09898) and HIV-1 DNA vs viremia (p=0.1687=, r=0.1564) (Figure S1 in annex). However, all three were supported by a small absolute r in the previous analysis (<0.35), therefore already indicating a weak correlation between the variables. Undetectable measures of HIV-1 represent a considerably high proportion of our data; thus, it remained important to include them in our analysis. This exercise, however, demonstrated the influence of outliers on our statistical conclusions.
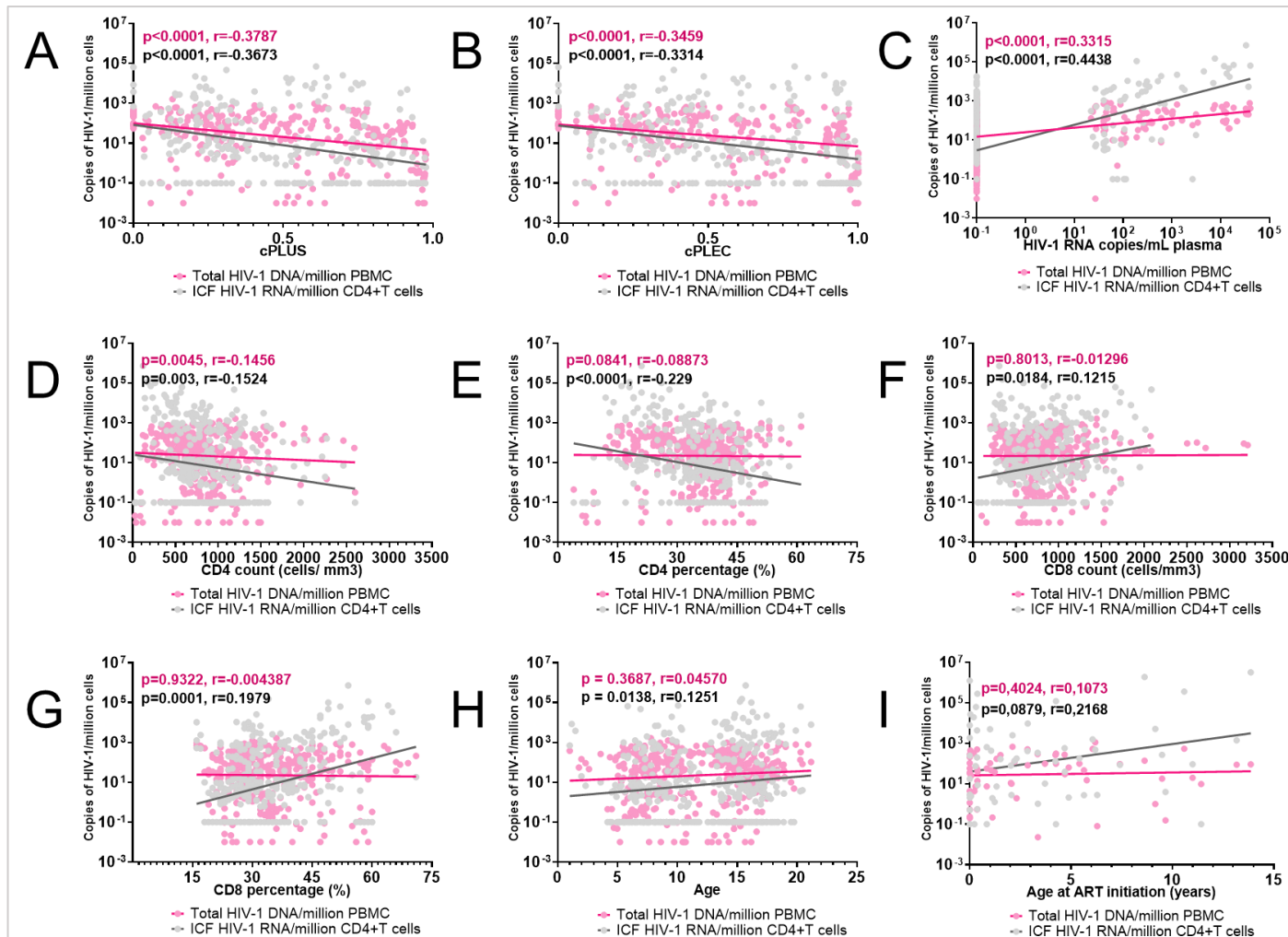
Figure 18. Impacts of various clinical and viral factors on the size of HIV-1 reservoirs in vertically infected children and adolescents under cART. The viral reservoir was quantified at different time-points using two methods: the SUW013-stimulation assay (grey) and the total HIV-1 DNA assay (pink). The studied factors include the cumulative proportion of life under sustained viral suppression (cPLUS) (A) and under effective treatment (cPLEC) (B), viremia (C), CD4+ T cell counts and frequencies (D and E), CD8+ T cell counts and frequencies (F and G), age (H) and age at ART initiation (I). Each dot represents a time point. Correlations were assessed using Spearman's non-parametric correlation test. ICF = Inducible cell-free.

We also assessed the impact of age at ART initiation. Surprisingly, when looking at the whole study cohort, no significant impact was noticed on the reservoir size (RNA: p=0.0879, r=0.2168; DNA: p=0.4024, r=0.2168) (Figure 18I). Even by divided the participants into smaller groups according to ART initiation, this variable still showed no influence over levels of HIV-1 DNA (Figure 19A). And although RNA levels were lower in participants who initiated ART in the first week after birth, this difference was strangely only noticeable in comparison to children who initiated ART between 1 week to 1 year after birth and not with those who started ART after a year (Figure 19A).

Additionally, the timing of ART was similar in all groups based on achievement of SVS, with the majority having started after 12 months of life, followed by those who started between 6 week and 12 months of life and finally children who started treatment within 24 hours postpartum (Figure 19B). We also studied the relationship between ART timing and reservoir size within each group and found a single significant positive correlation in regard to the inducible reservoir of the *SVS* group (p=0.0156, r=0.4605) (Figure 19C). This seems to highlight the importance of both adequate virological control and early initiation of ART in limiting the viral reservoir.

As expected, due to the stability of the measured reservoirs during the period that participants were followed, no significant impact of the different factors on the slopes, and thus the trajectory of the HIV-1 reservoirs, was identified (Figure 20).
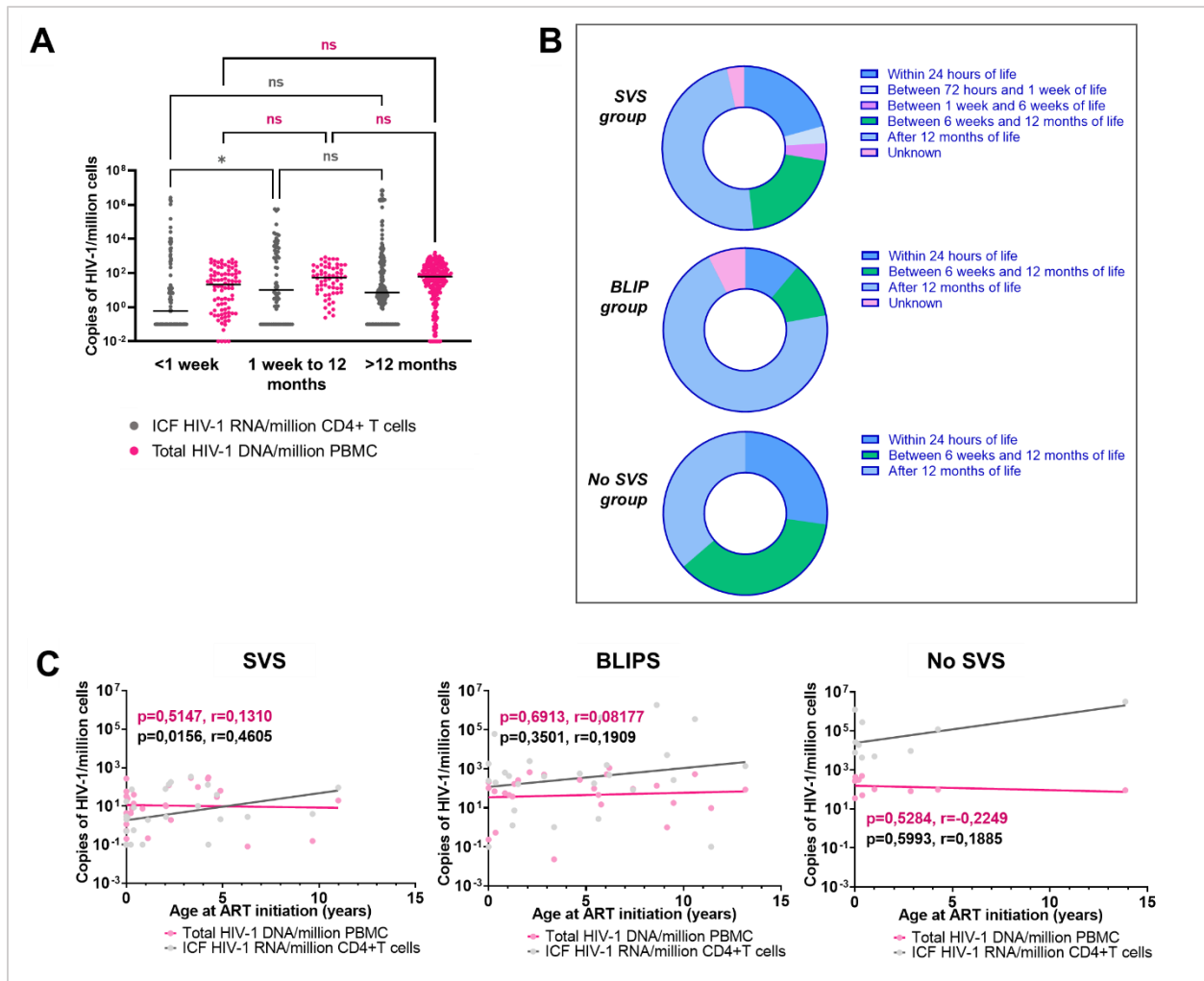
Figure 19. Relationship between timing of ART initiation and the size of HIV-1 reservoirs in vertically infected children and adolescents. A. Impact of really early (<1 week of life), early (1 week to 12 months) and late (>12 months) ART initiation on the size of the viral reservoir. Comparison between groups was done using the Kruskal-Wallis test and Dunn's multiple comparisons test. * = p<0.01; ns = not significant. B. Distribution of participants depending on ART initiation in the SVS, BLIP and No SVS groups. C. Impact of timing of ART initiation on the viral reservoir size in the three viral control groups: SVS (left), Blips (middle) and No SVS (right). Correlations were assessed using Spearman's non-parametric correlation test. The reservoir was quantified using the SUW013-stimulation assay (grey) and the total HIV-1 DNA assay (pink). Horizontal lines indicate median values. ICF = Inducible cell-free.

59
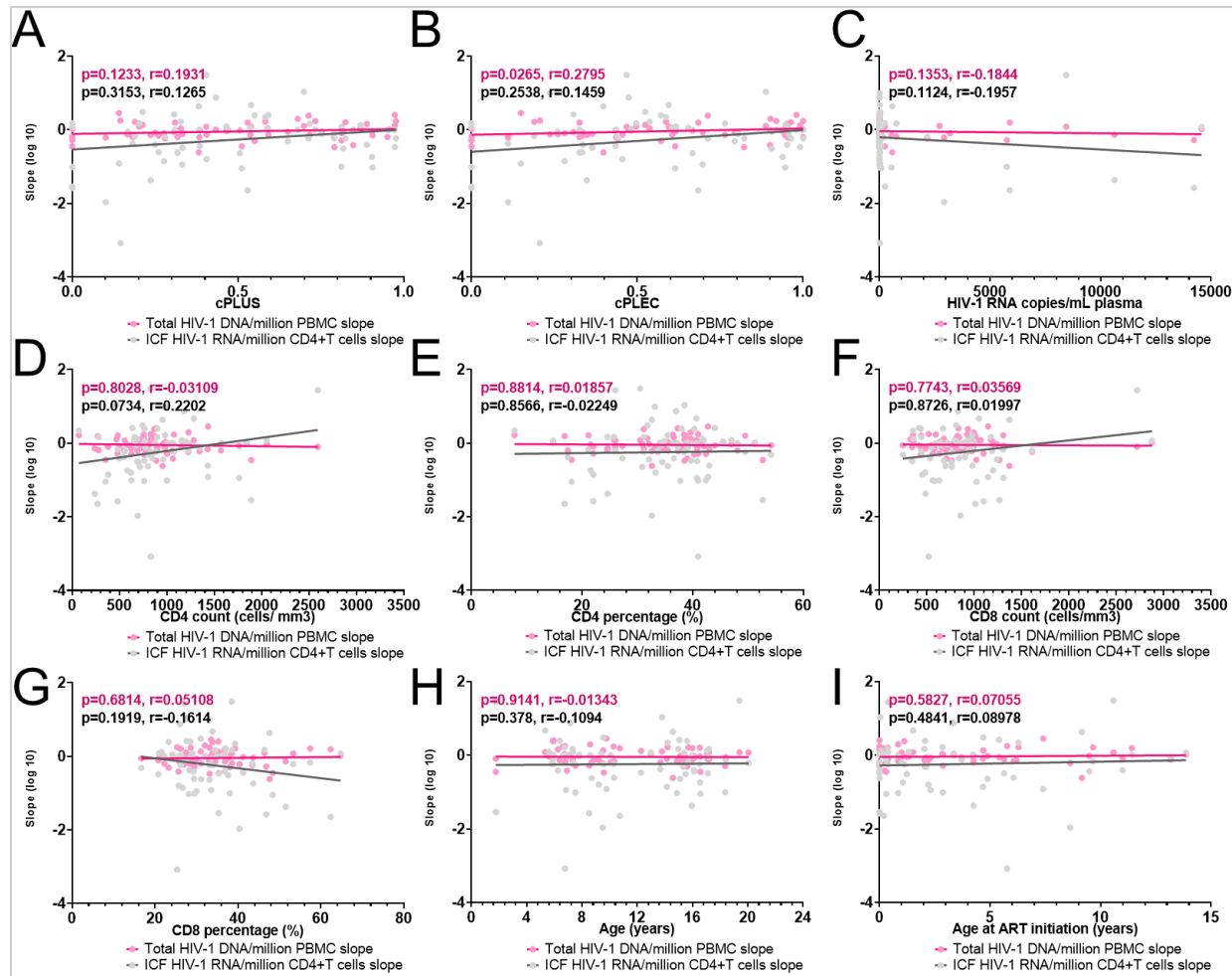
Figure 20. Impacts of various clinical and viral factors on the evolution of HIV-1 reservoirs in 67 vertically infected children and adolescents under cART. The viral reservoir was quantified at different time-points using two methods: the SUW013-stimulation assay (grey) and the total HIV-1 DNA assay (pink). Slopes were calculated for each participant using a linear regression model. The studied factors include the cumulative proportion of life under sustained viral suppression (cPLUS) (A) and under effective treatment (cPLEC) (D), CD4+ T cell counts and frequencies (B and C), CD8+ T cell counts and frequencies (E and F), age (G) and viremia (H). Each dot represents a time point analysis. Statistical significance of correlations was assessed using Spearman's non-parametric correlation test. ICF = Inducible cell-free.

60

Finally, we tried to analyze the impact of HIV-1 subtypes. Subtype B was prevalent in each viral control group, closely followed by subtype C (Figure 21A). The genetic diversity was also similar in the three groups. Unfortunately, the low number of participants in each category made it difficult to study their relationship with the inducible viral RNA reservoir and the HIV-1 DNA reservoir. Because of this, no clear cut correlations were observed between subtypes and the size and trajectory of the viral reservoirs (Figure 21B and 21C).
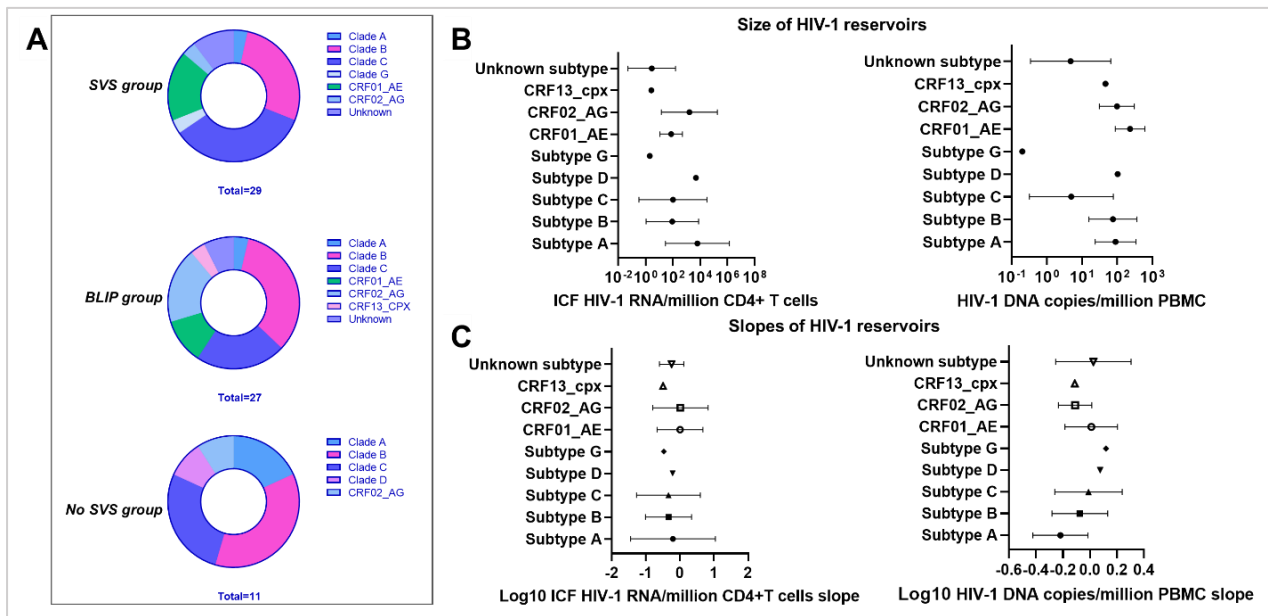
Figure 21. Relationship between HIV-1 subtypes and the size of the viral reservoirs in vertically infected children and adolescents. A. Distribution of the viral subtypes in the SVS, BLIP and No SVS groups. B. Impact of HIV-1 subtypes on the size of the viral reservoir. C. Impact of HIV-1 subtypes on the evolution of the viral reservoir. The reservoir was quantified using the SUW013-stimulation assay (left graph [B and C]) and the total HIV-1 DNA assay (right graph [B and C]). Graphs represent mean with error bars showing the standard deviation. Comparison between groups was done using the Kruskal-Wallis test and Dunn's multiple comparisons test. ICF = Inducible cell-free. ICF = Inducible cell-free.

CHAPTER 4 – DISCUSSION

4.1 Phylogenetic study of HIV-1 isolates

The goal of the first study was to determine the HIV-1 subtype infecting 64 EPIC[4] participants under cART. The majority (87.5%) were able to sustain suppression of viral replication throughout the retrospective study, meaning that viremia was undetectable at all time-points. In the past, a very low level of HIV in samples often made it difficult to isolate and study the virus. Nowadays, the advancement of molecular techniques, often associated with a higher sensitivity, a lower limit of detection and an easier access, has facilitated the process. Here, we show how we were able to successfully amplify the highly conserved HIV-1 *gag* gene in 95.3% (61/64) of our young participants.

Eight participants were over the age of twenty and had remained in the EPIC[4] study group as a part of a protocol seeking to help them manage the challenges that occur during the transition from pediatric to adult health care. This transition can be accompanied with a complex range of medical and psychosocial issues, often resulting from the sudden loss of the thorough guidance and support typically present in pediatric care, a lack of communication between institutions and/or stigma from the health-care workers.

We started by performing a nested PCR on lysates of PBMC dry pellets, which allowed us to obtain a final viral DNA fragment of 561 bp. Some of the participants we call « blippers » presented interrupted viral suppression. By prioritizing the selection of time-points where viremia was detectable, we were able to effectively isolate the virus in all blippers. We also noted the importance of diluting the amplicons of the first-round PCR, as the absence of this step often resulted in the failure of second-round amplification. The three participants for which the HIV-1 *gag* gene could not be amplified were 01-002-BLY, 05-028-IGT and 09-009-SOF. We noted that these participants spent long periods of time under effective treatment (median: 84% of their life [range: 72-97]) and under sustained viral suppression (median: 94% of their life [range: 89-100]). This could explain our difficulty in isolating the virus, since a long-term suppressive ART is associated with lower levels of HIV-1 DNA [149-151]. However, we were able to accomplish amplification with samples from other participants with similar characteristics. The reason for the lack of success might be in the PBMC samples. The rareness of HIV-1 DNA in

the samples might require repeating the experiment with a larger volume of PBMC lysate to increase the probability of finding a template for PCR.

The final PCR products were migrated on agarose gel, then cut and purified in preparation for cloning. As an RNA virus, HIV-1 expresses a high level of heterogeneity between patients but also within a single host, which contributes to the virus evading the immune system [152]. To isolate individual clones of the *gag* gene for each participant, purified DNA fragments were subcloned into pCR4-TOPO plasmid vectors which we used to transform competent *E. coli* cells.

The phylogenetic analysis began with the verification of the position of *gag* sequences on the genome of the HIV-1 reference strain HXB2. Clones which positioned outside of the *gag* gene were eliminated and those which were inserted backward in the vector were reversed in the correct direction relative to HXB2. An alignment was then made with our sequences and the reference *gag* sequences of HIV-1. We built phylogenetic trees rooted on a strain of SIVcpz, using with the Neighbor-Joining method with the bootstrap test at 1'000 replicates. In the first tree, we included all CRFs and groups of HIV-1 (M, N O and P). We studied the evolutionary relatedness among sequences and then built a second tree in which we excluded groups that did not cluster with our sequences in the first tree. We were left with the subtypes of group M and CRFs 01 and 02. This was expected, given that group M accounts for 90% of all HIV infections and that CRF01_AE and 02_AG are the most widespread recombinant forms [153].

We determined that the predominant subtype in our study group was C (39.3% of participants), followed by subtype A (34.4%), then subtype B (22.9%), CRF01_AE (19.7%), CRF02_AG (6.6%), and finally subtype G (3.2%). Notably, one participant of the subtype A cluster (04-021-XBD), grouped more specifically with clade A3, an embranchment supported at 73%.

As expected, only one HIV-1 subtype was found within each participant. The same cannot be said for adults, where there could be cases of reinfection, associated with sexual intercourse or drug injection, resulting in the presence of multiple subtypes in one host [154]. In fact, due to the vertical path of transmission, children are infected by the same subtype of HIV-1 found in their mothers. This is demonstrated by the siblings in our study cohort (05-25-UHW and 05-26-HVX / 09-003-TPH and 09-004-UKN), whose *gag* gene clones intertwined and clustered with

high bootstrap values of 99 to 100% and a small evolutionary distance. Except for these 4 participants, all clones originating from a singular host closely grouped separately from others, confirming the lack of contamination between samples.

All groupings were supported with a bootstrap value >70%. However, since the presence of a single recombinant sequence can greatly influence the branching order and branch lengths of a phylogenetic tree [155], we turned to HIV LANL tools to further study recombination in the recovered *gag* sequences [156]. We were only able to confirm the findings of our phylogenetic analysis and did not discover a new recombinant form among the different clones. A future investigation on the whole sequence of HIV-1 will be needed to confirm these findings.

Many questions were raised regarding the potential impact of HIV-1 subtypes on the outcome of the infection. Some studies have demonstrated a link between the biological differences among the clades and clinical outcomes [157]. For example, Kiwanuka et al. observed a faster disease progression and rate of decline of CD4+ T cells in patients infected with subtype D in comparison to subtype A [158]. In the present study, we did not detect a relationship between the subtypes infecting participants and clinical factors measured during EPIC[4], such as viral load, the number of CD4+ and CD8+ T cells and the cPLUS. This is most likely due to the small number of participants.

As the pandemic progresses, the genetic diversity of HIV-1 keeps expanding mainly due to the extremely high mutation rate and the selective pressure exerted by the hosts' immune system. We investigated the evolutionary divergence for *gag* fragments positioned from the 802nd to the 1327th nucleotide on the HXB2 genome and calculated a genetic distance of 0.18 substitutions per site between all sequences. The mean variance within a single subtype was more than half as high (0.062 substitutions per site). Interestingly, clade C, which is globally predominant, presented the highest variability. It was closely followed by clade B, then clades A and G along with CRF01-AE, all three showing similar values, and finally CRF02-AG. However, due to the small number of participants in some categories, this conclusion remains a mere observation. Indeed, clade C included the highest number of sequences, which could explain why it demonstrated the highest diversity.

There has been an increase in the prevalence of non-B subtypes in North America, the west of Europe and Australia [24]. This is also revealed in our results, where non-B infections amounted to 77%. This is no surprise as most of our participants were born outside of Canada. Overall, we noted a strong correlation between the genotype of the HIV-1 isolates infecting our participants and the prevalent HIV strain in the birth countries of their mothers. There was a concordance 83% of the time. For example, 100% of HIV-1 strains from participants of Vietnamese origin were identified as the recombinant CRF01_AE, which is predominant in that country [159]. Same with participants from countries in Southern Africa, where we mostly found subtype C [160]. Additionally, 66% of participants from Canada were infected with subtype B, which predominates in North America [161].

4.2. HIV-1 reservoir study

The second goal of this master's project was to characterize the size and evolution of the HIV-1 reservoir in perinatally infected children and adolescents under cART, and then determine the impact of multiple clinical and viral factors on the dynamics of said reservoir. 67 participants were selected from the multicentric EPIC[4] study. To demonstrate the longitudinal evolution of the reservoir throughout childhood and adolescence, participants were distributed in three main groups, depending on their ability to control viral replication (*SVS*, *BLIP*, *No SVS*), and further stratified in three age subgroups (<6, 6 to 10 and >10 years old). The *SVS* group represented participants with undetectable viremia at all time-points; the *BLIP* group presented interrupted SVS and the *No SVS* group included participants with no control over viral replication.

The viral reservoir was quantified using two methods in PBMCs samples collected every 3 months for approximatively 2.63 years (Range: 0.94 – 3.53). The first assay consisted of negatively isolating CD4+ T cells and stimulating *ex-vivo* virus production with the compound SUW013, an analogue of the PKC activator prostratin. This synthetic analogue was designed for an improved binding to PKC and thus has a greater ability at inducing the expression of the silent provirus [123]. Following a 48-hour stimulation with the inducer and IL-2, a digital droplet

PCR was performed on the culture supernatants. This allowed us to quantify the inducible cell-free HIV-1 RNA per million CD4+ T cells. With the second method, the HIV-1 DNA assay, we measured the total viral DNA present in PBMC lysate, using real time quantitative PCR.

Many quantitative assays have been developed to study HIV-1 reservoirs, each presenting their own set of advantages and challenges. The Total HIV-1 DNA assay has long been recognized as a standard technique based on its clinical relevance. It is commonly used, cost-effective, sensitive and requires a low volume of samples. However, this assay overestimates the reservoir by quantifying the entire pool of viral DNA, which includes only a small proportion of replication-competent proviruses [120]. The SUW013-stimulation assay allowed us to counteract this limitation by measuring the inducible and transcription-competent viral reservoir. However, this second technique is not without disadvantages. Indeed, the quantification of high levels of targets might be a limitation of the ddPCR. 7 participants from the **BLIP** and **No SVS** groups presented measures above the upper limit of detection (AUDL) in ddPCR due to a high saturation of positive droplets [162]. A calculation was thus made to estimate the reservoir (Table 5 in annex) and the calculated values were excluded in the correlation analysis between the size of the reservoir and suspected influencers. Although dilution of the cell samples could have resolved this issue, repeated measurements for the impacted time-points were not conducted due to the low number of samples available. Indeed, the volume of blood that was collected from our pediatric participants was limited. Therefore, the remaining samples were conserved for further studies. This mainly impacted the **NoSVS** group, as less time-point samples were available for experimentation. Despite this limitation, we observed a strong positive correlation between the measurements of viral DNA and inducible cell-free RNA, as was shown in our previously published study [148].

Time-point analysis showed that the ranges of measured RNA and DNA did not significantly differ. However, we observed an overall 4.25-time lower range of values with the second quantification method, perhaps hinting at a higher stability in viral DNA levels over time. Indeed, the median slope of the evolution of the reservoir was twice as high for the inducible HIV-1 RNA (-0.12 $\log_{10}$ ICF HIV-1 RNA/10^6 CD4+ T cells) in comparison to total HIV-1 DNA (-0.056 $\log_{10}$ HIV-1 DNA/10^6 PBMC). Additionally, in 73% (48/67) of participants, the regression line between the

size of the reservoir and time did not significantly deviate from zero. For those in whom a significant line could be observed, 72% experienced a slow decrease. This is consistent with the findings of multiple studies such as the 2003 study by Siliciano et al., where they demonstrated the extremely slow decay rate of the HIV-1 reservoir in patients under cART [163]. They estimated that in the absence of viremic blips, it would take an average of 51.2 years of therapy to eradicate one million infected cells, and the number jumped to 95.8 years in the presence of viremic blips [163].

The size and trajectory of the viral reservoir was mainly influenced by the control of viremia and although we found reservoir size tended to correlate with the age of the participants, the measured reservoir did not significantly differ between children in early/late childhood and adolescents. This can also be explained by the stability of the HIV-1 reservoir. In fact, a study by Persaud et al. has shown that, for perinatally infected children, after an initially rapid decay in the first three months following ART initiation, the frequency of infected CD4+ T cells persists with little or no decay [164]. They also estimated the half-time of the viral reservoir in adults to be similar in children (44 months) [164].

The similarity between age-subgroups in our study might also be linked to the unbalanced number of participants, which has impacted our statistical analysis. In reality, most people in the EPIC[4] cohort are teenagers who suppressed viremia very well, making it difficult to select participants for the **BLIPS** and **No SVS** groups, as well as the younger age-subgroups. A larger sample size of participants will thus be needed to further explore the evolution of the viral reservoir through childhood and adolescence.

HIV-1 ICF RNA and total DNA levels were highest amongst children who showed detectable viremia at most time-points (**No SVS** group). Blippers came second and participants with SVS had the lowest levels (Table 6 in annex). To further support these findings, we found that a lower viremia at the time of sample collection significantly correlated with lower amounts of viral DNA and inducible RNA. The ratio of ICF RNA in CD4+ T cells and DNA in PBMCs tended to be higher in children without viral suppression and the opposite trend was noted in children with viral suppression. Although this was not supported in statistical analyses, it suggests a

lower inducibility in the absence of SVS which perhaps results from a smaller pool of replication competent proviruses.

In the **No SVS** group, participants spent significantly less time under effective treatment and SVS compared to the other groups. The median amount of time being almost half as much as participants of the **SVS** group. We also observed at baseline a lower number and frequency of CD4+ T cells along with a higher frequency of CD8+ T cells, a dynamic which is typically seen in cases where virological failure occurs [165]. This is also reflected in the high levels of detectable viremia at almost every time point for this group.

Participants within the same age-subgroup exhibited a similar linear relationship between time and the size of their reservoirs. Divergence between participants was only observed in subgroups composed of children with interrupted suppression of viremia. These intermittent viremic blips following the achievement of viral suppression have long been the source of questioning. In theory, they are thought to be caused by a multitude of factors, such as a lower concentration of antiretrovirals, immune activation (due to vaccination or infections), the treatment regimen or virological failure [166, 167]. We analyzed the clinical history of each of our participants and indeed found a correlation between viral suppression and adherence to therapy. A lack of proper adherence was indicated in only 22% of time-points in the **SVS** group, whereas in the **BLIP** and **No SVS** groups, the amount jumped to 43% and 71.4% respectively. Non-adherence has been shown to be one of the most important determinants of disease progression and the development of drug resistance under antiretroviral therapy [168]. Our findings underline the benefits of maintaining a good level of adherence to ART as it significantly improves the control of viral replication and thus diminishes the size of the viral reservoir.

Interestingly, the viral reservoir was inducible in all but 8 participants (11.9%), 6 of which belonged to the **SVS** group and 2 in the **BLIP** group. They shared similar characteristics with the rest of the cohort, including the absolute numbers of CD4+ and CD8+ T cells, the cPLUS and the cPLEC. Although they tended to have a lower age at first-ART initiation (median: 0.12 years [range: 0.00 to 11.42], p=0.0723), this association was not statistically significant. In fact, the differentiating factor seemed to be the median level of viral DNA, which was 26.8-times lower in

these 8 children (2,172 HIV-1 DNA/10^6 PBMC, p<0.0001) compared to the rest of the cohort. This might suggest a smaller pool of HIV DNA-harbouring cells in these participants, and thus a lower amount of functional proviruses capable of producing viral RNA.

We also found that levels of viral ICF RNA and total DNA negatively correlated with the cPLUS and the cPLEC in our cohort. This is consistent with the fact that participants that spend less time on effective ART take longer to develop a robust control of viral replication which could result in an increased viral reservoir. Although viral RNA and DNA both correlated negatively with the CD4+ T cell counts, only RNA levels had a significant relationship with CD8+ T cell counts and the frequency of CD4+ or CD8+ T cells. Indeed, a smaller level of inducible reservoir was associated with higher frequency of CD4+ T cells and less CD8+ T cells in circulation, which indicates a better control over the viral infection.

We analyzed the impact of HIV-1 subtypes but could not draw any conclusions due to the small number of participants in certain categories. Besides, the genetic diversity was similar in our three viral control groups, with subtype B and C being prevalent.

Our investigation of the influence of the timing of ART on the size and trajectory of the reservoir yielded unexpected results. Early initiation of ART did not impact the level of viral DNA as we would have expected [169]. The only significant correlation was observed in the group of *SVS* participants. In these children, an early initiation of ART was associated with a smaller reservoir, but only in terms of ICF HIV-1 RNA. All these results indicate that starting ART at an early age is not enough to eradicate the reservoir or obtain ART-free remission. Sustained suppression of viral replication along with a strong level of adherence during cART might be the key in maintaining a small-sized viral reservoir.

Overall, the parameters we examined had little to no significant impact on the evolution of the reservoir. We did find a link between the cPLEC and viral DNA. Surprisingly, it suggested that participants who spent more time under effective cART had higher levels of proviruses. However, due to the general stability of the measured HIV-1 RNA and DNA in the few years our participants were followed, further investigation will be needed to confirm our finding and to better understand the impact of our factors on the evolution of the reservoir. For example, a

future project could be to measure the reservoir over an extended period in a bigger pool of participants.

Overall, the SUW013-stimulation assay was shown to be more sensitive to the effects of the different determinants we studied. In fact, in comparison to the viral DNA reservoir measured with the total DNA assay, the inducible reservoir was revealed to have a significant relationship with the level of immune T cells and the amount of time spent under treatment and SVS. This method of quantification might be a better tool in assessing the efficacy of therapy and the control over the viral infection in patients.

CHAPTER 5 – CONCLUSIONS AND PERSPECTIVES

The goals of this master's project, which was centered on the EPIC[4] pediatric cohort, were to (1) determine the subtype of HIV-1 isolates infecting participants and (2) describe the evolution of viral reservoir throughout childhood and adolescence.

We demonstrated how we were able to isolate and amplify the HIV-1 *gag* gene in a pool of participants under cART who mostly exhibited SVS. The phylogenetic analysis showed the predominance of non-B clades in our Canadian cohort and the consistent relation between HIV-1 subtypes in participants and the prevalent subtype in the birth countries of their mothers. These results fall in line with the evolution of the global distribution of HIV-1 and could be used in studies on transmission linkage.

Further investigation will be necessary to evaluate the presence of recombination in the viral sequences. This could be accomplished with a phylogenetic analysis on full-length sequences, using recombination breakpoint analysis software, such as SIMPLOT or RDP4, which can detect the exchange of genetic information between nucleotide sequences [170, 171].

We could not establish a relationship between subtypes and the outcome of HIV infection, due to the low number of participants. It would be interesting to increase the pool of samples to prove the impact they can have on different clinical factors, as well as the viral reservoir.

In this project, we measured the transcription-competent reservoir, as well as the levels of HIV-1 DNA in vertically infected children and adolescents. We found that the size of the reservoir was greatly influenced by the control of viral replication. Participants with sustained viral suppression presented the lowest median levels of RNA and DNA which were more than 10'000-times higher for participants without SVS in terms of RNA, and 8-times higher in terms of DNA. The presence of viremic blips correlated with a larger viral reservoir, an increase in CD8+ T cells, a loss of CD4+ T cells and imperfect adherence, thereby confirming the biological and potentially clinical significance of these isolated peaks and the importance of proper adherence to treatment.

Two other factors that influenced reservoir size were the cPLEC and the cPLUS, as our results show that participants who spent more time under effective treatment and SVS presented a smaller viral reservoir. The age at ART initiation only influenced the inducible reservoir of

participants with SVS, highlighting again the importance of early ART initiation on decreasing the establishment of the viral reservoir.

The use of two quantification methods allowed us to target different aspects of the complex HIV-1 reservoir. We demonstrated the positive correlation between HIV-1 DNA in PBMCs and inducible RNA in CD4+ T cells and noted an insignificant decline in the levels of HIV-1 through time. The stability of the reservoir and the fact that we were able to detect viral DNA even in *SVS* children who started treatment very early showed that the duration of ART and the timing of initiation are not enough to eradicate the virus. In fact, we measured similar levels of viral RNA and DNA between children younger than 6 years, those aged 6 to 10 years and adolescents.

Overall, we hope our results will help to better understand the dynamics of the HIV-1 reservoir in vertically infected hosts and serve in the development of eradication strategies and/or a long-term functional cure for children.

BIBLIOGRAPHY

1.   Centers for Disease, C., *Kaposi's sarcoma and Pneumocystis pneumonia among homosexual men--New York City and California.* MMWR Morb Mortal Wkly Rep, 1981. **30**(25): p. 305-8.

2.   Gottlieb, M.S., et al., *Pneumocystis carinii pneumonia and mucosal candidiasis in previously healthy homosexual men: evidence of a new acquired cellular immunodeficiency.* N Engl J Med, 1981. **305**(24): p. 1425-31.

3.   Greene, W.C., *A history of AIDS: looking back to see ahead.* Eur J Immunol, 2007. **37 Suppl 1**: p. S94-102.

4.   UNAIDS, *Fact Sheet 2021: Global HIV & AIDS statistics*. 2021.

5.   Canada, P.H.A.o., *Estimates of HIV incidence, prevalence and Canada's progress on meeting the 90-90-90 HIV targets*. 2020.

6.   UNAIDS, *90-90-90: An ambitious treatment target to help end the AIDS epidemic*. 2014.

7.   UNAIDS, *Global AIDS Update 2020 : Seizing the moment*. 2020.

8.   Nall, R. *The History of HIV and AIDS in the United States*. 2013 February 28, 2021 2021, Aug. 16]; Available from: https://www.healthline.com/health/hiv-aids/history.

9.   Bhaskaran, K., et al., *HIV infection and COVID-19 death: a population-based cohort analysis of UK primary care data and linked national death registrations within the OpenSAFELY platform.* Lancet HIV, 2021. **8**(1): p. e24-e32.

10.   Mirzaei, H., et al., *COVID-19 Among People Living with HIV: A Systematic Review.* AIDS Behav, 2021. **25**(1): p. 85-92.

11.   Bajunirwe, F., et al., *Towards 90-90-90 Target: Factors Influencing Availability, Access, and Utilization of HIV Services-A Qualitative Study in 19 Ugandan Districts.* Biomed Res Int, 2018. **2018**: p. 9619684.

12.   UNAIDS. *2025 AIDS Targets - Putting people living with HIV and communities at risk at the centre*. 2020 2021, Aug. 16]; Available from: https://aidstargets2025.unaids.org/.

13.   Barre-Sinoussi, F., et al., *Isolation of a T-lymphotropic retrovirus from a patient at risk for acquired immune deficiency syndrome (AIDS).* Science, 1983. **220**(4599): p. 868-71.

14.   Levy, J.A., et al., *Isolation of lymphocytopathic retroviruses from San Francisco patients with AIDS.* Science, 1984. **225**(4664): p. 840-2.

15.   Popovic, M., et al., *Detection, isolation, and continuous production of cytopathic retroviruses (HTLV-III) from patients with AIDS and pre-AIDS.* Science, 1984. **224**(4648): p. 497-500.

16.   Coffin, J., et al., *What to call the AIDS virus?* Nature, 1986. **321**(6065): p. 10.

17.   Sharp, P.M. and B.H. Hahn, *Origins of HIV and the AIDS pandemic.* Cold Spring Harb Perspect Med, 2011. **1**(1): p. a006841.

18.   Zhu, T., et al., *An African HIV-1 sequence from 1959 and implications for the origin of the epidemic.* Nature, 1998. **391**(6667): p. 594-7.

19.   Peeters, M., M. Jung, and A. Ayouba, *The origin and molecular epidemiology of HIV.* Expert Rev Anti Infect Ther, 2013. **11**(9): p. 885-96.

20.   Nyamweya, S., et al., *Comparing HIV-1 and HIV-2 infection: Lessons for viral immunopathogenesis.* Rev Med Virol, 2013. **23**(4): p. 221-40.

21.   Vicenzi, E. and G. Poli, *Novel factors interfering with human immunodeficiency virus-type 1 replication in vivo and in vitro.* Tissue Antigens, 2013. **81**(2): p. 61-71.

22.   Taylor, B.S., et al., *The challenge of HIV-1 subtype diversity.* N Engl J Med, 2008. **358**(15): p. 1590-602.

23.   Plantier, J.C., et al., *A new human immunodeficiency virus derived from gorillas.* Nat Med, 2009. **15**(8): p. 871-2.

24.   Santoro, M.M. and C.F. Perno, *HIV-1 Genetic Variability and Clinical Implications.* ISRN Microbiol, 2013. **2013**: p. 481314.

25.   Robertson, D.L., et al., *HIV-1 nomenclature proposal.* Science, 2000. **288**(5463): p. 55-6.

26.   Yamaguchi, J., et al., *Brief Report: Complete Genome Sequence of CG-0018a-01 Establishes HIV-1 Subtype L.* J Acquir Immune Defic Syndr, 2020. **83**(3): p. 319-322.

27.   Mokili, J.L., et al., *Identification of a novel clade of human immunodeficiency virus type 1 in Democratic Republic of Congo.* AIDS Res Hum Retroviruses, 2002. **18**(11): p. 817-23.

28.   Hemelaar, J., *The origin and diversity of the HIV-1 pandemic.* Trends Mol Med, 2012. **18**(3): p. 182-92.

29.   Hemelaar, J., et al., *Global and regional molecular epidemiology of HIV-1, 1990-2015: a systematic review, global survey, and trend analysis.* Lancet Infect Dis, 2019. **19**(2): p. 143-155.

30.   Bbosa, N., P. Kaleebu, and D. Ssemwanga, *HIV subtype diversity worldwide.* Curr Opin HIV AIDS, 2019. **14**(3): p. 153-160.

31.   Ng, K.T., et al., *Genome sequence of a novel HIV-1 circulating recombinant form 54_01B from Malaysia.* J Virol, 2012. **86**(20): p. 11405-6.

32.   Database, L.A.N.L.H.S., *HIV Circulating Recombinant Forms (CRFs)*.

33.   Watts, J.M., et al., *Architecture and secondary structure of an entire HIV-1 RNA genome.* Nature, 2009. **460**(7256): p. 711-6.

34.   Gelderblom, H.R., *Assembly and morphology of HIV: potential effect of structure on viral function.* AIDS, 1991. **5**(6): p. 617-37.

35.   Munro, J.B. and W. Mothes, *Structure and Dynamics of the Native HIV-1 Env Trimer.* J Virol, 2015. **89**(11): p. 5752-5.

36.   Pancera, M., et al., *Structure and immune recognition of trimeric pre-fusion HIV-1 Env.* Nature, 2014. **514**(7523): p. 455-61.

37.   German Advisory Committee Blood, S.A.o.P.T.b.B., *Human Immunodeficiency Virus (HIV).* Transfus Med Hemother, 2016. **43**(3): p. 203-22.

38.   Splettstoesser, T., *Diagram of the HIV virion*. 2014, SciStyle.

39.   Moore, M.D. and W.S. Hu, *HIV-1 RNA dimerization: It takes two to tango.* AIDS Rev, 2009. **11**(2): p. 91-102.

40.   Shan, L., et al., *Stimulation of HIV-1-specific cytolytic T lymphocytes facilitates elimination of latent viral reservoir after virus reactivation.* Immunity, 2012. **36**(3): p. 491-501.

41.   Perelson, A.S., et al., *HIV-1 dynamics in vivo: virion clearance rate, infected cell life-span, and viral generation time.* Science, 1996. **271**(5255): p. 1582-6.

42.   Seelamgari, A., et al., *Role of viral regulatory and accessory proteins in HIV-1 replication.* Front Biosci, 2004. **9**: p. 2388-413.

43.   Deeks, S.G., et al., *HIV infection.* Nat Rev Dis Primers, 2015. **1**: p. 15035.

44. Freed, E.O., *HIV-1 assembly, release and maturation.* Nat Rev Microbiol, 2015. **13**(8): p. 484-96.

45. Wagner, T.A., et al., *HIV latency. Proliferation of cells with HIV integrated into cancer genes contributes to persistent infection.* Science, 2014. **345**(6196): p. 570-3.

46. Griffin, G.E., et al., *Activation of HIV gene expression during monocyte differentiation by induction of NF-kappa B.* Nature, 1989. **339**(6219): p. 70-3.

47. Nabel, G. and D. Baltimore, *An inducible transcription factor activates expression of human immunodeficiency virus in T cells.* Nature, 1987. **326**(6114): p. 711-3.

48. Malim, M.H., et al., *The HIV-1 rev trans-activator acts through a structured target sequence to activate nuclear export of unspliced viral mRNA.* Nature, 1989. **338**(6212): p. 254-7.

49. Kariuki, S.M., et al., *The HIV-1 transmission bottleneck.* Retrovirology, 2017. **14**(1): p. 22.

50. Organization, W.H. *Global HIV Programme: Mother-to-child transmission of HIV*. 2018 Aug. 25, 2021]; Available from: https://www.who.int/teams/global-hiv-hepatitis-and-stis-programmes/hiv/prevention/mother-to-child-transmission-of-hiv.

51. UNAIDS, *Report on the global AIDS epidemic 2010*. 2010.

52. Groot, F., et al., *Differential susceptibility of naive, central memory and effector memory T cells to dendritic cell-mediated HIV-1 transmission.* Retrovirology, 2006. **3**: p. 52.

53. Blanpain, C., et al., *CCR5 and HIV infection.* Recept Channels, 2002. **8**(1): p. 19-31.

54. Bleul, C.C., et al., *The HIV coreceptors CXCR4 and CCR5 are differentially expressed and regulated on human T lymphocytes.* Proc Natl Acad Sci U S A, 1997. **94**(5): p. 1925-30.

55. Naif, H.M., *Pathogenesis of HIV Infection.* Infect Dis Rep, 2013. **5**(Suppl 1): p. e6.

56. Grossman, Z., et al., *Pathogenesis of HIV infection: what the virus spares is as important as what it destroys.* Nat Med, 2006. **12**(3): p. 289-95.

57. Okoye, A.A. and L.J. Picker, *CD4(+) T-cell depletion in HIV infection: mechanisms of immunological failure.* Immunol Rev, 2013. **254**(1): p. 54-64.

58. Goulder, P.J., S.R. Lewin, and E.M. Leitman, *Paediatric HIV infection: the potential for cure.* Nat Rev Immunol, 2016. **16**(4): p. 259-71.

59.   Evans, C., C.E. Jones, and A.J. Prendergast, *HIV-exposed, uninfected infants: new global challenges in the era of paediatric HIV elimination.* Lancet Infect Dis, 2016. **16**(6): p. e92-e107.

60.   McHenry, M.S., et al., *Neurodevelopment in Young Children Born to HIV-Infected Mothers: A Meta-analysis.* Pediatrics, 2018. **141**(2).

61.   *Rates of mother-to-child transmission of HIV-1 in Africa, America, and Europe: results from 13 perinatal studies. The Working Group on Mother-To-Child Transmission of HIV.* J Acquir Immune Defic Syndr Hum Retrovirol, 1995. **8**(5): p. 506-10.

62.   Kumar, S.B., et al., *Elevated cytokine and chemokine levels in the placenta are associated with in-utero HIV-1 mother-to-child transmission.* AIDS, 2012. **26**(6): p. 685-94.

63.   Wabwire-Mangen, F., et al., *Placental membrane inflammation and risks of maternal-to-child transmission of HIV-1 in Uganda.* J Acquir Immune Defic Syndr, 1999. **22**(4): p. 379-85.

64.   Tobin, N.H. and G.M. Aldrovandi, *Immunology of pediatric HIV infection.* Immunol Rev, 2013. **254**(1): p. 143-69.

65.   Biggar, R.J., et al., *The role of transplacental microtransfusions of maternal lymphocytes in HIV transmission to newborns.* AIDS, 2008. **22**(17): p. 2251-6.

66.   Lee, T.H., et al., *The role of transplacental microtransfusions of maternal lymphocytes in in utero HIV transmission.* J Acquir Immune Defic Syndr, 2010. **55**(2): p. 143-7.

67.   Kessler, P.A., *Potential Role of Regulatory T Cells in Mother-to-Child Transmission of HIV.* Curr HIV Res, 2018. **16**(6): p. 396-403.

68.   Mold, J.E., et al., *Maternal alloantigens promote the development of tolerogenic fetal regulatory T cells in utero.* Science, 2008. **322**(5907): p. 1562-5.

69.   Parren, P.W., et al., *Antibody protects macaques against vaginal challenge with a pathogenic R5 simian/human immunodeficiency virus at serum levels giving complete neutralization in vitro.* J Virol, 2001. **75**(17): p. 8340-7.

70.   Stiehm, E.R., et al., *Efficacy of zidovudine and human immunodeficiency virus (HIV) hyperimmune immunoglobulin for reducing perinatal HIV transmission from HIV-infected*

women with advanced disease: results of Pediatric AIDS Clinical Trials Group protocol 185. J Infect Dis, 1999. **179**(3): p. 567-75.

71. Ng, C.T., et al., *Passive neutralizing antibody controls SHIV viremia and enhances B cell responses in infant macaques.* Nat Med, 2010. **16**(10): p. 1117-9.

72. Thobakgale, C.F., et al., *Impact of HLA in mother and child on disease progression of pediatric human immunodeficiency virus type 1 infection.* J Virol, 2009. **83**(19): p. 10234-44.

73. Tiemessen, C.T. and L. Kuhn, *Immune pathogenesis of pediatric HIV-1 infection.* Curr HIV/AIDS Rep, 2006. **3**(1): p. 13-9.

74. Simon, A.K., G.A. Hollander, and A. McMichael, *Evolution of the immune system in humans from infancy to old age.* Proc Biol Sci, 2015. **282**(1821): p. 20143085.

75. Tobin, N.H. and G.M. Aldrovandi, *Are infants unique in their ability to be "functionally cured" of HIV-1?* Curr HIV/AIDS Rep, 2014. **11**(1): p. 1-10.

76. Gibbons, D.L., et al., *Neonates harbour highly active gammadelta T cells with selective impairments in preterm infants.* Eur J Immunol, 2009. **39**(7): p. 1794-806.

77. Ziegner, U., et al., *Deficient antibody-dependent cellular cytotoxicity against human immunodeficiency virus (HIV)-expressing target cells in perinatal HIV infection.* Clin Diagn Lab Immunol, 1999. **6**(5): p. 718-24.

78. Brenchley, J.M., et al., *Microbial translocation is a cause of systemic immune activation in chronic HIV infection.* Nat Med, 2006. **12**(12): p. 1365-71.

79. Sandler, N.G. and D.C. Douek, *Microbial translocation in HIV infection: causes, consequences and treatment opportunities.* Nat Rev Microbiol, 2012. **10**(9): p. 655-66.

80. Veazey, R.S., *Intestinal CD4 Depletion in HIV / SIV Infection.* Curr Immunol Rev, 2019. **15**(1): p. 76-91.

81. Richman, D.D., et al., *The toxicity of azidothymidine (AZT) in the treatment of patients with AIDS and AIDS-related complex. A double-blind, placebo-controlled trial.* N Engl J Med, 1987. **317**(4): p. 192-7.

82. Arts, E.J. and D.J. Hazuda, *HIV-1 antiretroviral drug therapy.* Cold Spring Harb Perspect Med, 2012. **2**(4): p. a007161.

83. James, J.S., *Saquinavir (Invirase): first protease inhibitor approved--reimbursement, information hotline numbers.* AIDS Treat News, 1995(no 237): p. 1-2.

84. Gulick, R.M., et al., *Treatment with indinavir, zidovudine, and lamivudine in adults with human immunodeficiency virus infection and prior antiretroviral therapy.* N Engl J Med, 1997. **337**(11): p. 734-9.

85. Sansone, G.R. and J.D. Frengley, *Impact of HAART on causes of death of persons with late-stage AIDS.* J Urban Health, 2000. **77**(2): p. 166-75.

86. Heendeniya, A. and Bogoch, II, *HIV prevention with post-exposure prophylaxis-in-pocket.* Lancet Public Health, 2019. **4**(10): p. e494.

87. Adolescents., P.o.A.G.f.A.a. *Guidelines for the Use of Antiretroviral Agents in Adults and Adolescents with HIV. Department of Health and Human Services.* 2021 Apr. 18, 2022]; Available from: https://clinicalinfo.hiv.gov/en/guidelines/adult-and-adolescent-arv.

88. Tressler, R. and C. Godfrey, *NRTI backbone in HIV treatment: will it remain relevant?* Drugs, 2012. **72**(16): p. 2051-62.

89. Organization, W.H., *WHO recommends dolutegravir as preferred HIV treatment option in all populations*. 2019.

90. Transmission., P.o.T.o.H.D.P.a.P.o.P. *Recommendations for the Use of Antiretroviral Drugs During Pregnancy and Interventions to Reduce Perinatal HIV Transmission in the United States*. 2021 Apr. 18, 2022]; Available from: https://clinicalinfo.hiv.gov/en/guidelines/perinatal.

91. HIV, P.o.A.T.a.M.M.o.C.L.w. *Guidelines for the Use of Antiretroviral Agents in Pediatric HIV Infection*. 2021 Apr. 18, 2022]; Available from: https://clinicalinfo.hiv.gov/en/guidelines/pediatric-arv.

92. Link, J.O., et al., *Clinical targeting of HIV capsid protein with a long-acting small molecule.* Nature, 2020. **584**(7822): p. 614-618.

93. Beccari, M.V., et al., *Ibalizumab, a Novel Monoclonal Antibody for the Management of Multidrug-Resistant HIV-1 Infection.* Antimicrob Agents Chemother, 2019. **63**(6).

94. *Cabotegravir/rilpivirine (Cabenuva) for HIV-1 infection.* Med Lett Drugs Ther, 2021. **63**(1625): p. 81-83.

95.   Richman, D.D., et al., *The challenge of finding a cure for HIV infection.* Science, 2009. **323**(5919): p. 1304-7.

96.   Chun, T.W., et al., *Quantification of latent tissue reservoirs and total body viral load in HIV-1 infection.* Nature, 1997. **387**(6629): p. 183-8.

97.   Brown, T.R., *I am the Berlin patient: a personal reflection.* AIDS Res Hum Retroviruses, 2015. **31**(1): p. 2-3.

98.   Gupta, R.K., et al., *Evidence for HIV-1 cure after CCR5Delta32/Delta32 allogeneic haemopoietic stem-cell transplantation 30 months post analytical treatment interruption: a case report.* Lancet HIV, 2020. **7**(5): p. e340-e347.

99.   Hutter, G., et al., *Long-term control of HIV by CCR5 Delta32/Delta32 stem-cell transplantation.* N Engl J Med, 2009. **360**(7): p. 692-8.

100.   Henrich, T.J., et al., *Antiretroviral-free HIV-1 remission and viral rebound after allogeneic stem cell transplantation: report of 2 cases.* Ann Intern Med, 2014. **161**(5): p. 319-27.

101.   Kordelas, L., et al., *Shift of HIV tropism in stem-cell transplantation with CCR5 Delta32 mutation.* N Engl J Med, 2014. **371**(9): p. 880-2.

102.   Salgado, M., et al., *Mechanisms That Contribute to a Profound Reduction of the HIV-1 Reservoir After Allogeneic Stem Cell Transplant.* Ann Intern Med, 2018. **169**(10): p. 674-683.

103.   Darcis, G., B. Van Driessche, and C. Van Lint, *HIV Latency: Should We Shock or Lock?* Trends Immunol, 2017. **38**(3): p. 217-228.

104.   Cohn, L.B., N. Chomont, and S.G. Deeks, *The Biology of the HIV-1 Latent Reservoir and Implications for Cure Strategies.* Cell Host Microbe, 2020. **27**(4): p. 519-530.

105.   Chomont, N., et al., *HIV reservoir size and persistence are driven by T cell survival and homeostatic proliferation.* Nat Med, 2009. **15**(8): p. 893-900.

106.   Luzuriaga, K., *Early Combination Antiretroviral Therapy Limits HIV-1 Persistence in Children.* Annu Rev Med, 2016. **67**: p. 201-13.

107.   Mavigner, M., et al., *Simian Immunodeficiency Virus Persistence in Cellular and Anatomic Reservoirs in Antiretroviral Therapy-Suppressed Infant Rhesus Macaques.* J Virol, 2018. **92**(18).

108.   Wong, J.K. and S.A. Yukl, *Tissue reservoirs of HIV.* Curr Opin HIV AIDS, 2016. **11**(4): p. 362-70.

109.   Catalfamo, M., et al., *HIV infection-associated immune activation occurs by two distinct pathways that differentially affect CD4 and CD8 T cells.* Proc Natl Acad Sci U S A, 2008. **105**(50): p. 19851-6.

110.   Rong, L. and A.S. Perelson, *Modeling HIV persistence, the latent reservoir, and viral blips.* J Theor Biol, 2009. **260**(2): p. 308-31.

111.   Martinez-Picado, J. and S.G. Deeks, *Persistent HIV-1 replication during antiretroviral therapy.* Curr Opin HIV AIDS, 2016. **11**(4): p. 417-23.

112.   Whitney, J.B., et al., *Rapid seeding of the viral reservoir prior to SIV viraemia in rhesus monkeys.* Nature, 2014. **512**(7512): p. 74-7.

113.   Besson, G.J., et al., *HIV-1 DNA decay dynamics in blood during more than a decade of suppressive antiretroviral therapy.* Clin Infect Dis, 2014. **59**(9): p. 1312-21.

114.   *Special issue dedicated to Dr. Sidney Udenfriend.* Neurochem Res, 1990. **15**(4): p. 371-474.

115.   Veldsman, K.A., et al., *Rapid decline of HIV-1 DNA and RNA in infants starting very early antiretroviral therapy may pose a diagnostic challenge.* AIDS, 2018. **32**(5): p. 629-634.

116.   Rouzioux, C. and D. Richman, *How to best measure HIV reservoirs?* Curr Opin HIV AIDS, 2013. **8**(3): p. 170-5.

117.   Lewin, S.R. and C. Rouzioux, *HIV cure and eradication: how will we get from the laboratory to effective clinical trials?* AIDS, 2011. **25**(7): p. 885-97.

118.   Avettand-Fenoel, V., et al., *Total HIV-1 DNA, a Marker of Viral Reservoir Dynamics with Clinical Implications.* Clin Microbiol Rev, 2016. **29**(4): p. 859-80.

119.   Wong, J.K., et al., *Recovery of replication-competent HIV despite prolonged suppression of plasma viremia.* Science, 1997. **278**(5341): p. 1291-5.

120.   Alidjinou, E.K., L. Bocket, and D. Hober, *Quantification of viral DNA during HIV-1 infection: A review of relevant clinical uses and laboratory methods.* Pathol Biol (Paris), 2015. **63**(1): p. 53-9.

121. Ho, Y.C., et al., *Replication-competent noninduced proviruses in the latent reservoir increase barrier to HIV-1 cure.* Cell, 2013. **155**(3): p. 540-51.

122. Plantin, J., M. Massanella, and N. Chomont, *Inducible HIV RNA transcription assays to measure HIV persistence: pros and cons of a compromise.* Retrovirology, 2018. **15**(1): p. 9.

123. Beans, E.J., et al., *Highly potent, synthetically accessible prostratin analogs induce latent HIV expression in vitro and ex vivo.* Proc Natl Acad Sci U S A, 2013. **110**(29): p. 11698-703.

124. Massanella, M., et al., *Improved assays to measure and characterize the inducible HIV reservoir.* EBioMedicine, 2018. **36**: p. 113-121.

125. Cuevas, J.M., et al., *Extremely High Mutation Rate of HIV-1 In Vivo.* PLoS Biol, 2015. **13**(9): p. e1002251.

126. Bhargava, M., et al., *Do HIV-1 non-B subtypes differentially impact resistance mutations and clinical disease progression in treated populations? Evidence from a systematic review.* J Int AIDS Soc, 2014. **17**: p. 18944.

127. Wymant, C., et al., *A highly virulent variant of HIV-1 circulating in the Netherlands.* Science, 2022. **375**(6580): p. 540-545.

128. Bitnun, A., et al., *Early initiation of combination antiretroviral therapy in HIV-1-infected newborns can achieve sustained virologic suppression with low frequency of CD4+ T cells carrying HIV in peripheral blood.* Clin Infect Dis, 2014. **59**(7): p. 1012-9.

129. Butler, K.M., et al., *Rapid viral rebound after 4 years of suppressive therapy in a seronegative HIV-1 infected infant treated from birth.* Pediatr Infect Dis J, 2015. **34**(3): p. e48-51.

130. Frange, P., et al., *HIV-1 virological remission lasting more than 12 years after interruption of early antiretroviral therapy in a perinatally infected teenager enrolled in the French ANRS EPF-CO10 paediatric cohort: a case report.* Lancet HIV, 2016. **3**(1): p. e49-54.

131. Giacomet, V., et al., *No cure of HIV infection in a child despite early treatment and apparent viral clearance.* Lancet, 2014. **384**(9950): p. 1320.

132.   Hocqueloux, L., et al., *Long-term immunovirologic control following antiretroviral therapy interruption in patients treated at the time of primary HIV-1 infection.* AIDS, 2010. **24**(10): p. 1598-601.

133.   Luzuriaga, K., et al., *Viremic relapse after HIV-1 remission in a perinatally infected child.* N Engl J Med, 2015. **372**(8): p. 786-8.

134.   Persaud, D., et al., *Absence of detectable HIV-1 viremia after treatment cessation in an infant.* N Engl J Med, 2013. **369**(19): p. 1828-35.

135.   Rosenberg, E.S., et al., *Immune control of HIV-1 after early treatment of acute infection.* Nature, 2000. **407**(6803): p. 523-6.

136.   Saez-Cirion, A., et al., *Post-treatment HIV-1 controllers with a long-term virological remission after the interruption of early initiated antiretroviral therapy ANRS VISCONTI Study.* PLoS Pathog, 2013. **9**(3): p. e1003211.

137.   Violari, A., et al., *A child with perinatal HIV infection and long-term sustained virological control following antiretroviral treatment cessation.* Nat Commun, 2019. **10**(1): p. 412.

138.   Persaud, D., et al., *Dynamics of the resting CD4(+) T-cell latent HIV reservoir in infants initiating HAART less than 6 months of age.* AIDS, 2012. **26**(12): p. 1483-90.

139.   Rainwater-Lovett, K., P. Uprety, and D. Persaud, *Advances and hope for perinatal HIV remission and cure in children and adolescents.* Curr Opin Pediatr, 2016. **28**(1): p. 86-92.

140.   Gabant, P., et al., *Bifunctional lacZ alpha-ccdB genes for selective cloning of PCR products.* Biotechniques, 1997. **23**(5): p. 938-41.

141.   Kuiken, C., B. Korber, and R.W. Shafer, *HIV sequence databases.* AIDS Rev, 2003. **5**(1): p. 52-61.

142.   Tamura, K., G. Stecher, and S. Kumar, *MEGA11: Molecular Evolutionary Genetics Analysis Version 11.* Mol Biol Evol, 2021. **38**(7): p. 3022-3027.

143.   Thompson, J.D., et al., *The CLUSTAL_X windows interface: flexible strategies for multiple sequence alignment aided by quality analysis tools.* Nucleic Acids Res, 1997. **25**(24): p. 4876-82.

144.   Saitou, N. and M. Nei, *The neighbor-joining method: a new method for reconstructing phylogenetic trees.* Mol Biol Evol, 1987. **4**(4): p. 406-25.

145.	Tamura, K., M. Nei, and S. Kumar, *Prospects for inferring very large phylogenies by using the neighbor-joining method.* Proc Natl Acad Sci U S A, 2004. **101**(30): p. 11030-5.

146.	Vandergeeten, C., et al., *Cross-clade ultrasensitive PCR-based assays to measure HIV persistence in large-cohort studies.* J Virol, 2014. **88**(21): p. 12385-96.

147.	Clouse, K.A., et al., *Monokine regulation of human immunodeficiency virus-1 expression in a chronically infected human T cell clone.* J Immunol, 1989. **142**(2): p. 431-8.

148.	Bitnun, A., et al., *Clinical Correlates of Human Immunodeficiency Virus-1 (HIV-1) DNA and Inducible HIV-1 RNA Reservoirs in Peripheral Blood in Children With Perinatally Acquired HIV-1 Infection With Sustained Virologic Suppression for at Least 5 Years.* Clin Infect Dis, 2020. **70**(5): p. 859-866.

149.	Bachmann, N., et al., *Determinants of HIV-1 reservoir size and long-term dynamics during suppressive ART.* Nat Commun, 2019. **10**(1): p. 3193.

150.	Chun, T.W., et al., *Decay of the HIV reservoir in patients receiving antiretroviral therapy for extended periods: implications for eradication of virus.* J Infect Dis, 2007. **195**(12): p. 1762-4.

151.	Payne, H., et al., *Early ART-initiation and longer ART duration reduces HIV-1 proviral DNA levels in children from the CHER trial.* AIDS Res Ther, 2021. **18**(1): p. 63.

152.	Domingo, E. and C. Perales, *Viral quasispecies.* PLoS Genet, 2019. **15**(10): p. e1008271.

153.	Hemelaar, J., et al., *Global trends in molecular epidemiology of HIV-1 during 2000-2007.* AIDS, 2011. **25**(5): p. 679-89.

154.	Chohan, B., et al., *Evidence for frequent reinfection with human immunodeficiency virus type 1 of a different subtype.* J Virol, 2005. **79**(16): p. 10701-8.

155.	Posada, D., K.A. Crandall, and E.C. Holmes, *Recombination in evolutionary genomics.* Annu Rev Genet, 2002. **36**: p. 75-97.

156.	Siepel, A.C., et al., *A computer program designed to screen rapidly for HIV type 1 intersubtype recombinant sequences.* AIDS Res Hum Retroviruses, 1995. **11**(11): p. 1413-6.

157. Keller, M., et al., *Impact of HIV-1 viral subtype on CD4+ T-cell decline and clinical outcomes in antiretroviral naive patients receiving universal healthcare.* AIDS, 2009. **23**(6): p. 731-7.

158. Kiwanuka, N., et al., *HIV-1 viral subtype differences in the rate of CD4+ T-cell decline among HIV seroincident antiretroviral naive persons in Rakai district, Uganda.* J Acquir Immune Defic Syndr, 2010. **54**(2): p. 180-4.

159. Lan, N.T., et al., *HIV type 1 isolates from 200 untreated individuals in Ho Chi Minh City (Vietnam): ANRS 1257 Study. Large predominance of CRF01_AE and presence of major resistance mutations to antiretroviral drugs.* AIDS Res Hum Retroviruses, 2003. **19**(10): p. 925-8.

160. Giovanetti, M., et al., *Molecular Epidemiology of HIV-1 in African Countries: A Comprehensive Overview.* Pathogens, 2020. **9**(12).

161. Hemelaar, J., et al., *Global and regional distribution of HIV-1 genetic subtypes and recombinants in 2004.* AIDS, 2006. **20**(16): p. W13-23.

162. Pinheiro, L.B., et al., *Evaluation of a droplet digital polymerase chain reaction format for DNA copy number quantification.* Anal Chem, 2012. **84**(2): p. 1003-11.

163. Siliciano, J.D., et al., *Long-term follow-up studies confirm the stability of the latent reservoir for HIV-1 in resting CD4+ T cells.* Nat Med, 2003. **9**(6): p. 727-8.

164. Persaud, D., et al., *A stable latent reservoir for HIV-1 in resting CD4(+) T lymphocytes in infected children.* J Clin Invest, 2000. **105**(7): p. 995-1003.

165. Chereau, F., et al., *Impact of CD4 and CD8 dynamics and viral rebounds on loss of virological control in HIV controllers.* PLoS One, 2017. **12**(4): p. e0173893.

166. Darcis, G., et al., *Detectability of HIV Residual Viremia despite Therapy Is Highly Associated with Treatment with a Protease Inhibitor-Based Combination Antiretroviral Therapy.* Antimicrob Agents Chemother, 2020. **64**(3).

167. Nettles, R.E., et al., *Intermittent HIV-1 viremia (Blips) and drug resistance in patients receiving HAART.* JAMA, 2005. **293**(7): p. 817-29.

168. Lucas, G.M., *Antiretroviral adherence, drug resistance, viral fitness and HIV disease progression: a tangled web is woven.* J Antimicrob Chemother, 2005. **55**(4): p. 413-6.

169. Henrich, T.J., et al., *HIV-1 persistence following extremely early initiation of antiretroviral therapy (ART) during acute HIV-1 infection: An observational study.* PLoS Med, 2017. **14**(11): p. e1002417.

170. Lole, K.S., et al., *Full-length human immunodeficiency virus type 1 genomes from subtype C-infected seroconverters in India, with evidence of intersubtype recombination.* J Virol, 1999. **73**(1): p. 152-60.

171. Martin, D.P., et al., *RDP4: Detection and analysis of recombination patterns in virus genomes.* Virus Evol, 2015. **1**(1): p. vev003.

ANNEX SUPPLEMENTARY TABLES AND FIGURES

Table 5. Raw results of total HIV-1 DNA and inducible cell-free RNA for the 67 participants in the reservoir study. Some measures of viral RNA were estimated (indicated by *) due to a saturation of positive droplets in digital droplet PCR. Our calculations were based on a theoretical dynamic range of 10^5 target copies per 20,000-droplet reaction (1 reaction = 20 μL) for a 99.5% saturation of the droplets [162]. As ddPCR was performed on 1000 μL samples (50x20 μL), we divided 50-times 10^5 copies by the number of CD4+ T cells counted during the stimulation protocol and thus obtained the estimated ICF HIV-1 RNA per million CD4+ T cells.

Link to the Google Excel sheet:

https://docs.google.com/spreadsheets/d/1yQkwb68RvMnckP9Z4QAvcSeUwXw7BDAo/edit?usp =sharing&ouid=112458619558678595515&rtpof=true&sd=true

Table 6. Median levels and slope of total HIV-1 DNA and inducible cell-free RNA for the 67 participants in the reservoir study.

Caracterisitics	Children with sutained viral suppression during study; <SVS> (n=29)	Children presenting occasional viremic blips; <BLIPS> (n=27)	Children without sutained viral suppression; <No SVS> (n=11)	P value <SVS> vs <BLIPS>	P value <SVS> vs <No SVS>	P value <BLIPS> vs <No SVS>
Median Inducible cell-free HIV-1 RNA levels (ICF HIV-1 RNA/10^6 CD4+ T cells) (Interquartile range: 25%,75%)	0.6174(0.1000,6.034)	9.884 (0.3094,664.1)	6953 (295.0-561010)	<0.0001	<0.0001	<0.0001
Median Total HIV-1 DNA levels (log10 HIV-1 DNA/10^6 PBMC) (Interquartile range: 25%,75%)	16.64 (0.801,74.09)	63.99 (17.70,221.3)	132.0 (50.27,308.4)	0,0001	<0.0001	0.2784
Median Inducible cell-free HIV-1 RNA slope (log10 ICF HIV-1 RNA/10^6 CD4+ T cells) (Interquartile range: 25%,75%)	0.000 (-0.3079,0.09862)	-0.4408 (-0.9164,0,08759)	-0.2014 (-1.370,0.1729)	0.5491	>0.9999	>0.9999
Median Total HIV-1 DNA Slope (log10 HIV-1 DNA/10^6 PBMC) (Interquartile range: 25%,75%)	-0.05452 (-0.1976,0.1734)	-0.05947 (-0.1614,0.04301)	-0.09516 (-0.2383,0.08924)	>0.9999	>0.9999	>0.9999
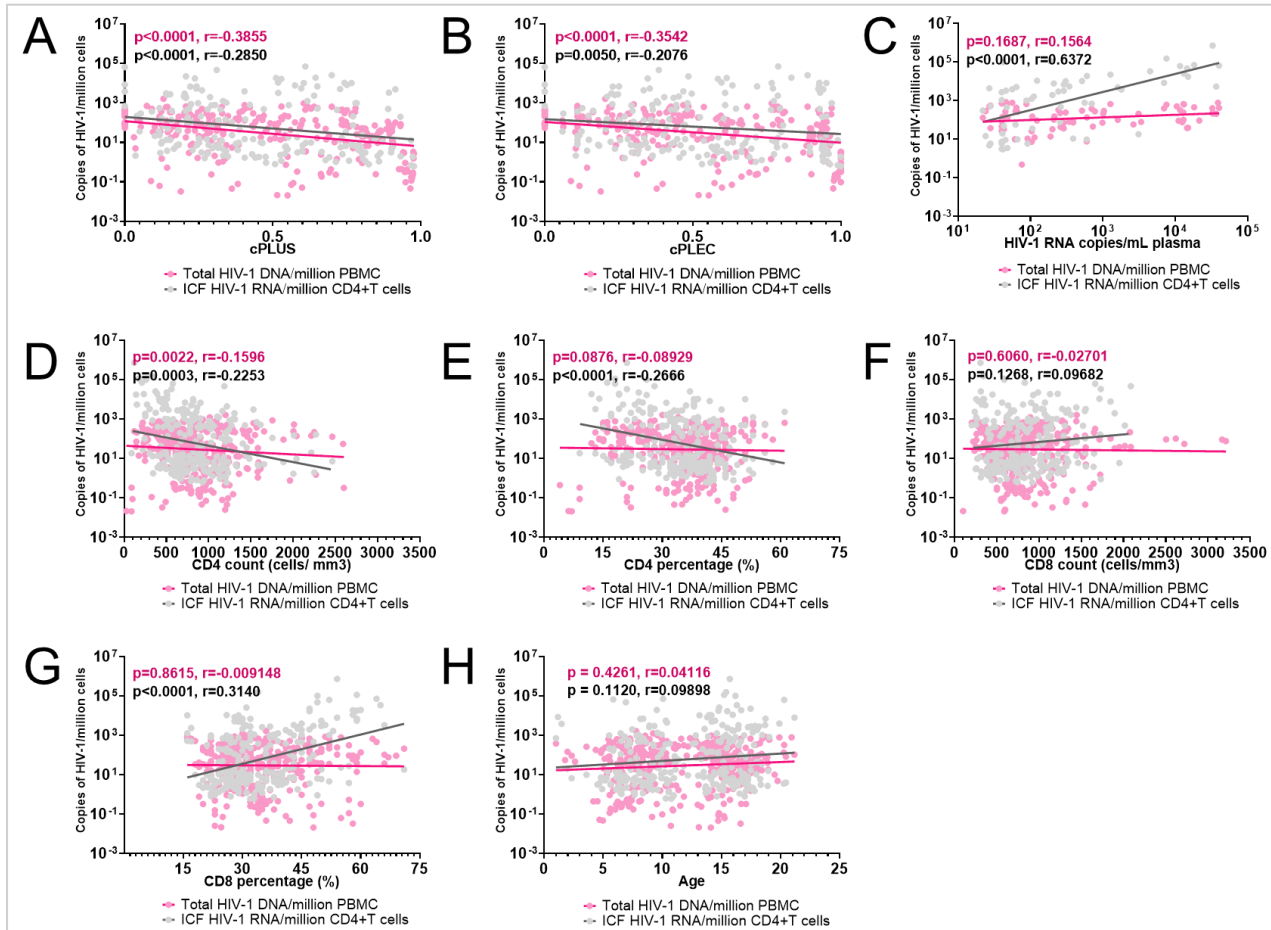
Figure S1. Impacts of various clinical and viral factors on the size of HIV-1 reservoirs in vertically infected children and adolescents under cART. The viral reservoir was quantified at different time-points using two methods: the SUW013-stimulation assay (grey) and the total HIV-1 DNA assay (pink). In this graph, undetectable measures for viral load, ICF HIV-1 RNA and total HIV-1 DNA were excluded. The studied factors include the cumulative proportion of life under sustained viral suppression (cPLUS) (A) and under effective treatment (cPLEC) (B), viremia (C), CD4+ T cell counts and frequencies (D and E), CD8+ T cell counts and frequencies (F and G), and age (H). Age at initiation was not included due to the lack of outliers in the data set. Each dot represents a time point. Correlations were assessed using Spearman's non-parametric correlation test. ICF = Inducible cell-free.